***Response to Reviewer 1***

*We thank the reviewer for their time and patience in re-reviewing our revised manuscript. We greatly appreciate the extremely helpful, detailed, and constructive comments they provided. They identified remaining weaknesses our analysis, which we have addressed, and we believe this has significantly improved the manuscript. We have numbered each reviewer comment below and responded in italicized text.*

Review

**General Comments:**
I appreciate the effort the authors have taken to substantially revise and focus the manuscript, including new data on 14CO2 and CO isotope data from an additional site. The evaluation of the Indianapolis dataset is presented in a more adequate way, although I have a doubt whether the error estimate is correct (the standard error of the mean has apparently been used for averaging measurements on clearly different air masses). The uncertainty may be underestimated.
It is nice that Beech Island data are shown, but the straightforward analysis with a Keeling plot model is questionable. The authors already discuss this in some detail, but do not attempt to estimate additional errors. This analysis is in my opinion too qualitative, and it may be useful to compare the Beech Island data to other stations (see below).
I also miss a discussion on the possible role of ozonolysis in producing CO from unsaturated hydrocarbons (e.g. isoprene), in particular the effect that this source would have on the d18O values.

***Response to the General Comments:*** *These comments are addressed individually next to the specific comments the Reviewer made below, thus please refer to our responses below.*

**Comment 1**
P2, l17: remove “mole fraction of”

***Response to Comment 1:*** *Completed as requested.*

**Comment 2**
P3, l2: It may be good to include some other key references that determined the isotopic composition of sources, rather than only the review by Brenninkmeijer et al.

***Response to Comment 2:*** *We have updated Table 1 with key references for the sources, as well as the OH sink.*

**Comment 3**
P8, l11 ff: I suggest replacing carbon-13 by 13C etc.

***Response to Comment 3:*** *Completed as requested.*

**Comment 4**
P8, l14: Mak and Yang are only one of the studies that state this formula, I think it was first explicitly stated in Brenninkmeijer 1993.

***Response to Comment 4:*** *We added this reference as requested, as well as original Stevens and Krout (1972) reference which present this correction in a different form, but nonetheless were the first to detail this correction method when using Schütze's Reagent.*

**Comment 5:** P8-9: This paragraph is about the 17O excess of CO. Minor issue: This is NOT observed "particularly in the high northern latitudes" but was also observed at Tenerife. It is a global effect. Further, the authors do not mention or are not aware of the fact that the 17O excess can also be created by ozonolysis of VOC, where the strong 17O excess of O3 is transferred to CO (Röckmann et al., J. Geophys. Res., 103, 1463-1470, 1998). This should be discussed, since it may be particularly relevant for the VOC oxidation source. The effect on the 17O correction for 13C is likely still small, but this source will also affect 18O, which is the target of the present study (see below).

***Response to Comment 5:*** *We have both corrected the error as requested for the "high northern latitudes", and have also discussed the ozonolysis source in this section as well. Further, we discuss the ozonolysis source at length in a new discussion section (section 3.4).*

**Comment 6**
P10, l6: Independent of what?

***Response to Comment 6:*** *We removed this statement. After re-reading the paragraph, it appeared to be confusing and not relevant to the description of the method.*

**Comment 7**
P10, L22: Is there a reason why you use the symbol I_delta18O here, instead of directly writing delta_source? In the next sentence you write that it is the source signature, so it may not be necessary to introduce a new symbol that is usually not used in the literature.

***Response to Comment 7:*** *We have changed the intercept to δs as requested here. The reason Iδ was used in this equation was because the original source (Keeling, 1958) used this notation*.

**Comment 8**
P12, l24 ff: You mention that you filter unphysical data, and data with less than 5% VOC contribution. In table 2 I see two data points that have about 10% VOC contribution, but for which the signatures are strongly deviating. I understand that these points are included in the evaluation.

***Response to Comment 8:*** *We are uncertain what the reviewer is trying to ask for in this comment. All of the statements in this comment are correct, but we do not see a clear request* *for changes. However, in response to the reviewer's comment below (Comment 12), we have reformulated our data filtering (described in section 2.6). These two points are no longer included in the data set. This change is discussed more below in our response to Comment 12.*

**Comment 9**
P13, l1: The sentence "It is unclear from our data why the XCO2-FF enhancements are occasionally near or below zero." is a unsatisfactory. Reformulate (at least provide some thoughts) since you have the 14C experts in your author team.

***Response to Comment 9:*** *We have reformulated this sentence. It now reads:*

*"Large overestimates of XCO-VOC arise because the ratio method can produce unrealistically low calculated XCO-FF values if the XCO2-FF enhancements are not significantly different from zero. XCO2-FF enhancements near or below zero are a result of possible local contamination at or near the background tower, which violates the assumption of well mixed background air flowing across the city."*

**Comment 10**
P14, l 8 and 10: Help the reader by writing down the differences (values) between summer and winter for both signatures.

***Response to Comment 10:*** *Added in the differences as requested. Additionally, for 18O, we reversed the order in the sentence to be consistent with the previously mentioned 13C differences.*

**Comment 11**
L17: strongly contributes

***Response to Comment 11:*** *Completed as requested*

**Comment 12**
P15, l3-5: These numbers seem to be the standard error of the mean of your observations. Is it adequate to use the standard error of the mean? It is clear that you do NOT make repeated measurements of the same samples. So it is in my view not adequate to assume that by making more measurements you reduce the error statistically. When I see the large range of values I think that the errors are underestimated.

***Response to Comment 12:*** *Our original approach using the mean and standard error of the mean was done because we were sampling the same overall process. In light of the reviewer's comment, however, we have adjusted the approach and performed a bootstrap Monte Carlo, (described in section 2.5) for the δVOC sample sets. This approach samples with replacement, which we believe is needed given the outlier data points we have in relation to the total number of data. This approach provides a metric to determine the probability of the mean value by* *randomly replacing points within the data set with other points from the data set, which helps to assess the effect of the outliers.*

*Furthermore, we reconsidered our data filtering approach. The method we use to calculate the δ values for CO derived from oxidized VOC's becomes biased when XCO-VOC is calculated to be either a very small or a very large percentage of the total urban enhancement. Small percentages produce large negative outliers, such as the points referred to by the reviewer in comment X, while large percentages are biased towards the urban enhancement isotopic signatures. We applied a new filter so data with XCO-VOC values below 15% and above 85% are excluded, to eliminate the outlier issues. The revised data filtering approach is detailed in the text, section 2.6.*

*These two changes reduce the scatter in the calculated dVOC values, and we believe provide a more robust metric for the uncertainty bounds placed on our estimates of the mean δVOC signatures. The results are still within 1σ uncertainty, lending further confidence to this estimate.*

**Comment 13**
P15-16: In the discussion of the VOC source signature, I miss the aspect that unsaturated HC can also be oxidized by ozonolysis, where the strong enrichment in both 17O and 18O would be transferred to CO (Röckmann et al., J. Geophys. Res., 103, 1463-1470, 1998). This was originally suggested as a source for the 17O excess of CO (see above), but it would also strongly affect the d18O values since O3 is so enriched in d18O. Does the low value for oxidation of VOC that is found here suggest that ozonolysis of VOC is not a significant source of CO compared to oxidation by OH? Do you have estimates from models on how much of the photochemically produced CO would be produced via ozonolysis?

***Response to Comment 13:*** *We thank the reviewer for pointing this out. To address this comment, we have included a new section, Section 3.4: Discussion of the role of ozonolysis in the VOC-derived CO δ18O signature. In this section we discuss the ozonolysis source, and its possible impact on our observations. The effect on VOC-derived CO from Indianapolis measurements is expected to be minimal due to the short reaction times in the INFLUX experiment (detailed in the text). We currently do not have chemistry-transport model results for CO produced by ozonolysis at our sites. While such estimates could be useful, performing such simulations is beyond the scope of this study. Instead, we discuss the effect this source would have on δ18O of CO assuming source isotopic values reported by Röckmann et al. (1998), and that our δ18O time series are not consistent with a significant contribution from this source.*

**Comment 14**
P16, section 3.3: You apply the Keeling plot approach to the Beech Island data, but I wonder whether this is appropriate. You discuss several aspects, but assess the effect of different processes on the results mainly qualitatively (e.g. would go in a different direction). As you state the assumption of the Keeling plot model is that the bg is constant, but we know that this is not the case since OH strongly affects and processes CO during summer. You conclude from

qualitative statements that the Keeling plot approach is still appropriate, but this is not substantiated by quantitative numbers.

An example: The application of the Keeling plot technique conceptually implies that the sample collected on August 8 with 87.9 ppb CO is a “near-background” sample and the sample on July 27 with 179.2 ppb is a contaminated sample and that the additional 90 ppb comes from the local contamination for which you calculate the isotope signature. Including the 87.9 ppb sample has a large effect on the source signature (you would get very different source signatures, outside the reported errors, if you left this one sample out), but does this sample represent the background well?

Can you make some assumptions on the seasonal changes in a conceptual model and assess the effect on the results (similar to conceptual model calculations in the Brenninkmeijer 1999 review, Fig 2)? Or can you try to quantify the effect by comparing to CO isotope measurements at other stations, e.g. Barbados, Montauk Pt, LI or Izana, similar to Mak et al., in their analysis of the Barbados data? Could this provide background values to better assess the total and VOC sources?

***Response to Comment 14:*** *We have addressed this comment using the method of including prior data from another station as background for Beech Island, as per the Reviewers suggestion. This provides an independent method of assessing the validity of the Keeling plot analysis. We used CO mole fraction and isotopic data from Tennerife for this purpose from Braunlich, (2000). Using these data, we calculated monthly averaged Xco, δ13C, and δ18O data from Tennerife. Using this as a background signal, we then applied a Miller Tans approach to the Beech Island data (figure 6 in revised manuscript). While this approach also has weaknesses, they are different than those of the Keeling analysis. The Miller-Tans approach using the Tennerife data produces similar results to the Keeling plot analysis, and should address the reviewers concern about the background assumptions at Beech Island.*

**Comment 15**

P18. ,l4: cite original references. They may also give uncertainties for Table 1.

***Response to Comment 15:*** *This section of the text has been removed and replaced by our analysis of the Beech Island data relative to Tennerife (discussed in the above comment). We have, however, consulted and cited original references for Table 1 (discussed in the response to comment 16).*

**Comment 16**

Table 1: Why are the uncertainties for the OH reaction unknown? Please check original references, they should be given there. Where do the uncertainty estimates on the source signatures come from?

***Response to Comment 16:*** *We remade Table 1, and included estimates for the isotopic signatures of the main sources. Further, we have consulted both Röckmann et al (1998) and Stevens et al. (1980) for CO+OH sink fractionation factors, and uncertainty estimates. We could* *not find a clear ± uncertainty stated in either publication. Therefore, have reported the full range of fractionation factors as reported by both of these references as the uncertainty on these factors. We have reported the Brenninkmeijer et al. (1999) recommended values for the factors, and explained the values and uncertainties in the foot note.*

**Comment 17**
Table 2: Add statement that this table is for the Indianapolis measurements. Can you provide the equation that converts D14C to XCO2 in section 2.4?

***Response to Comment 17:*** *We have added the requested statement to the Table 2 caption. We have added the equation (and description of variables) to section 2.4.*

**Comment 18**
Figure 4: Indicate which data were taken for summer and winter periods.

***Response to Comment 18:*** *We have added these arrows to figure 4 as requested, as well as described them in the caption.*

**Comment 19**
Figure 5: See arguments above on the suitability of the Keeling plot approach.

***Response to Comment 19:*** *We have added a Miller Tans Analysis using Tennerife as a background (and added this analysis as figure 6) as detailed above in Comment 14. We believe our response to Comment 14 has addressed this comment about figure 5.*

**References**

Bräunlich, M.: Study of atmospheric carbon monoxide and methane using isotopic analysis, PhD, Institute of Environmental Physics, Rupertus Carola University, Heidelberg, Germany, 2000.

Brenninkmeijer, C. A. M., Röckmann, T., Braunlich, M., Jockel, P., and Bergamaschi, P.: Review of Progress in Isotope Sutdies of Atmospheric Carbon Monoxide, ChemoSphere- Global Change Science, 1, 33-52, 1999.

Röckmann, T., Brenninkmeijer, C. A. M., Saueressig, G., Bergamaschi, P., Crowley, J. N., Fischer, H., and Crutzen, P. J.: Mass-Independent Oxygen Isotope Fractionation in Atmospheric CO as a Result of the Reaction CO+OH, Science, 281, 544-546, 10.1126/science.281.5376.544, 1998.

Stevens, C. M., Kaplan, L., Gorse, R., Durkee, S., Compton, M., Cohen, S., and Bielling, K.: The kinetic isotope effect for carbon and oxygen in the reaction CO + OH, Int. J. Chem. Kinet., 12, 935-948, 10.1002/kin.550121205, 1980.

**Response to Reviewer 2**

*We thank the Reviewer for taking the time to provide comments to our revised manuscript. We have responded to the comments the Reviewer made below in italicized text.*

**Comment 1**
Figures 1
It is better to change the background color of the balloon of station 1 (dark blue) to lighter color (sky blue).

***Response to Comment 1:*** *Completed as Requested*

**Comment 2**
Figure S1(b) horizontal axis
Could you change the scale of the horizontal axis? It seems to be too large.

***Response to Comment 2:*** *Completed as Requested*

**Comment 3**
Figure S1(c) caption
δ13O → δ13C

***Response to Comment 3w:*** *Completed as Requested*

**Comment 4**
Page 5 Section 2.1
Could you add information about the amount of forest area in the total land area and vegetation type?

***Response to Comment 4:*** *We have provided the land cover percentage of leafy trees and shrubs as described by the MEGAN 2.1 plant functional type data. These plants are the primary producers of biogenic VOC's such as isoprene, and therefore the most relevant to our study. These data are included in the supplement, in figure S1. Our revised language to section 2.1 reads:*

*"It is surrounded by mostly agricultural land, interspersed with trees and foliage. Broadleaf and deciduous foliage comprises approximately 25-100% of the vegetative cover, both inside and outside of Indianapolis' borders (figure 1, Guenther et al. (2012), figure S1). "*

**Comment 5**
Page 7 Section 2.2

We need more information about Beech Island; such as population and population density, land cover use, the amount of forest area in the total land area, vegetation type, and temperature. Please write the sampling period, too.

***Response to Comment 5:*** *We have added population and population density for Beech Island and the surrounding region. As with Indianapolis in section 2.1, we have included the vegetative ground cover for Beech Island from the MEGAN 2.1 model. We have also included temperature ranges. Our revised language to Section 2.2 reads:*

*"The Beech Island sampling site is located approximately 5.5 km from the town of Beech Island, in a sparsely populated region of South Carolina. The climate is temperate with annual temperature varying between 6°C and 28°C (NOAA Center for Environmental Information, https://www.ncdc.noaa.gov/). The town of Beech Island has a population of approximately 8,500, and the surrounding region population density is about 150 people per square mile (US Census Bureau, www.census.gov). However, the sampling site is 15.5 miles from Augusta, Georgia, a metropolitan center of approximately 200,000 (US Census Bureau, www.census.gov). Deciduous, broad leaf trees and shrubs compose ~80% of the ground cover for much of the area surrounding the sampling site (MEGAN 2.1, Guenther et al., 2012, Figure S2)."*

**Comment 6**
Page 17, Line 21
Densely forested → please show us the amount of forest area in the total land area and vegetation type.

***Response to Comment 6:*** *We have addressed this comment through our response and corrections in Comment 5 above.*

**Comment 7**
Page 19, Line 5
Could you add some information about the fossil fuel use in Beech Island (compare the fossil fuel use between summer and winter) to support and/or deepen your explanation?

***Response to Comment 7:*** *We attempted to find this data for Beech Island, but were unable to do so. We could find only yearly energy production by various power plants and utilities for South Carolina and Georgia. Those data did not provide actual fossil fuel use, nor could we find reasonable estimates for gasoline or diesel use, which would be necessary since the majority of fossil fuel produced CO is attributable to the mobile sector.*

*Further, our discussion in this section is focused on the change from winter to summer. As stated above, the bulk of fossil CO emissions are produced by vehicles (e.g. US Environmental Protection Agency National Emissions Inventory 2014, https://www.epa.gov/air-emissions-inventories/2014-national-emissions-inventory-nei-data). While some seasonality in fossil CO production could certainly alter the CO budget slightly, it would not account for a significant reduction in 18O for the combined local source signatures, which our analysis suggests. Further,* *to address a comment from Reviewer 1, we have added a seasonally varying background to the Beech Island analysis using Tennerife data published by Bräunlich (2000), which accounts for seasonal changes in the CH4 oxidation source of CO and the OH sink (discussed in detail in the text). This added analysis supports our interpretation that the primary driver of the winter to summer CO source signature change is most likely the VOC oxidation source.*

## References

Bräunlich, M.: Study of atmospheric carbon monoxide and methane using isotopic analysis, PhD, Institute of Environmental Physics, Rupertus Carola University, Heidelberg, Germany, 2000.

Guenther, A. B., Jiang, X., Heald, C. L., Sakulyanontvittaya, T., Duhl, T., Emmons, L. K., and Wang, X.: The Model of Emissions of Gases and Aerosols from Nature version 2.1 (MEGAN2.1): an extended and updated framework for modeling biogenic emissions, Geosci. Model Dev., 5, 1471-1492, 10.5194/gmd-5-1471-2012, 2012.

## Title:

# An improved estimate for the $\delta^{13}C$ and $\delta^{18}O$ signatures of carbon monoxide produced from atmospheric oxidation of volatile organic compounds

## Authors:

*Isaac J Vimont[1,2,3], Jocelyn C. Turnbull[3,4], Vasilii V. Petrenko[5], Philip F. Place[5], Colm Sweeney[2], Natasha Miles[6], Scott Richardson[6], Bruce H. Vaughn[1], James W.C. White[1]

1. Institute of Arctic and Alpine Research, Boulder, CO USA
2. National Oceanic and Atmospheric Administration, Global Monitoring Division, Boulder, CO USA
3. CIRES, University of Colorado, Boulder, CO, USA
4. GNS Science, Lower Hutt, New Zealand
5. University of Rochester Earth and Environmental Science Department, Rochester, NY, USA
6. Pennsylvania State University, College Station, PA USA

* Corresponding Author: Isaac.vimont@colorado.edu

## Abstract:

Atmospheric carbon monoxide (CO) is a key player in global atmospheric chemistry and a regulated pollutant in urban areas. Oxidation of volatile organic compounds (VOCs) is an important component of the global CO budget and has also been hypothesized to contribute substantially to the summertime urban CO budget. In principle, stable isotopic analysis of CO could constrain the magnitude of this source. However, the isotopic signature of VOC-produced CO has not been well quantified, especially for the oxygen isotopes. We performed measurements of CO stable isotopes on air samples from two sites around Indianapolis, USA over three summers to investigate the isotopic signature of VOC-produced CO. One of the sites is located upwind of the city, allowing us to quantitatively remove the background air signal and isolate the urban CO enhancements as well as the isotopic signature of these enhancements. In addition, we use measurements of $\Delta^{14}CO_2$ in combination with the $CO:CO_2$ emission ratio from fossil fuels to constrain the fossil fuel-

**Deleted:** ¶ ... [1]
**Style Definition** ... [10]
**Style Definition** ... [9]
**Style Definition** ... [8]
**Style Definition** ... [7]
**Style Definition** ... [6]
**Style Definition** ... [5]
**Formatted** ... [11]
**Formatted** ... [12]
**Formatted** ... [13]
**Formatted** ... [14]
**Formatted** ... [15]
**Formatted** ... [16]
**Formatted** ... [17]
**Formatted** ... [18]
**Formatted** ... [19]
**Formatted** ... [20]
**Formatted** ... [21]
**Formatted** ... [22]
**Formatted** ... [23]
**Formatted** ... [24]
**Formatted** ... [25]
**Formatted** ... [26]
**Formatted** ... [27]
**Formatted** ... [28]
**Formatted** ... [29]
**Formatted** ... [30]
**Formatted** ... [31]
**Formatted** ... [32]
**Formatted** ... [33]
**Formatted** ... [34]
**Formatted** ... [35]
**Formatted** ... [36]
**Formatted** ... [37]
**Formatted** ... [38]
**Formatted** ... [39]
**Formatted** ... [40]
**Formatted** ... [41]
**Formatted** ... [2]
**Formatted** ... [3]
**Formatted** ... [4]

derived CO and thereby isolate the VOC-derived component of the CO enhancement. Combining these measurements and analyses, we are able to determine the carbon and oxygen isotopic signatures of CO derived from VOC oxidation as -32.8‰ ± 0.5‰ and 3.6‰ ± 1.2‰, respectively. Additionally, we analyzed CO stable isotopes for one year at Beech Island, South Carolina, USA, a site thought to have large VOC-derived contributions to the summertime CO budget. The Beech Island results are consistent with isotopic signatures of VOC-derived CO determined from the Indianapolis data. This study represents the first direct determination of the isotopic signatures of VOC-derived CO and will allow for improved use of isotopes in constraining the global and regional CO budgets.

## 1. Introduction

The global carbon monoxide (CO) budget, along with regional and local CO budgets, remain uncertain (e.g. Holloway et al., 2000; Duncan et al., 2007; Granier et al., 2011; Zhou et al., 2017; Strode et al., 2018). CO stable isotope measurements can aid in the partitioning of the sources of CO, and hence improve global and regional budgets (e.g. Brenninkmeijer et al., 1999). Several studies have incorporated stable isotopes of CO to independently constrain the sources of CO (Manning et al., 1997; Bergamaschi et al., 2000; Park et al., 2015). On the global scale, carbon monoxide (CO) has four major sources which include biomass/biofuel burning, oxidation of methane ($CH_4$), the incomplete combustion of fossil fuels and the oxidation of volatile organic compounds (VOCs) (Logan et al., 1981; Duncan et al., 2007; Table 1). These sources are balanced by the oxidation of CO by the hydroxyl radical (OH) and a small soil sink, resulting in a residence time of CO in the atmosphere that is ≈2 months on average but varies by location and time of year (Logan et al., 1981; Duncan et al., 2007). Each CO source has a unique isotopic signature which is determined by the isotopic signature of the source material (e.g., $CH_4$) and the process(es) by which the CO is formed. The carbon isotopic signature of methane-derived CO is much more negative than that of the other sources, largely due to the depleted carbon isotopic signature of methane (Table 1, Brenninkmeijer et al., 1999). The oxygen isotopic signature can help distinguish between combustion (fossil fuel and biomass burning) and oxidation sources (methane and

**Deleted:** ¶

**Deleted:** -33.6‰ ± 1.0‰

**Formatted:** Font color: Text 1

**Deleted:**

**Formatted:** Font color: Text 1

**Deleted:** 3‰ ±

**Formatted:** Font color: Text 1

**Deleted:** 1.3‰ ± 2..7‰,

**Formatted:** Font color: Text 1

**Formatted:** Font: 10 pt, Font color: Text 1

**Formatted:** Font color: Text 1

**Formatted:** Font: 10 pt, Font color: Text 1

**Formatted:** Font color: Text 1

**Deleted:** mole fraction of

**Deleted:** 2

VOC-derived CO), with combustion sources having more positive isotopic values than oxidation sources (Table 1, Brenninkmeijer et al., 1999).

The isotopic signatures of CO from fossil fuel combustion and biomass burning have been relatively well quantified (Table 1). The $^{13}$CO produced by oxidation of methane has also been well quantified, although the C$^{18}$O signature remains more uncertain (Brenninkmeijer et al., 1999). However the isotopic signatures of CO produced by the oxidation of volatile organic compounds (VOCs) remain poorly known ( Brenninkmeijer and Röckmann (1997), Brenninkmeijer et al. (1999), and Gros et al. (2001). The carbon isotopic signature of CO produced by oxidation of VOCs has been estimated to around -32‰, from atmospheric measurements (Stevens and Wagner, 1989) and through analysis of the isotopic signature of isoprene, accounting for fractionation during the oxidation reaction (Sharkey et al., 1991; Conny and Currie, 1996, Conny et al., 1997).

Only two prior studies have tried to estimate the oxygen isotopic signature of VOC-derived CO, yielding very different values: 0‰ (Brenninkmeijer and Röckmann, 1997) or 15‰ (Stevens and Wagner, 1989), with a reported uncertainty of “greater than 3‰” (e.g. Gros et al., 2001; Table 1). As VOC oxidation is a major source of CO on global and regional scales (e.g. Logan et al., 1981; Guenther et al., 1995; Duncan et al., 2007), the large uncertainty in the associated isotopic signatures presents a major obstacle to using isotopes in investigations of the atmospheric CO budget.

Our study uses a new set of measurements to evaluate the carbon and oxygen isotopic signatures of CO produced from VOCs by analyzing the urban CO isotopic enhancements at Indianapolis, IN, USA. An urban setting for determining the isotopic signature of CO from oxidized VOCs may not seem like an obvious choice, because of the large CO enhancements from fossil fuel burning (EPA, 2014 , Mak and Kra, 1999; Popa et al., 2014; Turnbull et al., 2015; Vimont et al., 2017; Turnbull et al., 2018). However, previous literature suggests that during the summer months there may also be a large urban source of CO from the oxidation of VOCs, likely from biogenic sources (Guenther et al., 1993, 1995; Carter and

**Deleted:** ¶

**Formatted:** Font: 10 pt, Font color: Text 1

**Formatted:** Font color: Text 1

**Deleted:** Brenninkmeijer et al., 1999;

**Formatted:** Font: 10 pt, Font color: Text 1

**Formatted:** Font color: Text 1

**Formatted:** Font: 10 pt, Font color: Text 1

**Formatted:** Font color: Text 1

**Formatted:** Position: Horizontal: Center, Relative to: Margin, Vertical: 0", Relative to: Paragraph, Wrap Around

**Formatted:** Page Number

**Formatted:** Page Number

**Deleted:** ¶

Atkinson, 1996; Kanakidou and Crutzen, 1999; Cheng et al., 2017, Turnbull et al. (2006) Miller et al. (2012)).

**Formatted:** Font: 10 pt, Font color: Text 1

**Formatted:** Font color: Text 1

Some of these studies aimed to quantify fossil fuel $CO_2$ enhancements ($CO_{2FF}$) by using CO enhancements as a proxy measurement but noted that the ratio of CO:$CO_{2FF}$ enhancements was higher in the summer than the winter at several sites in the eastern United States (Turnbull et al., 2006; Miller et al., 2012). A higher CO:$CO_{2FF}$ ratio is inconsistent with a stronger sink process such as an increase in OH during the summer months. Instead, a seasonal increase in a non-fossil fuel source provides the most likely explanation for the increase in the CO:$CO_{2FF}$ ratio. These studies hypothesized, but could not confirm, that oxidation of VOCs may be the source of this summertime increase in CO:$CO_{2FF}$ ratio.

**Formatted:** Font: 10 pt, Font color: Text 1

**Formatted:** Font color: Text 1

Studies that model the effect of CO sources on the measured CO mole fraction have also indicated that oxidation of VOCs (particularly from biogenic sources) contributes significantly to the global and regional CO budget (e.g. Kanakidou and Crutzen, 1999). Isoprene and terpene emissions from broadleaf species have been shown to be a large source of VOCs (Guenther et al., 1995; Helmig et al., 1998; Harley et al., 1999), particularly in the southeastern United States (e.g. Chameides et al., 1988). Griffin et al. (2007) used the Caltech Atmospheric Chemistry Mechanism to investigate CO production by VOC oxidation at a regional scale in the United States. Their model determined that VOC oxidation could provide as much as 10-20% of the CO observed in parts of New England, but in a heavily polluted region such as the Los Angeles Basin, the percentage was much lower, on the order of 1% or less. Cheng et al. (2017) measured $O_3$ and CO mole fractions and then modeled CO production from the various sources using $O_3$-to-CO ratios. Their model suggested the oxidation of isoprene might equal or exceed the total anthropogenic production of CO within the urban region of Baltimore, USA.

**Formatted:** Font: 10 pt, Font color: Text 1

**Formatted:** Font color: Text 1

This study focuses mainly on measurements from the Indianapolis FLUX project (INFLUX). INFLUX provides a sampling methodology that allows for quantitative removal of background air signals, which isolates the urban enhancement, and simplifies the source and sink budget analysis (Turnbull et al., 2015; Vimont et al., 2017; Turnbull et al., 2018). Measurements are made not only at tower sites within and downwind of the city, but also

**Deleted:** 4

directly upwind of the city, so that the changes in CO mole fraction and isotopic values due to the urban influence can be isolated. The short transit time of air across the city means that removal of CO by OH (and the associated impact on the isotopic signature) can be ignored. Methane oxidation is similarly minimal in the short transit time, and biomass burning is known to be very small within the urban confines.

In addition to the CO mole fraction and stable isotopic measurements, $^{14}CO_2$ measurements were also performed on the INFLUX samples, allowing for accurate quantification of $CO_{2FF}$ (Turnbull et al., 2015). This allowed us to partition the urban CO enhancement between fossil fuel and VOC-derived sources. We were then able to isolate the carbon and oxygen isotopic signatures of CO produced from VOC oxidation.

To further examine our estimates of the isotopic signatures of CO produced from oxidized VOCs, we analyzed bi-monthly samples from a site at Beech Island, South Carolina, USA. This site is heavily forested and the CO mole fraction at this site should be strongly influenced by isoprene oxidation during the summer. By analyzing the isotopic signatures at this site, we were able to compare the Beech Island isotopic signals to our estimates for VOC-derived CO.

## 2. Methods

### *2.1 Tower Sampling at Indianapolis*

Indianapolis, Indiana is a metropolitan area of over one million people in the Mid-West region of the United States. It is surrounded by mostly agricultural land, interspersed with trees and foliage. Broadleaf and deciduous foliage comprises approximately 25-100% of the vegetative cover, both inside and outside of Indianapolis' borders (Figure 1, Guenther et al. (2012), Figure S1). It has hot summers (25 to 30°C) and cold winters (-8 to 1°C) that result in a distinct growing season, with the winter being relatively devoid of biogenic fluxes of CO and $CO_2$ (Turnbull et al., 2015). INFLUX aims to develop and assess methods

**Deleted:** ¶

**Formatted:** Font: 10 pt, Font color: Text 1

**Formatted:** Font color: Text 1

**Formatted:** Font: 10 pt, Font color: Text 1

**Formatted:** Font color: Text 1

**Formatted:** Font: 10 pt, Font color: Text 1

**Formatted:** Font color: Text 1

**Formatted:** Level 1

**Formatted:** Font: 10 pt, Font color: Text 1

**Formatted:** Font color: Text 1

**Formatted:** Level 1

**Formatted:** Font: 10 pt, Font color: Text 1

**Formatted:** Font color: Text 1

**Formatted:** Font color: Text 1

**Deleted:** its

**Formatted:** Font color: Text 1

**Deleted:** figure

**Formatted:** Font color: Text 1

**Deleted:** ).

**Formatted:** Font color: Text 1

**Deleted:** □

**Formatted:** Font color: Text 1

**Deleted:** □

**Formatted:** Font color: Text 1

**Formatted:** Position: Horizontal: Center, Relative to: Margin, Vertical: 0", Relative to: Paragraph, Wrap Around

**Formatted:** Page Number

**Formatted:** Page Number

for determining urban greenhouse gas emissions. CO, though not a primary greenhouse gas, is measured and used as a tracer for fossil fuel $CO_2$ emissions and to provide information for source attribution.

INFLUX has twelve instrumented towers within and around the urban boundary (Miles et al., 2017). The flask-sampling regime was described in detail by Vimont et al. (2017) and Turnbull et al. (2015). In brief, discrete hourly-integrated air samples are collected at six of the towers, although the integrated samplers (Turnbull et al., 2012) are moved between the twelve towers occasionally. Three of the towers have had continuous flask samples and were sampled for CO isotopes (towers 1-3, Turnbull et al., 2015; Miles et al., 2017; Turnbull et al., 2019) approximately six days per month, during the early afternoon when the strongest boundary layer mixing occurs (19:00 UTC, 14:00 local). Stable isotope measurements of CO were made on samples collected from July 2013 to July 2015. In this paper, we consider only the summer samples that were collected in July and August 2013, May-August 2014, and May – July 2015 (inclusive) from tower 1 (121 m above ground level (AGL), 39.5805° N, 86.4207° W), and tower 2 (136 m AGL, 39.7978° N, 86.0183° W) (Figure 1). The winter samples were examined in a previous study (Vimont et al., 2017) that determined in winter, CO enhancements in Indianapolis are primarily derived from fossil fuel combustion; the CO isotopic signature of the fossil fuel combustion source was also constrained. Though summer samples were also collected at tower 3 (39.7833° N, 86.1652° W), its proximity to Indianapolis' downtown district and its lower elevation above the ground (54 m AGL) meant that the signals there were strongly dominated by fossil fuel combustion sources, even in summer. Tower 2, located to the east of the urban region, was the ideal candidate for determining the isotopic signature of the oxidized VOC source of CO. Tower 2 "sees" a more mixed signal of urban and suburban sources including both fossil fuel sources and the influence of the substantial suburban vegetation (Turnbull et al., 2015; Turnbull et al., 2018).

For the samples in this study, collection was done when the wind was approximately from the west, so that Tower 1 provides a clean-air background for the towers further to the east (Turnbull et al., 2012). Tower 2 is east of the city, with only a small residential influence

**Deleted:** ¶

**Formatted:** Font: 10 pt, Font color: Text 1

**Formatted:** Font color: Text 1

**Formatted:** Font: 10 pt, Font color: Text 1

**Formatted:** Font color: Text 1

**Deleted:** figure

**Formatted:** Font color: Text 1

**Formatted:** Font: 10 pt, Font color: Text 1

**Formatted:** Font color: Text 1

**Deleted:** 6

and one major highway nearby, with significant foliage within its influence footprint (Turnbull et al., 2015). The distance between towers 1 and 2 is 51 km, and the average wind speed during the period sampled for this study was 4.4 m $s^{-1}$, which results in an average transit time of air from tower 1 to tower 2 of 3.2 hours.

The air samples were collected in Portable Flask Packages (PFP's) provided by the National Oceanic and Atmospheric Administration Global Reference Network (NOAA GRN)(https://www.esrl.noaa.gov/gmd/ccgg/aircraft/sampling.html). One-hour integrated samples were collected; this sampling regime allows for smoothing of very short-term variability that may be difficult to interpret (Turnbull et al., 2012). NOAA's Earth System Research Laboratory (ESRL) provides the infrastructure and logistical support for these PFP's, and the CO mole fraction measurements used in this study (Novelli et al., 2003). $^{14}CO_2$ measurements were performed at GNS Science with support from University of Colorado INSTAAR (Turnbull et al., 2015).

### *2.2 Tower Sampling at Beech Island, South Carolina*

Beech Island, South Carolina, USA (33.4057 °N, 81.8334°W) is a tall tower (305m AGL) site in the NOAA Global Greenhouse Gas Reference Network (GGGRN). The Beech Island sampling site is located approximately 5.5 km from the town of Beech Island, in a sparsely populated region of South Carolina. The climate is temperate with annual temperature varying between 6°C and 28°C (NOAA Center for Environmental Information, https://www.ncdc.noaa.gov/). The town of Beech Island has a population of approximately 8,500, and the surrounding region population density is about 150 people per square mile (US Census Bureau, www.census.gov). However, the sampling site is 15.5 miles from Augusta, Georgia, a metropolitan center of approximately 200,000 (US Census Bureau, www.census.gov). Deciduous, broad leaf trees and shrubs compose ~80% of the ground cover for much of the area surrounding the sampling site (Guenther et al., 2012, Figure S2). Samples for CO stable isotopes were collected approximately bi-monthly for one year (April 2015 – March 2016) from this site. This site uses "grab sampling" rather than the integrating sampling used at the INFLUX towers. Flasks are flushed and then filled

**Deleted:** ¶

**Formatted:** Font: 10 pt, Font color: Text 1

**Formatted:** Font color: Text 1

**Deleted:** https://www.esrl.noaa.gov/gmd/ccgg/aircraft/sampling.html).

**Formatted:** Font color: Text 1

**Deleted:** b

**Formatted:** Font: 10 pt, Font color: Text 1

**Formatted:** Font color: Text 1

**Formatted:** Font: 10 pt, Italic, Font color: Text 1

**Formatted:** Font color: Text 1

**Formatted:** Font color: Text 1

**Formatted:** Position: Horizontal: Center, Relative to: Margin, Vertical: 0", Relative to: Paragraph, Wrap Around

**Formatted:** Page Number

**Formatted:** Page Number

and pressurized over about a two minute period. Flasks are measured by the same methods as the INFLUX samples. However, although $^{14}CO_2$ measurements are made on some flasks from this site, limitations on the available air in each flask mean that the CO stable isotopes were measured on different flasks (collected on different dates) than the $^{14}CO_2$ measurements.

### *2.3 Stable Isotope Analysis*

The stable isotopic measurement procedure is described in detail in Vimont et al. (2017). Briefly, the air is extracted from the PFP by vacuum transfer through a cold loop trap at -70° C that removes water vapor. Next, a mass flow controller is used to regulate the flow of the sample through a second cryogenic trap at -196° C that removes $CO_2$, $N_2O$, and any other condensable species. The remaining air is passed through acidified $I_2O_5$ suspended on a silica gel matrix (Schutze's reagent, (Schutze, 1944)) that quantitatively oxidizes CO to $CO_2$, adding an oxygen with a consistent isotopic signature. The sample passes through a second cold loop trap (-70° C) to remove any traces of sulfuric acid that has evolved from the reagent and finally the CO-derived $CO_2$ is trapped on a third cryogenic trap (-196° C) while the remaining gasses are pumped away. The CO-derived $CO_2$ is then transferred to a cryogenic focusing trap and finally released through a GC column (PoraBond Q) to the isotope ratio mass spectrometer (GV Instruments IsoPrime 5KeV).

Following convention, we use delta notation to report our isotopic results:

$$\delta^{13}C_{VPDB} = \left(\frac{R_s}{R_{VPDB}} - 1\right) * 10^3‰ \qquad (1)$$

where $R_s$ is the ratio of $^{13}C$ to $^{12}C$ in the sample and $R_{VPDB}$ is the ratio of $^{13}C$ to $^{12}C$ in the international standard Vienna Pee Dee Belemnite. The same notation describes $\delta^{18}O$ except the international standard of reference is Vienna Standard Mean Ocean Water (VSMOW). Because we are oxidizing CO to $CO_2$ in this analysis, we correct our $CO_2$ $\delta^{18}O$ data to account for the added oxygen, as described in Stevens and Krout (1972), Brenninkmeijer (1993), and Mak and Yang (1998):

$$\delta^{18}O_{CO}=2\delta^{18}O_{CO_2}-\left(2\delta^{18}O_{CO_2std}-\delta^{18}O_{COstd}\right) \qquad (2)$$

**Deleted:** ¶

**Formatted:** Font: 10 pt, Font color: Text 1

**Formatted:** Font color: Text 1

**Formatted:** Level 1

**Formatted:** Font: 10 pt, Font color: Text 1

**Formatted:** Font color: Text 1

**Deleted:** ⍰

**Formatted:** Font color: Text 1

**Formatted:** Font: 10 pt, Font color: Text 1

**Formatted:** Font color: Text 1

**Formatted:** Font: 10 pt, Font color: Text 1

**Deleted:** 13-carbon

**Deleted:** 12-carbon

**Deleted:** 13-carbon

**Deleted:** 12-carbon

**Deleted:** ⍰

**Formatted:** Font color: Text 1

**Deleted:** ⍰

**Formatted:** Font color: Text 1

**Formatted:** Font color: Text 1

**Formatted:** Font color: Text 1

**Formatted:** Font: 10 pt, Font color: Text 1

**Deleted:** 8

where the subscript CO indicates the original $\delta^{18}O$ signature of the sample, $CO_2$ indicates the $\delta^{18}O$ of the $CO_2$ measured in the mass spectrometer, $CO_2std$ indicates the $\delta^{18}O$ of the $CO_2$ measured on the standard gas and $CO_{std}$ indicates the calibrated $\delta^{18}O$ of the CO in the same standard gas (standard gas procedure was described in Vimont et al. (2017)). Once the samples have been analyzed in the mass spectrometer, a correction for the $^{17}O$ contribution to the $\delta^{13}CO$ measurement is applied to the data based on the recommendations of Brand et al. (2009) (Vimont et al., 2017). This correction is required because $^{13}CO$ and $C^{17}O$ are indistinguishable in our mass spectrometer. The 1σ repeatability over two years for our analysis system is 0.23‰ for $\delta^{13}C$ and 0.46‰ for $\delta^{18}O$. For a more complete description of system performance, see Vimont et al. (2017).

We note that a significant deviation from the standard $CO_2$ $^{17}O$ correction has been observed and quantified for CO (Röckmann and Brenninkmeijer, 1998; Röckmann et al., 1998). This so called "$^{17}O$ excess", or $\Delta^{17}O$, is a result of mass-independent fractionation (MIF) that arises in OH photolytic formation, which in turn affects CO during removal by OH (Röckmann et al., 1998b; Huff and Thiemens, 1998). Ozonolysis of VOC's also contributes to $^{17}O$ excess, (Röckmann et al., 1998 a,b). The source of CO from ozonolysis of VOC's is discussed in more detail in section 3.4. The combined $\Delta^{17}O$ from these processes can introduce error of up to 0.35‰ in the corrected $\delta^{13}C$ values, and the error is only quantifiable by measuring $\delta^{17}O$ (Röckmann and Brenninkmeijer, 1998b). However, though we do not measure $\delta^{17}O$ for our samples, our data analysis approach (section 2.5) eliminates the need for this correction because both background and urban samples will see similar $\Delta^{17}O$ effects. Additionally, because of the short transit time between our background and polluted tower sites (3.2 hours, section 2.1), and the long lifetime of most VOC ozonolysis relative to OH oxidation (Atkinson and Arey, 2003a), we expect any effect of ozonolysis produced $\Delta^{17}O$ error to our $\delta^{13}C$ measurements to be insignificant relative to our measurement uncertainty.

*2.4 Radiocarbon $CO_2$ Analysis*

**Deleted:** ¶

**Deleted:** ⍰

**Formatted:** Font color: Text 1

**Deleted:** ⍰

**Deleted:** ⍰

**Formatted:** Font color: Text 1

**Formatted:** Font color: Text 1

**Deleted:** ⍰

**Formatted:** Font color: Text 1

**Deleted:** ⍰

**Formatted:** Font color: Text 1

**Deleted:** ⍰

**Deleted:** ⍰

**Formatted:** Font color: Text 1

**Formatted** ... [44]

**Formatted:** Font color: Text 1

**Deleted:** , particularly in the high northern latitudes

**Formatted:** Font color: Text 1

**Deleted:** s

**Deleted:** s

**Formatted:** Font color: Text 1

**Deleted:** but this source of $^{17}O$ is difficult to interpret due to the extreme $\delta^{18}O$ enrichment that ... [45]

**Deleted:** is...effect ...$^{17}O$ from these processes can ... [46]

**Formatted:** Font color: Text 1

**Deleted:** and is ...nly quantifiable by measuring δ ... [47]

**Formatted:** Font color: Text 1

**Deleted:** ⍰

**Formatted:** Font color: Text 1

**Commented [Vas Petre1]:** Although this ... [48]

**Deleted:** .

**Formatted:** Font: 10 pt, Font color: Text 1

**Formatted** ... [49]

**Formatted** ... [50]

**Formatted:** Font color: Text 1

**Formatted** ... [42]

**Formatted** ... [43]

Each of the INFLUX samples analyzed for the stable isotopes of CO was also analyzed for $^{14}CO_2$. $^{14}CO_2$ is the best tracer for fossil fuel produced $CO_2$ because fossil fuels contain no $^{14}C$ (Levin et al., 2003; Turnbull et al., 2006). $^{14}CO_2$ measurements were made by extracting $CO_2$ from whole air in each flask at INSTAAR, University of Colorado, followed by graphitization and AMS $^{14}C$ measurement at GNS Science, New Zealand (Turnbull et al., 2015b). $CO_2ff$ was determined for each sample using Tower 1 as background, and the $^{14}CO_2$ results for these and other INFLUX flask samples were reported in detail by Turnbull et al (2015) and Turnbull et al (2019). $^{14}C$ measurements of $CO_2$ are reported as $\Delta^{14}C$, or the permil deviation of the measured $^{14}C$ from a standard material, corrected for fractionation effects and radioactive decay between sampling and measurement (Stuiver and Polach, 1977; Turnbull et al., 2015). The conversion of the $^{14}CO_2$ measurements to $CO_2ff$ enhancements is done by:

$$X_{CO2ffenh} = \frac{X_{CO2obs}\,(\Delta_{obs}-\Delta_{bg})}{(\Delta_{ff}-\Delta_{bg})} - \frac{X_{CO2other}(\Delta_{other}-\Delta_{bg})}{(\Delta_{ff}-\Delta_{bg})} \qquad (3)$$

(Turnbull et al., 2015). $X_{CO2ffenh}$ is calculated using the observed ($\Delta$obs) and background ($\Delta$bg) $\Delta^{14}C$ values and the observed CO2 mole fraction ($X_{CO2obs}$). $\Delta_{ff}$ is the $\Delta^{14}C$ value of fossil fuel $CO_2$ (by definition -1000‰). $X_{CO2other}$ is a small correction that applied and consists primarily of sources from the nuclear industry and heterotrophic respiration Typical values for $X_{CO2other}$ are 0. equation 2 - 0.5 ppm when a continental background is used (e.g.in Turnbull et al., 2006; Miller et al., 2012; Turnbull et al., 2015). The measurement precision of ~1.8‰ results in uncertainties in $CO_{2FF}$ of better than 1 µmol:mol $CO_{2FF}$ for these samples.

*2.5 Regression Plot Analysis*

At Indianapolis, the CO measured at tower 2 is typically 20 nmol:mol higher than the background CO of ~150 nmol:mol at tower 1. It is necessary to remove the background signal from the polluted tower to accurately constrain the urban CO signals. Using the method described by Miller and Tans (2003), we calculate the isotopic signature of the urban source:

**Deleted:** ¶

**Deleted:** 8

**Formatted** ... [51]

**Formatted:** Centered

**Formatted** ... [52]

**Formatted** ... [53]

**Formatted:** Level 1

**Formatted:** Font: 10 pt, Font color: Text 1

**Formatted:** Font color: Text 1

**Formatted:** Font: 10 pt, Font color: Text 1

**Deleted:** 10

$$\delta_s=\frac{\left(\delta_{meas}X_{CO_{meas}}-\delta_{bkg}X_{CO_{bkg}}\right)}{\left(X_{CO_{meas}}-X_{CO_{bkg}}\right)} \qquad (4)$$

where $\delta_s$ is the $\delta^{13}C$ or $\delta^{18}O$ of the urban source (Figure 2), X indicates the mole fraction and the subscript “meas” indicates the $\delta^{13}C$ (or $\delta^{18}O$) and CO mole fraction measured at tower 2. The subscript “bkg” indicates the $\delta^{13}C$ (or $\delta^{18}O$) and CO mole fraction measured at tower 1. In order to obtain a best-fit solution using (4) for all the data, we regressed the numerator against the denominator using an ordinary least squares (model 1) Y|X approach (Isobe et al.,1990; Zobitz et al., 2006).

To account for uncertainty in our measurements, we used a Monte Carlo technique. Using the propagated measurement uncertainties, we assigned an error distribution to each point. We assumed a normally distributed error curve based on QQ plot analysis of our data against a synthetic normally distributed data set (not shown). This analysis allows us to assess if two data sets have the same distribution. 10,000 regressions were run, randomly selecting values for each data point from that point’s error distribution. The reported slopes are the median values from the 10,000 regressions. The reported errors on the slope are 1σ for the slopes of each simulation.

At the Beech Island measurement site, no local background measurement site with CO isotope measurements exists. Therefore, we performed a Keeling plot analysis, as well as a Miller-Tans plot analysis using monthly averaged CO mole-fraction, $\delta^{13}C$, and $\delta^{18}O$ data from Izaña, Tenerife in the Canary Islands (28ºN, 16ºW, 2370 masl) as a background for Beech Island (Bräunlich, 2000, Table S4). The Beech Island Miller Tans analysis was performed in the same manner as the Indianapolis source signatures, described above.

In the Keeling plot approach, isotopic measurements are plotted against the reciprocal of the mole fraction (Keeling, 1958). This method uses the relationship:

$$\delta_{obs}=\delta_s+M(X_{CO}^{-1}) \qquad (5)$$

where $\delta_{obs}$ is the observed $\delta^{13}C$ or $\delta^{18}O$ at the measurement site, M is the slope determined from a regression of the data, and $X_{CO}$ is the observed CO mole fraction. $\delta_s$ is the intercept

**Deleted:** ¶ ... [54]
**Deleted:** (3)
**Formatted** ... [57]
**Deleted:** ⍰
**Formatted** ... [59]
**Deleted:** ⍰
**Formatted** ... [60]
**Deleted:** ⍰
**Formatted** ... [58]
**Formatted** ... [61]
**Deleted:** figure
**Formatted** ... [62]
**Deleted:** ⍰
**Formatted** ... [63]
**Deleted:** ⍰
**Formatted** ... [64]
**Deleted:** ⍰
**Formatted** ... [65]
**Deleted:** ⍰
**Formatted** ... [66]
**Deleted:** (3)
**Formatted** ... [67]
**Deleted:** , which assumes mole-fraction to be ... [68]
**Formatted** ... [69]
**Formatted** ... [70]
**Formatted** ... [71]
**Formatted** ... [72]
**Deleted:** , and the Miller Tans plots cannot be ... [73]
**Deleted:** and
**Formatted** ... [74]
**Deleted:** representative
**Formatted** ... [75]
**Formatted** ... [76]
**Deleted:** T
**Formatted** ... [77]
**Deleted:** plots
**Deleted:** in which the
**Formatted** ... [78]
**Deleted:** are plotted
**Formatted** ... [79]
**Deleted:** $\delta^{18}O_{obs}$
**Formatted** ... [80]
**Deleted:** $I_{\delta180}$
**Formatted** ... [81]
**Deleted:** (4)
**Formatted** ... [82]
**Deleted:** ⍰$^{18}$O
**Formatted** ... [83]
**Deleted:** ⍰
**Formatted** ... [84]
**Deleted:** $I_{\delta180}$
**Formatted** ... [55]
**Formatted** ... [56]

determined from a regression of the data. The intercept represents the isotopic signature of the sources influencing the measurement site (Keeling, 1958). The Keeling plot assumes that the background concentration and isotopic values are constant over the period of analysis, which is a reasonable but imperfect assumption for this dataset measured over the summer season. The benefits and limitations of this approach are discussed more fully in section 3.3.

To assess the uncertainty of our Keeling plot analysis, we perform a standard Monte Carlo analysis and additionally use a sampling with replacement Monte Carlo method (often referred to as a bootstrap Monte Carlo). Briefly, the boot strap Monte Carlo consist of calculating a linear regression for 1000 randomly chosen sample sets. These sets are chosen from the original data, at random, such that the number of data points is always constant (n=7 for both summer and winter at Beech Island). However, in some sample sets, points may be selected more than once, or not at all. In this way, any disproportionately large influence on the model by outlier points can be assessed, and the distribution of the model parameter of interest (in our case, the intercept) is representative of data as a whole. We report the mean of the 1000 intercepts, and both the 1σ standard deviation as well as the standard error of the mean are reported for the error on that value. The bootstrap Monte Carlo distributions are shown in the supplementary material (section S3).

### *2.6 Calculation of the VOC oxidation isotopic signatures using mass balance*

The $CH_4$ oxidation source, the biomass-burning source, and the OH oxidation sink have negligible impacts for the Indianapolis CO budget (detailed calculations can be found in the supplementary material, section S2). In order to constrain the remaining two sources (fossil fuel combustion and VOC oxidation), we use a simple isotope mass balance approach. We assume that the $\delta_s$ calculated at each polluted tower (section 2.5, equation (4)) can be represented by:

$$\delta_s = f_{VOC}\delta_{VOC} + f_{FF}\delta_{FF} \qquad (6a)$$

**Deleted:** ¶

**Formatted:** Font: 10 pt, Font color: Text 1

**Formatted:** Font color: Text 1

**Deleted:** section S2

**Formatted:** Font color: Text 1

**Formatted:** Font: 10 pt, Font color: Text 1

**Formatted:** Font color: Text 1

**Formatted:** Level 1

**Formatted:** Font: 10 pt, Font color: Text 1

**Formatted:** Font color: Text 1

**Deleted:** section S1

**Formatted:** Font color: Text 1

**Deleted:** ☐

**Formatted:** Font color: Text 1

**Deleted:** (3)

**Formatted:** Font color: Text 1

**Formatted:** Font: 10 pt, Font color: Text 1

**Deleted:** (5a)

**Formatted:** Font color: Text 1

**Deleted:** 12

$$f_{VOC}=\frac{X_{CO\text{-}VOC}}{X_{CO\text{-}ENH}} \qquad (6b)$$

$$f_{FF}=\frac{X_{CO\text{-}FF}}{X_{CO\text{-}ENH}} \qquad (6c)$$

where $f_{VOC}$ and $\delta_{VOC}$ are the fraction (as compared to total urban CO enhancement) and isotopic signature of CO added from VOC oxidation, and $f_{FF}$ and $\delta_{FF}$ are the fraction and isotopic signature of CO added from fossil fuel combustion. $X_{CO\text{-}VOC}$, $X_{CO\text{-}FF}$, and $X_{CO\text{-}ENH}$ are the mole fractions for VOC-produced CO, the fossil fuel-produced CO, and the total urban CO enhancement, respectively. The isotopic signatures of fossil fuel combustion at Indianapolis were previously determined from wintertime measurements when fossil fuel combustion is the only significant CO source in Indianapolis and are -27.7 ± 0.5‰ and 17.7± 1.1‰ for $\delta^{13}C$ and $\delta^{18}O$ respectively (Vimont et al., 2017). That study found that the isotopic signature in the winter did not vary significantly with temperature, and that the primary source within the city was emissions from transportation (Vimont et al., 2017). Therefore, we use these values as the fossil fuel produced CO isotopic signatures for Indianapolis. Because we have only two sources (supplementary material, section S2), we can derive $X_{CO\text{-}VOC}$ as:

$$X_{CO\text{-}VOC}=X_{CO\text{-}ENH}-X_{CO\text{-}FF} \qquad (7)$$

In order to determine $X_{CO\text{-}VOC}$ we need to determine $X_{CO\text{-}FF}$. This is done using the fossil fuel CO to $CO_2$ ratio:

$$X_{CO\text{-}FF}=R_{COFF:CO2FF}{}^{*}\, X_{CO2\text{-}FF} \qquad (8)$$

where $X_{CO2\text{-}FF}$ is the fossil fuel produced enhancement in the $CO_2$ mole fraction, determined by $^{14}CO_2$ measurements (section 2.4). $R_{COFF:CO2FF}$ is the ratio of $CO_{FF}$ to $CO_{2FF}$ and was determined to be 7 ± 1 nmol:µmol for Indianapolis in the winter, when nearly all CO produced is from fossil fuel combustion, primarily vehicles (Turnbull et al., 2018). We assume that this ratio holds across all seasons. We then solve equations (8), (7) and (6a) to determine $\delta_{VOC}$. In order to estimate a mean value for our limited sample set, we perform a bootstrap Monte Carlo approach, similar to that described in the previous section. We perform 10,000 calculations of the mean. We report the mean and standard deviation of

**Deleted:** ¶

**Deleted:** (5b)

**Formatted:** Font color: Text 1

**Deleted:** (5c)

**Formatted:** Font color: Text 1

**Deleted:**

**Formatted:** Font color: Text 1

**Deleted:**

**Formatted:** Font color: Text 1

**Deleted:**

**Formatted:** Font color: Text 1

**Deleted:**

**Formatted:** Font color: Text 1

**Deleted:** Section S1

**Formatted:** Font color: Text 1

**Formatted:** Font: 10 pt, Font color: Text 1

**Deleted:** (6)

**Formatted:** Font color: Text 1

**Formatted:** Level 1

**Formatted:** Font: 10 pt, Font color: Text 1

**Deleted:** (7)

**Formatted:** Font color: Text 1

**Deleted:** (7)

**Formatted:** Font color: Text 1

**Deleted:** (6)

**Formatted:** Font color: Text 1

**Deleted:** (5a)

**Formatted:** Font color: Text 1

**Formatted:** Font color: Text 1

**Deleted:** error of the

**Formatted:** Position: Horizontal: Center, Relative to: Margin, Vertical: 0", Relative to: Paragraph, Wrap Around

**Formatted:** Page Number

**Formatted:** Page Number

the 10,000 individual mean values for our bootstrap Monte Carlo simulation as our estimate of the isotopic value and uncertainty of $\delta_{VOC}$.

Simple filtering is applied to these data. Any samples with calculated $X_{CO\text{-}VOC}$ values that were near zero, negative, or exceeded the total urban enhancement were removed. $X_{CO\text{-}VOC}$ values that are negative or exceed the total enhancement are obviously non-physical. Positive values of $X_{CO\text{-}VOC}$ that are extremely low (less than 5% of the total enhancement), while physical, create extreme outliers when $\delta^{13}C_{VOC}$ or $\delta^{18}O_{VOC}$ are calculated (in one case, several hundred ‰). Likewise, cases where $X_{CO\text{-}VOC}$ is calculated to be nearly the entire urban enhancement, our method will produce $\delta_{CO\text{-}VOC}$ estimates which approach or are equal to our urban enhancement δ values.

Large overestimates of $X_{CO\text{-}VOC}$ arise because the ratio method can produce unrealistically low calculated $X_{CO\text{-}FF}$ values if the $X_{CO2\text{-}FF}$ enhancements are not significantly different from zero. $X_{CO2\text{-}FF}$ enhancements near or below zero are a result of possible local contamination at or near the background tower, which violates the assumption of well mixed background air flowing across the city. Conversely, the ratio method can overestimate $X_{CO\text{-}FF}$ thereby underestimate $X_{CO\text{-}VOC}$ when $X_{CO2\text{-}FF}$ is highly elevated, without a corresponding elevation in $X_{CO\text{-}ENH}$. One example of how this can occur is if the local power plant (the Harding Street Power Plant) plume is sampled by the polluted tower. In the period of this study, the Harding Street Power Plant contributed about 28% of Indianapolis' $CO_{2FF}$ emissions and, while this source is often dispersed, the plume from this source is occasionally observed at tower 2. This source has a $CO:CO_{2FF}$ ratio of <0.1 nmol:μmol, due to CO emissions controls fitted to the exhaust stack. Because we use a constant value for $R_{CO:CO2FF}$, any day where tower 2 samples contain power plant emissions will produce low or negative $X_{CO\text{-}VOC}$ values. We do not attempt to identify specific causes for high or low $X_{CO\text{-}VOC}$ values. For our sample set, we simply filter samples in which $X_{CO\text{-}VOC}$ was less than 15% of the total enhancement, which produced strong outliers, and samples in which $X_{CO\text{-}VOC}$ was more than 85% of the total enhancement, which produced values equal to our calculated urban enhancements.

**Deleted:** ¶

**Deleted:** set of samples

**Deleted:** □

**Formatted:** Font color: Text 1

**Formatted:** Font: 10 pt, Font color: Text 1

**Formatted:** Font color: Text 1

**Deleted:** .

**Formatted:** Font color: Text 1

**Deleted:** It is unclear from our data why the

**Deleted:** are occasionally

**Deleted:** .

**Formatted:** Font color: Text 1

**Deleted:** the power plant plume, but as stated above, simply filter extremely low $X_{CO\text{-}VOC}$ values as outliers…

**Formatted:** Font color: Text 1

**Deleted:** 14

This filtering removed a total of 6 data points. The data used for calculating the isotopic signatures for VOC derived CO is shown in Table 2.

## 3. Results and Discussion

### *3.1 Determination of the urban enhancement CO isotopic signatures*

The full time series from Indianapolis was published in Vimont et al. (2017). However, we have reproduced the data from towers 1 and 2 (Figure 3) here to highlight the summertime data (not discussed in Vimont et al., 2017). The summertime mole fraction and isotopic data can be seen in Table S2 in the supplementary material. One of the more salient features of the summer Indianapolis data as compared to the winter data is that, while tower 2 CO mole fraction remains enhanced over tower 1 throughout the year, the $\delta^{18}$O values at tower 2 tend to be much closer to those of tower 1 during the summer, yet are more positive during the winter. This is consistent with the hypothesis that the wintertime urban enhancement is dominated by a fossil source, while the summertime enhancement is a mixed source. Further, this mixed source must be more depleted in $^{18}$O than fossil fuel produced CO. The $\delta^{13}$C results are more difficult to interpret from the time series alone, which underscores the need for the Miller Tans method at Indianapolis.

The Miller Tans Monte Carlo regression analysis produced isotopic results of -29.6 ± 1.0‰ for $\delta^{13}$C and 12.5 ± 2.1‰ for $\delta^{18}$O ($1\sigma$) for the overall urban summertime CO source (Figure 2). The $\delta^{13}$C source signature is very similar to that determined in winter (-27.7±0.5‰, Vimont et al., 2017). In contrast, the $\delta^{18}$O signature is substantially lower in summer than in winter (17.7±1.0‰ in winter, Vimont et al., 2017). These results are consistent with our hypothesized mixing of two sources of CO with different isotopic signatures contributing to the summertime CO enhancement. The determined $\delta^{13}$C of the urban CO source stays relatively consistent between winter and summer (-27.7±0.5‰ and -29.6±1.0‰, respectively), suggesting that the VOC oxidation source must have a $\delta^{13}$C signature that is only slightly more negative than the fossil fuel source. In contrast, $\delta^{18}$O of

**Deleted:** ¶

**Deleted:** ¶

**Formatted:** Font color: Text 1

**Formatted:** Font: 10 pt, Bold, Font color: Text 1

**Formatted:** Font color: Text 1

**Formatted:** Font: 10 pt, Font color: Text 1

**Formatted:** Font color: Text 1

**Deleted:** figure

**Formatted:** Font color: Text 1

**Deleted:** table

**Formatted:** Font color: Text 1

**Formatted:** Font: 10 pt, Font color: Text 1

**Formatted:** Font color: Text 1

**Deleted:** □

**Formatted:** Font color: Text 1

**Deleted:** □

**Formatted:** Font color: Text 1

**Formatted:** English (US)

**Deleted:** of

**Formatted:** Font color: Text 1

**Deleted:** figure

**Formatted:** Font color: Text 1

**Deleted:** □

**Formatted:** Font color: Text 1

**Deleted:** □

**Formatted:** Font color: Text 1

**Deleted:** □

**Formatted:** Font color: Text 1

**Deleted:** □

**Formatted:** Font color: Text 1

**Formatted:** Position: Horizontal: Center, Relative to: Margin, Vertical: 0", Relative to: Paragraph, Wrap Around

**Formatted:** Page Number

**Formatted:** Page Number

the urban source changes substantially from winter to summer (17.7±1.0‰ and 12.5±2.1‰, respectively), indicating a VOC $\delta^{18}O$ signature that is much more negative than the fossil fuel source. The increased scatter in the $\delta^{18}O$ regression relative to $\delta^{13}C$ is also consistent with this interpretation: variability in the relative contributions of fossil fuel and VOC CO sources for different samples will impart more variability in $\delta^{18}O$ than $\delta^{13}C$.

Day to day variability in the VOC oxidation source is expected and supports the hypothesis that secondary production of CO by VOCs strongly contributes to the urban enhancement. For example, isoprene has a short atmospheric lifetime in urban regions and rapidly forms CO (Atkinson and Arey, 2003). Isoprene oxidation is highly variable because isoprene emissions depend exponentially on the ambient temperature, and the rate at which isoprene is oxidized will increase as $NO_x$ increases (Guenther et al., 1995; Carter and Atkinson, 1996). Additionally, boundary layer mixing will vary day to day, affecting the magnitude and transport of all sources within the tower domain.

### *3.2 Determination of the VOC-produced CO $\delta^{13}C$ and $\delta^{18}O$ isotope signature*

To determine the VOC-produced CO isotopic signature, we first determined the fossil fuel-produced $CO_2$ source (section 2.4). The $^{14}CO_2$, the derived $CO_{2FF}$ mole fractions, and the calculated $CO_{FF}$ and $CO_{VOC}$ mole fractions are presented in Table 2. The uncertainties reported are 1σ for $CO_{2FF}$ and $\Delta^{14}CO_2$, while the uncertainties on the calculated $CO_{FF}$ and $CO_{VOC}$ values are the propagated errors for equations (7) and (8). Using the mass balance approach and bootstrap Monte Carlo method described in section 2.6 we use the isotopic source signatures determined in section 3.1 to calculate the isotopic signatures of VOC-derived CO (Table 2) and the associated bootstrap Monte Carlo mean values: -32.8‰ ± 0.5‰ for $\delta^{13}C$ and 3.6‰ ± 1.2‰ for $\delta^{18}O$ (1σ). The scatter in the VOC-derived CO isotopic signatures calculated for individual samples is relatively large (Table 2), and likely due to a combination of uncertainties discussed in Section 2.6 and real day-to-day variability in the isotopic signatures. However, it is the mean values that are of most interest for CO budget studies, and these appear to be well constrained by the data set.

**Deleted:** ¶

**Deleted:** summer to winter...inter to summer (17.7±1.0‰ and 12.5±2.1‰, respectively), indicating a VOC $\delta^{18}O$ signature that is much ... [85]

**Formatted** ... [86]

**Formatted:** Font color: Text 1

**Deleted:** is ...trongly contributing ... [87]

**Formatted:** Font: 10 pt, Font color: Text 1

**Formatted:** Font color: Text 1

**Deleted:**

**Formatted** ... [88]

**Formatted:** Font color: Text 1

**Deleted:** t

**Formatted:** Font color: Text 1

**Deleted:** (6)

**Deleted:** (7)

**Formatted:** Font color: Text 1

**Deleted:** ¶
¶

**Formatted:** Font color: Text 1

**Formatted** ... [89]

**Deleted:** mean ...sotopic signatures of VOC- ... [90]

**Formatted:** Font color: Text 1

**Deleted:** oxidation

**Formatted:** Font color: Text 1

**Deleted:** -33.6‰ ± 1.0‰

**Formatted:** Font color: Text 1

**Deleted:**

**Formatted:** Font color: Text 1

**Deleted:** 1.3‰ ± 2.7‰ ....6‰ ± 1.3‰ ± ... [91]

**Formatted:** Font color: Text 1

**Deleted:** .7

**Deleted:**

**Formatted:** Font color: Text 1

**Deleted:** ...1 sigma...)..... The scatter in the VOC-derived CO isotopic signatures calculated for individual samples pairs ...s relatively large (Table ... [92]

**Formatted:** Font color: Text 1

**Deleted:** 16

The $\delta^{13}$C results compare well to the later of previously published estimates of the VOC oxidation signature: -32 ± 2 ‰ (e.g. Brenninkmeijer et al., 1999). This value is reasonable given the expected carbon isotopic ratio of isoprene and the fractionation processes associated with the isoprene oxidation reaction (e.g. Sharkey et al., 1991). Our $\delta^{18}$O result compares well with the previously published estimate from Brenninkmeijer and Röckmann (1997) (~0‰) but contradicts Stevens and Wagner (1989) (~15‰). We re-examine the methods and uncertainties of the previous studies to understand what might cause this discrepancy.

Stevens and Wagner (1989) performed a Keeling plot analysis of samples collected in rural Illinois. They assumed a constant background, with VOC oxidation as the only added CO source, and performed a Keeling plot analysis. Their results indicated -32.2‰ for $\delta^{13}$C and 15‰ for $\delta^{18}$O of the added CO source. They also measured four samples from a coastal site in Australia and obtained an average $\delta^{18}$O of 5‰ for the atmospheric C$^{18}$O signature. They did not perform a Keeling analysis on the Australian data. They reasoned that the effect of oxidation by OH on the Australia samples would reduce the $\delta^{18}$O by 10‰, which meant the source (assumed to be dominated by VOC and methane oxidation) must have been 15‰, in agreement with their rural Illinois samples.

The value of 0‰ suggested by Brenninkmeijer and Röckmann (1997) was based on a model-driven interpretation of CO isotope measurements in the southern hemisphere. Using mass balance, they were able to determine the oxidation of methane and VOCs should produce CO with an oxygen isotopic value near to 0‰, while the value of 15‰ suggested by Stevens and Wagner (1989) could not be consistent with the measurements. Bergamaschi et al. (2000) used an atmospheric inversion combined with CO mole fraction and isotopic measurements in an attempt to determine the isotopic signatures of CO sources at the global scale. However, their study resulted in wide ranges for $\delta^{13}$C (-17‰ to -31‰) and $\delta^{18}$O (-30‰ to +23‰) isotopic values, dependent on the input parameters of their model. Later studies using $\delta^{18}$O to partition the global budget generally use the 0‰

**Deleted:** ¶

**Deleted:** We discuss the possible effects of ozonolysis of VOC's as a source of CO in section 3.4.

**Formatted:** Font color: Text 1

**Formatted:** Font: 10 pt, Font color: Text 1

**Formatted:** Font color: Text 1

**Deleted:** As stated above,

**Deleted:** t

**Deleted:** This

**Formatted:** Font color: Text 1

**Deleted:** ⍰

**Formatted:** Font color: Text 1

**Deleted:** results

**Formatted:** Font color: Text 1

**Formatted:** Font: 10 pt, Font color: Text 1

**Formatted:** Font color: Text 1

**Deleted:** ⍰

**Formatted:** Font color: Text 1

**Deleted:** ⍰

**Formatted:** Font color: Text 1

**Formatted:** Font: 10 pt, Font color: Text 1

**Formatted:** Font color: Text 1

**Formatted:** Position: Horizontal: Center, Relative to: Margin, Vertical: 0", Relative to: Paragraph, Wrap Around

**Formatted:** Page Number

**Formatted:** Page Number

value for $\delta^{18}$O despite the lack of consensus (e.g., Park et al., 2015). By leveraging the INFLUX measurements, we are able to place a constraint on the VOC-produced CO isotopic signatures without relying on the uncertain assumptions of a constant background / VOCs as the only source, or on the use of a model to derive the CO mass balance.

### *3.3 Beech Island South Carolina Isotopic Data*

The Beech Island results are shown in Figure 4, while the data can be found in the supplementary information (Table S3). One of the most striking features of this data set is that while the $\delta^{13}$C and $\delta^{18}$O both decrease from spring into summer and then increase into the fall and winter, the mole fraction values do not exhibit much seasonality. While any true seasonal cycles or trends are impossible to determine with only a single year of data, this nonetheless is consistent with a strong summer source of CO from VOC oxidation.

The Keeling plot-derived CO source isotopic signatures at Beech Island, South Carolina are shown in Figure 5. During the summer months (June-July-August-September), the Keeling plot analysis (section 2.5) produces a $\delta^{13}$C signature of -31.2‰ ± 0.2‰ and a $\delta^{18}$O signature of 5.8‰ ± 0.7‰ (1σ) using a standard Monte Carlo simulation and a $\delta^{13}$C signature of -30.9‰ ± 5.7‰, and a $\delta^{18}$O signature of 5.6‰ ± 2.4‰ (1σ) using the bootstrap Monte Carlo method. During the winter months (December-January-February-March), we obtain a $\delta^{13}$C signature of -27.3‰ ± 0.2‰ and a $\delta^{18}$O signature of 21.1‰ ± 0.3‰ (1σ) using the standard Monte Carlo method. Using the bootstrap Monte Carlo, we obtain a $\delta^{13}$C of -26.8‰ 3.7‰ and a $\delta^{18}$O of 20.4‰ ± 5.0‰ (1σ). The Keeling approach implicitly assumes constant background CO mole fraction and isotopic composition, which is unlikely to be correct for Beech Island for the entire duration of the summer. However, this approach is still useful for an approximate estimation of the CO source isotopic composition. This is particularly true for $\delta^{18}$O, where the difference between the inferred source isotopic signature and the measured $\delta^{18}$O values is larger than the scatter in the measured values.

**Deleted:** ¶ ... [93]
**Formatted** ... [94]
**Formatted** ... [95]
**Formatted** ... [96]
**Formatted** ... [97]
**Deleted:** figure
**Formatted** ... [98]
**Deleted:** table
**Formatted** ... [99]
**Deleted:** The
**Formatted** ... [100]
**Deleted:** feature
**Formatted** ... [101]
**Formatted** ... [102]
**Deleted:**
**Deleted:** oxidized VOC produced CO
**Formatted** ... [103]
**Formatted** ... [104]
**Formatted** ... [105]
**Formatted** ... [106]
**Deleted:**
**Formatted** ... [107]
**Deleted:** figure
**Formatted** ... [108]
**Formatted** ... [109]
**Formatted** ... [110]
**Deleted:** 0.2‰ (
**Deleted:** 1σ)
**Deleted:** ⍰
**Deleted:** 0.1‰ (
**Deleted:** 1σ)
**Formatted** ... [111]
**Formatted** ... [112]
**Formatted** ... [113]
**Deleted:** ± 0.1‰ (
**Deleted:** 1σ)
**Deleted:** ⍰$^{18}$O of 20.4‰ ± 0.2‰ (5.0‰ 1σ).
**Formatted** ... [114]
**Formatted** ... [115]
**Deleted:** 18

In an alternative approach, we apply a background seasonal signal from data published by Bräunlich (2000) from Izaña, Tennerife to allow for a Miller-Tans plot analysis. Tennerife is located in a similar latitudinal band to Beech Island (28ºN vs 33.4ºN), and the amplitude of the background seasonal signal should be similar between the two sites. However, the Tennerife data set is from sampling done approximately two decades before our Beech Island sampling, and therefore global changes to the CO budget between the two studies will introduce error to this analysis that is not easily quantified. Figure 6 shows the isotopic source signatures derived from a Monte Carlo simulation for a Miller Tans plot approach using monthly averaged data from Izaña, Tennerife (Bräunlich, 2000) as a background for Beech Island. This method produced summer (June-July-August-September) $\delta^{13}C$ and $\delta^{18}O$ source signatures of -29.5‰ ± 3.2‰ and 5.8‰ ± 0.3‰ (1σ) respectively. During the winter months (December, January, Febrary, March), we obtained $\delta^{13}C$ and $\delta^{18}O$ source signatures of -27.2‰ ± 3.7‰ and 20.5‰ ± 1.7‰ (1σ), respectively. These results are in good agreement with our Keeling plot results.

While both the Keeling and the Miller-Tans approaches for analyzing Beech Island data have important weaknesses as discussed above, these weaknesses are different. The close agreement between the Keeling and Miller Tans approaches for Beech Island therefore increases confidence in our findings and suggests that the primary drivers of the observed isotopic source signatures are local sources, rather than seasonal changes in background CO. The mean values (and standard deviations) of the isotopic signatures at Beech Island from our three analyses are -30.5‰ ± 3.2‰ and 5.7‰ ± 0.8‰ during the summer, and -27.1‰ ± 3.7‰ and 20.7‰ ± 1.7‰ during the winter for $\delta^{13}C$ and $\delta^{18}O$ respectively.

The wintertime source signatures derived at Beech Island are consistent with prior estimates of fossil fuel combustion sources ($\delta^{13}C$: ~-27.5‰, $\delta^{18}O$: ~23.5‰, Table 1). The Beech Island $\delta^{13}C$ value is consistent with the wintertime value found at Indianapolis (-27.7‰ ± 0.5‰, Vimont et al., 2017), while the $\delta^{18}O$ value differs slightly from the value found at Indianapolis during the winter (17.7‰ ± 1‰, Vimont et al., 2017). At Indianapolis, the winter CO urban enhancement was found to be primarily fossil fuel in origin, but it was noted that the oxygen isotopic signature was significantly different from

**Moved (insertion) [1]**

**Moved up [1]:** The merits of this approach relative to the Keeling plot are discussed further below.

**Deleted:** ¶

**Deleted:** ¶

**Formatted** ... [117]

**Moved (insertion) [1]**

**Deleted:** , and do not assume a constant background... The merits of this approach relative to the Keeling plot are discussed further below... [118]

**Formatted:** Font: 10 pt, Font color: Text 1

**Moved up [1]:** The merits of this approach relative to the Keeling plot are discussed further below.

**Formatted:** Font color: Text 1

**Deleted:** ¶

**Deleted:** ¶
While both the Keeling and the Miller-Tans approaches for analyzing Beech Island data have important weaknesses as discussed above, these weaknesses are different. The close agreement between the Keeling and Miller Tans approaches for Beech Island therefore increases confidence in our findings and suggests that the primary drivers of the observed isotopic source signatures are local source signatures..., rather than seasonal changes background CO. The mean values (and standard deviations?... ... [119]

**Formatted** ... [120]

**Formatted:** Font color: Text 1

**Deleted:** ▯

**Formatted:** Font color: Text 1

**Deleted:** Brenninkmeijer et al., 1999

**Formatted:** Font color: Text 1

**Formatted:** Position: Horizontal: Center, Relative to: Margin, Vertical: 0", Relative to: Paragraph, Wrap Around

**Formatted** ... [116]

prior estimates of fossil fuel combustion, possibly due to Indianapolis' emission regulation (Vimont et al., 2017). Nonetheless, this suggests that the main driver of CO variability during the winter at Beech Island is likewise fossil fuel combustion. In contrast, the summer CO source isotopic signatures at Beech Island ($\delta^{13}C$: -30.5‰, $\delta^{18}O$: 5.7‰) are lower than for Indianapolis ($\delta^{13}C$: -29.6‰, $\delta^{18}O$: 12.5‰), which is consistent with a larger relative contribution of CO from VOC oxidation. As stated above, the absence of a clear CO mole fraction summertime minimum at Beech Island (Figure 4) is likely due to the large influence from CO produced by oxidation of VOCs during the summer, which offsets the expected summertime CO decline, such as is seen at Indianapolis (Figure 3). The much higher contribution of CO produced by oxidized VOCs at Beech Island relative to Indianapolis is reasonable, given the more concentrated fossil fuel source in the Indianapolis urban area and the higher concentrations of biogenic VOCs expected at the densely forested and warmer Beech Island site.

While the small dataset from Beech Island does not allow for a direct estimate of the isotopic signatures of VOC-produced CO, it is consistent with the values we obtained from Indianapolis and with values estimated by Brenninkmeijer and Röckmann (1997). Additionally, the Beech Island data is not consistent with the 15‰ value for $\delta^{18}O$ of VOC-produced CO suggested by the prior Stevens and Wagner (1989) study. The Beech Island data suggest the dominant local CO wintertime source is fossil fuel combustion, with a $\delta^{18}O$ isotopic signature of approximately 20‰. During the summer months, the addition of VOC-produced CO shifts the overall source $\delta^{18}O$ to approximately 6‰. If the oxygen isotopic signature of CO produced by oxidation of VOCs was 15‰, as suggested by Stevens and Wagner (1989), this result would be impossible.

### *3.4 Discussion of the role of ozonolysis in the VOC-derived CO $\delta^{18}O$ signature*

As noted above, Röckmann et al. (1998) suggested ozonolysis of VOC's may be a cause of significant $\Delta^{17}O$ deviations resulting from mass independent fractionation (MIF) during the formation of $O_3$ (see Röckmann et al. (1998a,b) for a more detailed explanation of the MIF process). Hatakeyama et al. (1991), Röckmann et al. (1998a), and Atkinson and Arey

**Deleted:** ¶ ... [121]
**Deleted:** ~...30.51..., $\delta^{18}O$:~...5.76...) are ll ... [122]
**Deleted:** ighter
**Formatted** ... [123]
**Deleted:** ...which is consistent with a larger relative ... [124]
**Deleted:** more or less...bsence of a clear constant ... [126]
**Formatted** ... [125]
**Formatted** ... [127]
**Deleted:** time series
**Deleted:** figure
**Formatted** ... [128]
**Formatted** ... [129]
**Deleted:** mole fraction minimum
**Deleted:** figure
**Formatted** ... [130]
**Formatted** ... [131]
**Deleted:**
**Formatted** ... [132]
**Deleted:** ¶
**Formatted** ... [133]
**Deleted:** The Keeling approach implicitly assumes ... [134]
**Formatted** ... [135]
**Deleted:** would produce a shift in $\delta^{13}C$ towards ... [136]
**Deleted:** ¶
**Formatted** ... [137]
**Deleted:**
**Deleted:**
**Formatted** ... [138]
**Deleted:** Further
**Deleted:** it
**Deleted:** they
**Deleted:** helps us to rule out
**Formatted** ... [140]
**Deleted:**
**Formatted** ... [139]
**Formatted** ... [141]
**Deleted:** main driver of
**Formatted** ... [142]
**Deleted:** variability
**Formatted** ... [143]
**Formatted** ... [144]
**Deleted:** *T*
**Formatted** ... [145]
**Deleted:** *C*... ... [146]
**Formatted** ... [147]
**Formatted** ... [148]
**Formatted** ... [149]
**Deleted:** 20

(2003 a,b) have suggested that ozonolysis may be a large sink for terpenes in the atmosphere.

Röckmann et al., (1998a) found that $O_3$, and subsequently the CO produced from ozonolysis of VOC's, had a substantially enriched $\delta^{18}O$ signature relative to atmospheric oxygen and CO. The $\delta^{18}O$ of $O_3$ was shown to be around 80‰, and ethene, isoprene, and β-pinene produced CO with a $\delta^{18}O$ between 46‰ and 83‰ (relative to the original $O_2$ used in the experiments) (Röckmann et al., 1998a). The $\delta^{18}O$ of atmospheric $O_2$ is around 23‰, and therefore the CO produced by ozonolysis of these VOC's in the atmosphere would have a $\delta^{18}O$ of between 69‰ to 100‰. Röckmann et al. (1998a) acknowledge that a significant global source of CO with a $\delta^{18}O$ of 69‰-100‰ is difficult to reconcile with the overall CO $\delta^{18}O$ budget, and thus conclude that either a) ozonolysis of VOC's is not the primary source of the observed mass independent $^{17}O$ deviations, or b) a second source with sufficiently depleted $\delta^{18}O$ and similar seasonal cycle to ozone, VOC emissions, and CO must be countering the ozonolysis $\delta^{18}O$ contribution. Röckmann et al. (1998b) detail a second source of MIF from CO+OH, and concluded that the ozonolysis source was a small contributor to the overall CO budget.

Our $\delta^{18}O$ time series (Figures 3 and 4) as well as summertime source isotopic signature analyses (Figures 2, 5, 6) are not consistent with a summertime source with such a strong enrichment in $^{18}O$. Röckmann et al. (1998a) found no evidence for a seasonally covarying source that has depleted $^{18}O$ of a similar magnitude to the ozonolysis source, that could obscure the impact of ozonolysis on CO-$\delta^{18}O$. Thus, we conclude that CO produced by the ozonolysis of VOCs is not a major component of the CO budget at both Indianapolis and Beech Island, and that OH oxidation is the dominant source of VOC produced CO in our study.

Nonetheless, our $\delta^{18}O$ results do not preclude a minor source of CO from ozonolysis of VOCs and the VOC produced CO $\delta^{13}C$ and $\delta^{18}O$ signatures calculated in this study cannot be separated between OH oxidation and ozonolysis. We note that, as discussed in section 2.1, the mean transit time for air masses between our background and polluted sites is 3.2

**Deleted:** ¶

**Formatted** ... [151]

**Formatted:** Font color: Text 1

**Formatted** ... [152]

**Deleted:** measurements of

**Formatted** ... [153]

**Formatted:** Font color: Text 1

**Deleted:** Figure

**Deleted:** is

**Formatted** ... [154]

**Deleted:** d

**Formatted** ... [155]

**Deleted:** Likewise, we also have no evidence of such a phenomenon in the atmosphere.

**Formatted** ... [156]

**Deleted:** a minor

**Formatted:** Font color: Text 1

**Deleted:** observed

**Formatted:** Font: Cambria, Font color: Text 1

**Formatted:** Font color: Text 1

**Formatted:** Font color: Text 1

**Formatted:** Position: Horizontal: Center, Relative to: Margin, Vertical: 0", Relative to: Paragraph, Wrap Around

**Formatted** ... [150]

hours, which favors the oxidation of isoprene by OH (lifetime ~ 1.4 hours) relative to ozonolysis (lifetime ~1.3 day), depending on the OH and $O_3$ concentrations (Atkinson and Arey, 2003a). β-pinene (also tested by Röckmann et al. (1998a)) has similar OH and $O_3$ lifetimes (1.8 hours vs 1.1 days, respectively) (Atkinson and Arey, 2003a). Furthermore, Atkinson (2000) and Atkinson and Arey (2003a,b) have detailed the reaction schemes for VOCs, and the OH oxidation and ozonolysis pathways, which are complex. Ozonolysis of isoprene, for example, produces an ozonide which is then destroyed via three possible reaction pathways (Atkinson, 2000; Atkinson and Arey, 2003a,b). Only one of these pathways produces formaldehyde, which is subsequently photolyzed and the only pathway by which the oxygen isotopic signature of ozone could be guaranteed to be preserved in the resultant CO (Atkinson, 2000; Atkinson and Arey, 2003a,b). Other reaction pathways involve further interaction with OH or other molecules (Atkinson, 2000; Atkinson and Arey, 2003a,b), which provides for possible fractionation or exchange of the oxygen isotopes. Other terpenes also form higher order aldehydes, which primarily react with OH or $NO_3$, but do not react further with $O_3$ (Atkinson, 2000; Atkinson and Arey, 2003a,b). For reaction pathways other than photolysis of formaldehyde, the oxygen isotope fractionations or exchanges are difficult to trace and quantify, and are beyond the scope of this study.

To conclude, our results for the $\delta^{13}$C and $\delta^{18}$O signature of CO produced by oxidation of VOC's mainly represent OH oxidation processes with possible minor contributions from ozonolysis. Our atmospheric $\delta^{18}$O timeseries from Indianapolis and Beech Island are consistent with prior CO isotopic studies, for example Mak et al. (2003) and Röckmann et al. (2002): they do not show evidence for a strong source of CO from ozonolysis of VOCs.

## 4. Conclusions

We analyzed carbon monoxide stable isotopes and $\Delta^{14}CO_2$ during three summers at Indianapolis and determined the isotopic signature of the urban CO enhancement during the summer. Additionally, we analyzed CO stable isotopes approximately bi-monthly for one year at Beech Island, South Carolina. Using the $\Delta^{14}CO_2$ data and the ratio of CO:$CO_{2FF}$,

**Deleted:** ¶

**Formatted:** Font color: Text 1

**Formatted:** Font color: Text 1

**Formatted:** Font color: Text 1

**Formatted:** Font color: Text 1

**Formatted:** English (US)

**Formatted:** Font color: Text 1

**Formatted:** Font color: Text 1

**Formatted:** Font color: Text 1

**Deleted:** paper

**Formatted:** Font color: Text 1

**Formatted** ... [157]

**Formatted:** Font color: Text 1

**Deleted:** Therefore

**Formatted:** Font color: Text 1

**Deleted:** δ13C and

**Formatted:** Font color: Text 1

**Formatted** ... [158]

**Formatted:** Font color: Text 1

**Formatted:** Font color: Text 1

**Deleted:** is valid

**Formatted:** Font color: Text 1

**Deleted:** for

**Deleted:** and

**Formatted:** Font color: Text 1

**Formatted:** Font color: Text 1

**Formatted:** Font color: Text 1

**Deleted:** other

**Formatted:** Font color: Text 1

**Formatted:** Font color: Text 1

**Deleted:** globally

**Deleted:** However, further study of the ozonolysis ... [159]

**Formatted** ... [160]

**Formatted:** Font color: Text 1

**Formatted:** Font: 10 pt, Font color: Text 1

**Formatted:** Font color: Text 1

**Formatted:** Font color: Text 1

**Deleted:** 22

we calculated the fossil fuel component of the CO mole fraction enhancement at Indianapolis. We then used isotope mass balance and the Indianapolis $CO_{FF}$ isotopic signatures from prior work to calculate the isotopic signature of CO produced from VOCs: -32.8‰ ± 0.5‰ for $\delta^{13}C$ and 3.6‰ ± 1.2‰ for $\delta^{18}O$. This result mainly reflects oxidation of VOC's by OH, with a possible minor contribution from ozonolysis of VOC's. Our measurements from Beech Island, SC (a forest site strongly influenced by VOC-derived CO) are consistent with these results, and confirm that VOC-derived CO is a large component of the summer Beech Island CO budget. Our estimate for the carbon isotopic signature of VOC-produced CO agrees well with and confirms prior estimates. Our oxygen isotopic result agrees well with estimates made by Brenninkmeijer and Röckmann (1997) but does not support prior work by Stevens and Wagner (1989).

This result is an important step to improving the constraints on global and regional CO budgets. Additional studies that quantify the isotopic signature of VOC-produced CO could confirm whether our result is valid regionally and globally, as well as attempt to better quantify the global importance of CO produced via ozonolysis of VOCs.

*Author contributions:*

IJV performed the measurements, data analysis, and wrote the article. JCT assisted in data analysis and provided multiple coauthor revisions. VVP provided assistance with measurement issues, data analysis, and multiple coauthor revisions. PFP assisted in several of the measurements. CS provided several coauthor revisions. NM and SR provided logistical support for sample collection for the measurements. BHV and JWCW provided laboratory and equipment support.

*Competing Financial Interests:*

There are no competing financial interests for any of the authors.

*Funding Sources:*

**Deleted:** ¶

**Deleted:** .

**Formatted:** Font color: Text 1

**Deleted:** oxidized ...OCs: -33.6‰ ± 1.0‰ ... [163]

**Deleted:** ⍰

**Formatted:** Font color: Text 1

**Deleted:** 1.3‰ ± 2.7‰ ....6‰ ± 1.27 ... [164]

**Deleted:** includes both

**Formatted:** Font color: Text 1

**Formatted:** Font color: Text 1

**Formatted:** Font color: Text 1

**Deleted:** and

**Deleted:** , unquantified

**Formatted** ... [165]

**Deleted:** A separate set of CO isotopic measurements from a forest site strongly influenced by VOC-derived CO (Beech Island, SC) is consistent with these results. Our estimate for the carbon isotopic signature of VOC-produced CO agrees well with and confirms prior estimates. Our oxygen isotopic result agrees well with estimates made by Brenninkmeijer and Röckmann (1997) ... [166]

**Formatted** ... [167]

**Formatted:** Font color: Text 1

**Deleted:** help to further improve the associated ... [168]

**Formatted:** Font color: Text 1

**Deleted:** burden

**Formatted:** Font color: Text 1

**Deleted:** from the

**Formatted** ... [169]

**Formatted:** Font color: Text 1

**Formatted:** Font: 10 pt, Font color: Text 1

**Formatted** ... [170]

**Formatted:** Font color: Text 1

**Formatted:** Font: 10 pt, Font color: Text 1

**Formatted** ... [171]

**Formatted:** Font color: Text 1

**Formatted:** Font: 10 pt, Font color: Text 1

**Formatted** ... [161]

**Formatted** ... [162]

This research was generously funded by the National Institute of Standards and Technology (grant 60NANB10D023) and the National Oceanic and Atmospheric Administration Climate Program Office's AC4 program (award NA13OAR4310074). The lead author and the analysis system development were supported through funding in conjunction with the INSTAAR contract for isotopic analysis (RA-133R-15-CQ-0044) with The National Oceanic and Atmospheric Administration (NOAA) Earth System Research Laboratory (ESRL) Global Monitoring Division (GMD) Global Greenhouse Gas Reference Network (GGGRN).

*Materials and Correspondence:*

Please direct all requests for materials and correspondence to Isaac J Vimont, Isaac.vimont@colorado.edu

*Data Availability:*

Data for this experiment is available in Table 2 in the manuscript, and the supplemental material.

**Deleted:** ¶

**Formatted:** Font color: Text 1

**Formatted:** Font: 10 pt, Font color: Text 1

**Formatted:** Font color: Text 1

**Formatted:** Font: 10 pt, Font color: Text 1

**Formatted:** Font color: Text 1

**Deleted:** Isaac.vimont@colorado.edu

**Formatted:** Font: 10 pt, Font color: Text 1

**Formatted:** Font color: Text 1

**Formatted:** Font: 10 pt, Font color: Text 1

**Formatted:** Font color: Text 1

**Deleted:** table

**Formatted:** Font color: Text 1

**Formatted:** Font: 10 pt, Font color: Text 1

**Deleted:** ¶
¶

**Formatted:** Line spacing: 1.5 lines

**Formatted:** Font: Cambria, Font color: Text 1

**Formatted:** Font: Cambria, Bold, Font color: Text 1

**Deleted:** 24

## References

Atkinson, R., and Arey, J.: Gas-phase tropospheric chemistry of biogenic volatile organic compounds: a review, Atmospheric Environment, 37, Supplement 2, 197-219, http://dx.doi.org/10.1016/S1352-2310(03)00391-1, 2003a.

Atkinson, R., and Arey, J.: Atmospheric degradation of volatile organic compounds, Chem. Rev., 103, 4605-4638, 10.1021/cr0206420, 2003b.

Bergamaschi, P., Brenninkmeijer, C. A. M., Hahn, M., Röckmann, T., Scharffe, D. H., Crutzen, P. J., Elansky, N. F., Belikov, I. B., Trivett, N. B. A., and Worthy, D. E. J.: Isotope analysis based source identification for atmospheric CH4 and CO sampled across Russia using the Trans-Siberian railroad, J. Geophys. Res.-Atmos., 103, 8227-8235, 10.1029/97jd03738, 1998.

Bergamaschi, P., Hein, Ralf, Brenninkmeijer, Carl A.M., Crutzen, Paul J.: Inverse modeling of the global CO cycle 2. Inversion of 13C/12C and 18O/16O isotope ratios, Journal of Geophysical Research, 105, 1929-1945, 2000.

Brand, W. A., Assonov, S. S., and Coplen, T. B.: Correction for the 17O Interference in d13C Measurements When Analyzing CO2 with Stable Isotope Mass Spectrometry, International Union of Pure and Applied Chemistry Inorganic Chemistry Division Commission on Isotopic Abundances and Atomic Weights, 2009.

Bräunlich, M.: Study of atmospheric carbon monoxide and methane using isotopic analysis, PhD, Institute of Environmental Physics, Rupertus Carola University, Heidelberg, Germany, 2000.

Brenninkmeijer, C. A. M.: Measurement of the Abundance of 14CO in the Atmosphere and the 13C/12C and 18O/16O Ratio of Atmospheric CO with Applications in New Zealand and Antarctica, Journal of Geophysical Research, 98, 10,595-510,614, 1993.

Brenninkmeijer, C. A. M., and Röckmann, T.: Principal factors determining the18O/16O ratio of atmospheric CO as derived from observations in the southern hemispheric troposphere and lowermost stratosphere, Journal of Geophysical Research, 102, 25477, 10.1029/97jd02291, 1997.

Brenninkmeijer, C. A. M., Röckmann, T., Bräunlich, M., Jockel, P., and Bergamaschi, P.: Review of Progress in Isotope Sutdies of Atmospheric Carbon Monoxide, ChemoSphere- Global Change Science, 1, 33-52, 1999.

Carter, W. P. L., and Atkinson, R.: Development and evaluation of a detailed mechanism for the atmospheric reactions of isoprene and NOx, Int. J. Chem. Kinet., 28, 497-530, 10.1002/(sici)1097-4601(1996)28:7<497::aid-kin4>3.0.co;2-q, 1996.

**Deleted:** ¶

**Formatted:** Font color: Text 1

**Formatted:** From text: 0"

**Formatted:** Font: 10 pt, Font color: Text 1

**Formatted:** Font color: Text 1

**Formatted:** Font color: Text 1

**Formatted:** Font color: Text 1

**Formatted:** Font color: Text 1

**Formatted:** Font: 10 pt, Font color: Text 1

**Formatted:** Font color: Text 1

**Formatted:** Indent: Left: 0", First line: 0"

**Formatted:** Font color: Text 1

**Formatted:** Font: 10 pt, Font color: Text 1

**Formatted:** Font color: Text 1

**Deleted:** o

**Formatted:** Font color: Text 1

**Deleted:** a

**Formatted:** Font color: Text 1

**Formatted:** Font: 10 pt, Font color: Text 1

**Formatted:** Font color: Text 1

**Formatted:** Font: 10 pt, Font color: Text 1

**Formatted:** Font color: Text 1

**Deleted:** 25¶

Chameides, W. L., Lindsay, R. W., Richardson, J., and Kiang, C. S.: The role of biogenic hydrocarbons in urban photochemical smog - Atlanta as a case study, Science, 241, 1473-1475, 10.1126/science.3420404, 1988.

Cheng, Y., Wang, Y. H., Zhang, Y. Z., Chen, G., Crawford, J. H., Kleb, M. M., Diskin, G. S., and Weinheimer, A. J.: Large biogenic contribution to boundary layer O-3-CO regression slope in summer, Geophysical Research Letters, 44, 7061-7068, 10.1002/2017gl074405, 2017.

Conny, J. M., and Currie, L. A.: The isotopic characterization of methane, non-methane hydrocarbons and formaldehyde in the troposphere, Atmospheric Environment, 30, 621-638, 10.1016/1352-2310(95)00305-3, 1996.

Conny, J. M., Verkouteren, R. M., and Currie, L. A.: Carbon 13 composition of tropospheric CO in Brazil: A model scenario during the biomass burn season, J. Geophys. Res.-Atmos., 102, 10683-10693, 10.1029/97jd00407, 1997.

Daniel, J. S., and Solomon, S.: On the climate forcing of carbon monoxide, J. Geophys. Res.-Atmos., 103, 13249-13260, 10.1029/98jd00822, 1998.

Duncan, B. N., Logan, J. A., Bey, I., Megretskaia, I. A., Yantosca, R. M., Novelli, P. C., Jones, N. B., and Rinsland, C. P.: Global budget of CO, 1988–1997: Source estimates and validation with a global model, Journal of Geophysical Research: Atmospheres, 112, D22301, 10.1029/2007jd008459, 2007.

Granier, C., Bessagnet, B., Bond, T., D'Angiola, A., van der Gon, H. D., Frost, G. J., Heil, A., Kaiser, J. W., Kinne, S., Klimont, Z., Kloster, S., Lamarque, J. F., Liousse, C., Masui, T., Meleux, F., Mieville, A., Ohara, T., Raut, J. C., Riahi, K., Schultz, M. G., Smith, S. J., Thompson, A., van Aardenne, J., van der Werf, G. R., and van Vuuren, D. P.: Evolution of anthropogenic and biomass burning emissions of air pollutants at global and regional scales during the 1980-2010 period, Clim. Change, 109, 163-190, 10.1007/s10584-011-0154-1, 2011.

Griffin, R. J., Chen, J. J., Carmody, K., Vutukuru, S., and Dabdub, D.: Contribution of gas phase oxidation of volatile organic compounds to atmospheric carbon monoxide levels in two areas of the United States, J. Geophys. Res.-Atmos., 112, 19, 10.1029/2006jd007602, 2007.

Gros, V., Braunlich, M., Röckmann, T., Jockel, P., Bergamaschi, P., Brenninkmeijer, C. A. M., Rom, W., Kutschera, W., Kaiser, A., Scheel, H. E., Mandl, M., van der Plicht, J., and Possnert, G.: Detailed analysis of the isotopic composition of CO and characterization of the air masses arriving at Mount Sonnblick (Austrian Alps), Journal of Geophysical Research, 106, 3179-3193, 2001.

Guenther, A., Hewitt, C. N., Erickson, D., Fall, R., Geron, C., Graedel, T., Harley, P., Klinger, L., Lerdau, M., McKay, W. A., Pierce, T., Scholes, B., Steinbrecher, R., Tallamraju, R.,

**Deleted:** ¶

**Formatted:** Font: 10 pt, Font color: Text 1

**Formatted:** Font color: Text 1

**Formatted:** Font: 10 pt, Font color: Text 1

**Formatted:** Font color: Text 1

**Formatted:** Font: 10 pt, Font color: Text 1

**Formatted:** Font color: Text 1

**Formatted:** Font: 10 pt, Font color: Text 1

**Formatted:** Font color: Text 1

**Formatted:** Font: 10 pt, Font color: Text 1

**Formatted:** Font color: Text 1

**Formatted:** Font: 10 pt, Font color: Text 1

**Formatted:** Font color: Text 1

**Formatted:** Font: 10 pt, Font color: Text 1

**Formatted:** Font color: Text 1

**Formatted:** Font: 10 pt, Font color: Text 1

**Formatted:** Font color: Text 1

**Deleted:** o

**Formatted:** Font color: Text 1

**Formatted:** Font: 10 pt, Font color: Text 1

**Formatted:** Font color: Text 1

**Deleted:** 26¶

Taylor, J., and Zimmerman, P.: A global model of natural volitile organic compound emissions, J. Geophys. Res.-Atmos., 100, 8873-8892, 10.1029/94jd02950, 1995.

Guenther, A. B., Jiang, X., Heald, C. L., Sakulyanontvittaya, T., Duhl, T., Emmons, L. K., and Wang, X.: The Model of Emissions of Gases and Aerosols from Nature version 2.1 (MEGAN2.1): an extended and updated framework for modeling biogenic emissions, Geosci. Model Dev., 5, 1471-1492, 10.5194/gmd-5-1471-2012, 2012.

Guenther, A. B., Zimmerman, P. R., Harley, P. C., Monson, R. K., and Fall, R.: Isoprene and monoterpene emission rate variability - model evaluations and sensitivity analyses, J. Geophys. Res.-Atmos., 98, 12609-12617, 10.1029/93jd00527, 1993.

Harley, C. P., Monson, K. R., and Lerdau, T. M.: Ecological and evolutionary aspects of isoprene emission from plants, Oecologia, 118, 109-123, 10.1007/s004420050709, 1999.

Hatakeyama, S., Izumi, K., Fukuyama, T., Akimoto, H., and Washida, N.: Reactions of OH with alpha-pinene and beta-pinene in air- estimate of global CO production from the atmospheric oxidation of terpenes, J. Geophys. Res.-Atmos., 96, 947-958, 10.1029/90jd02341, 1991.

Helmig, D., Greenberg, J., Guenther, A., Zimmerman, P., and Geron, C.: Volatile organic compounds and isoprene oxidation products at a temperate deciduous forest site, J. Geophys. Res.-Atmos., 103, 22397-22414, 10.1029/98jd00969, 1998.

Holloway, T., Levy, H., and Kasibhatla, P.: Global distribution of carbon monoxide, J. Geophys. Res.-Atmos., 105, 12123-12147, 10.1029/1999jd901173, 2000.

Huff, A. K., and Thiemens, M. H.: O-17/O-16 and O-18/O-16 isotope measurements of atmospheric carbon monoxide and its sources, Geophysical Research Letters, 25, 3509-3512, 10.1029/98gl02603, 1998.

Isobe, T., Feigelson, E. D., Akritas, M. G., and Babu, G. J.: Linear Regression in Astronomy, Astrophys. J., 364, 104-113, 10.1086/169390, 1990.

Kanakidou, M., and Crutzen, P. J.: The photochemical source of carbon monoxide: Importance, uncertainties and feedbacks, Chemosphere - Global Change Science, 1, 91-109, 1999.

Keeling, C. D.: The concentration and isotopic abundances of atmospheric carbon dioxide in rural areas, Geochimica Et Cosmochimica Acta, 13, 322-334, 10.1016/0016-7037(58)90033-4, 1958.

Levin, I., Kromer, B., Schmidt, M., and Sartorius, H.: A novel approach for independent budgeting of fossil fuel CO2over Europe by14CO2observations, Geophysical Research Letters, 30, 10.1029/2003gl018477, 2003.

**Deleted:** ¶

**Formatted:** Font: 10 pt, Font color: Text 1

**Formatted:** Font color: Text 1

**Formatted:** Font color: Text 1

**Deleted:** ¶

**Formatted:** Font color: Text 1

**Formatted:** Indent: Left: 0", First line: 0"

**Formatted:** Font: 10 pt, Font color: Text 1

**Formatted:** Font color: Text 1

**Formatted:** Font color: Text 1

**Formatted:** Font: 10 pt, Font color: Text 1

**Formatted:** Font color: Text 1

**Formatted:** Font: 10 pt, Font color: Text 1

**Formatted:** Font color: Text 1

**Formatted:** Font: 10 pt, Font color: Text 1

**Formatted:** Font color: Text 1

**Formatted:** Font: 10 pt, Font color: Text 1

**Formatted:** Font color: Text 1

**Formatted:** Font: 10 pt, Font color: Text 1

**Formatted:** Font color: Text 1

**Formatted:** Font: 10 pt, Font color: Text 1

**Formatted:** Font color: Text 1

**Formatted:** Font: 10 pt, Font color: Text 1

**Deleted:** 27¶

Logan, J. A., Prather, M. J., Wopsy, S. C., and McElroy, M. B.: Tropospheric Chemistry: A Global Perspective, Journal of Geophysical Research, 86, 7210-7254, 1981.

Mak, J. E., and Kra, G.: The isotopic composition of carbon monoxide at Montauk Point, Long Island, ChemoSphere- Global Change Science, 1, 205-218, 1999.

Mak, J. E., Kra, G., Sandomenico, T., and Bergamaschi, P.: The seasonally varying isotopic composition of the sources of carbon monoxide at Barbados, West Indies, J. Geophys. Res.-Atmos., 108, 10.1029/2003jd003419, 2003.

Mak, J. E., and Yang, W.: Technique for Analysis of Air Samples for 13C and 18O in Carbon Monoxide via Continuous-Flow Isotope Ratio Mass Spectrometry, Analyitical Chemistry, 70, 5159-5161, 1998.

Manning, M. R., Brenninkmeijer, C. A. M., and Allan, W.: Atmospheric carbon monoxide budget of the southern hemisphere: Implications of13C/12C measurements, Journal of Geophysical Research, 102, 10673, 10.1029/96jd02743, 1997.

Miles, N. L., Richardson, S. J., Lauvaux, T., Davis, K. J., Balashov, N. V., Deng, A., Turnbull, J. C., Sweeney, C., Gurney, K. R., Patarasuk, R., Razlivanov, I., Cambaliza, M. O. L., and Shepson, P. B.: Quantification of urban atmospheric boundary layer greenhouse gas dry mole fraction enhancements in the dormant season: Results from the Indianapolis Flux Experiment (INFLUX), Elem Sci Anth, 5, http://doi.org/10.1525/elementa.127, 2017.

Miller, J. B., Lehman, S. J., Montzka, S. A., Sweeney, C., Miller, B. R., Karion, A., Wolak, C., Dlugokencky, E. J., Southon, J., Turnbull, J. C., and Tans, P. P.: Linking emissions of fossil fuel CO2 and other anthropogenic trace gases using atmospheric (CO2)-C-14, J. Geophys. Res.-Atmos., 117, 23, 10.1029/2011jd017048, 2012.

Miller, J. B., and Tans, P. P.: Calculating isotopic fractionation from atmospheric measurements at various scales, Tellus Ser. B-Chem. Phys. Meteorol., 55, 207-214, 10.1034/j.1600-0889.2003.00020.x, 2003.

Park, K., Emmons, L. K., Wang, Z. H., and Mak, J. E.: Joint Application of Concentration and delta O-18 to Investigate the Global Atmospheric CO Budget, Atmosphere, 6, 547-578, 10.3390/atmos6050547, 2015.

Popa, M. E., Vollmer, M. K., Jordan, A., Brand, W. A., Pathirana, S. L., Rothe, M., and Röckmann, T.: Vehicle emissions of greenhouse gases and related tracers from a tunnel study: CO: CO2, N2O: CO2, CH4 : CO2, O-2 : CO2 ratios, and the stable isotopes C-13 and O-18 in CO2 and CO, Atmospheric Chemistry and Physics, 14, 2105-2123, 10.5194/acp-14-2105-2014, 2014.

**Deleted:** ¶

**Formatted:** Font color: Text 1

**Formatted:** Font: 10 pt, Font color: Text 1

**Formatted:** Font color: Text 1

**Formatted:** Font: 10 pt, Font color: Text 1

**Formatted:** Font color: Text 1

**Formatted:** Font color: Text 1

**Formatted:** Font: 10 pt, Font color: Text 1

**Formatted:** Font color: Text 1

**Formatted:** Font: 10 pt, Font color: Text 1

**Formatted:** Font color: Text 1

**Formatted:** Font: 10 pt, Font color: Text 1

**Formatted:** Font color: Text 1

**Formatted:** Font: 10 pt, Font color: Text 1

**Formatted:** Font color: Text 1

**Formatted:** Font: 10 pt, Font color: Text 1

**Formatted:** Font color: Text 1

**Formatted:** Font: 10 pt, Font color: Text 1

**Formatted:** Font color: Text 1

**Deleted:** o

**Formatted:** Font color: Text 1

**Formatted:** Font: 10 pt, Font color: Text 1

**Formatted:** Font color: Text 1

**Deleted:** 28¶

Röckmann, T., and Brenninkmeijer, C. A. M.: The error in conventionally reported 13C/12C ratios of atmospheric CO due to the presence of mass independent oxygen isotope enrichment, Geophysical Research Letters, 25, 3163-3166, 1998.

Röckmann, T., Brenninkmeijer, C. A. M., Neeb, P., and Crutzen, P. J.: Ozonolysis of nonmethane hydrocarbons as a source of the observed mass independent oxygen isotope enrichment in tropospheric CO, J. Geophys. Res.-Atmos., 103, 1463-1470, 10.1029/97jd02929, 1998a.

Röckmann, T., Brenninkmeijer, C. A. M., Saueressig, G., Bergamaschi, P., Crowley, J. N., Fischer, H., and Crutzen, P. J.: Mass-Independent Oxygen Isotope Fractionation in Atmospheric CO as a Result of the Reaction CO+OH, Science, 281, 544-546, 10.1126/science.281.5376.544, 1998b.

Röckmann, T., Jockel, P., Gros, V., Bräunlich, M., Possnert, G., and Brenninkmeijer, C. A. M.: Using 14C, 13C, 18O, and 17O isotopic variations to provide insights into the high northern latitude surface CO inventory, Atmospheric Chemistry and Physics, 2, 147-159, 2002.

Saurer, M., Prevot, A. S. H., Dommen, J., Sandradewi, J., Baltensperger, U., and Siegwolf, R. T. W.: The influence of traffic and wood combustion on the stable isotopic composition of carbon monoxide, Atmospheric Chemistry and Physics, 9, 3147-3161, 2009.

Schutze, M.: New Oxidation Means for the Quantitative Crossover from carboxide to carbon dioxide- Article on the chemsitry of iodine pentoxide, Berichte der Deutschen Chemischen Gesellschaft, 77, 484-487, 1944.

Sharkey, T. D., Loreto, F., Delwiche, C. F., and Treichel, I. W.: Fractionation of carbon isotopes during biogenesis of atmospheric isoprene Plant Physiol., 97, 463-466, 10.1104/pp.97.1.463, 1991.

Stevens, C. M., Kaplan, L., Gorse, R., Durkee, S., Compton, M., Cohen, S., and Bielling, K.: The kinetic isotope effect for carbon and oxygen in the reaction CO + OH, Int. J. Chem. Kinet., 12, 935-948, 10.1002/kin.550121205, 1980.

Stevens, C. M., and Krout, L.: Method for the Determination of the Concentration and of the Carbon and Oxygen Isotopic Composition of Atmospheric Carbon Monoxide, International Journal of Mass Spectrometry and Ion Physics, 8, 265-275, 1972.

Stevens, C. M., Krout, L., Walling, D., and Venters, A.: The Isotopic Composition of Atmospheric Carbon Monoxide, Earth and Planetary Science Letters, 16, 147-165, 1972.

Stevens, C. M., and Wagner, A. F.: The role of isotope fractionation effects in atmospheric chemsitry, Z. Naturfors. Sect. A-J. Phys. Sci., 44, 376-384, 1989.

**Deleted:** ¶

**Deleted:** Rockmann

**Formatted:** Font color: Text 1

**Formatted:** Font: 10 pt, Font color: Text 1

**Formatted:** Font color: Text 1

**Deleted:** o

**Formatted:** Font color: Text 1

**Formatted:** Font color: Text 1

**Formatted:** Font color: Text 1

**Formatted:** Font color: Text 1

**Formatted:** Font: 10 pt, Font color: Text 1

**Formatted:** Font color: Text 1

**Formatted:** Font: 10 pt, Font color: Text 1

**Formatted:** Font color: Text 1

**Formatted:** Font: 10 pt, Font color: Text 1

**Formatted:** Font color: Text 1

**Formatted:** Font color: Text 1

**Formatted:** Font: 10 pt, Font color: Text 1

**Formatted:** Font color: Text 1

**Deleted:** 29¶

Strode, S. A., Liu, J. H., Lait, L., Commane, R., Daube, B., Wofsy, S., Conaty, A., Newman, P., and Prather, M.: Forecasting carbon monoxide on a global scale for the ATom-1 aircraft mission: insights from airborne and satellite observations and modeling, Atmospheric Chemistry and Physics, 18, 10955-10971, 10.5194/acp-18-10955-2018, 2018.

Stuiver, M., and Polach, H. A.: Reporting of C-14 data - discussion, Radiocarbon, 19, 355-363, 1977.

Turnbull, J., Guenther, D., Karion, A., Sweeney, C., Anderson, E., Andrews, A., Kofler, J., Miles, N., Newberger, T., and Richardson, S.: An integrated flask sample collection system for greenhouse gas measurements, Atmospheric Measurement Techniques, 5, 2321-2327, 2012.

Turnbull, J. C., Karion, A., Davis, K. J., Lauvaux, T., Miles, N. L., Richardson, S. J., Sweeney, C., McKain, K., Lehman, S. J., Gurney, K. R., Patarasuk, R., Liang, J. M., Shepson, P. B., Heimburger, A., Harvey, R., and Whetstone, J.: Synthesis of Urban CO2 Emission Estimates from Multiple Methods from the Indianapolis Flux Project (INFLUX), Environ. Sci. Technol., 53, 287-295, 10.1021/acs.est.8b05552, 2019.

Turnbull, J. C., Miller, J. B., Lehman, S. J., Tans, P. P., Sparks, R. J., and Southon, J.: Comparison of 14CO2, CO, and SF6 as tracers for recently added fossil fuel CO2in the atmosphere and implications for biological CO2 exchange, Geophysical Research Letters, 33, 10.1029/2005gl024213, 2006.

Turnbull, J. C., Sweeney, C., Karion, A., Newberger, T., Lehman, S. J., Tans, P. P., Davis, K. J., Lauvaux, T., Miles, N. L., and Richardson, S. J.: Toward quantification and source sector identification of fossil fuel CO2 emissions from an urban area: Results from the INFLUX experiment, Journal of Geophysical Research: Atmospheres, 2015.

Vimont, I. J., Turnbull, J. C., Petrenko, V. V., Place, P. F., Karion, A., Miles, N. L., Richardson, S. J., Gurney, K. R., Patarasuk, R., Sweeney, C., Vaughn, B., and White, J. W. C.: Carbon monoxide isotopic measurements in Indianapolis constrain urban source isotopic signatures and support mobile fossil fuel emissions as the dominant wintertime CO source, Elem Sci Anth, 5, 10.1525/elementa.136, 2017.

Zhou, Y., Mao, H., Demerjian, K., Hogrefe, C., and Liu, J.: Regional and hemispheric influences on temporal variability in baseline carbon monoxide and ozone over the Northeast US, Atmospheric Environment, 164, 309-324, 10.1016/j.atmosenv.2017.06.017, 2017.

Zobitz, J. M., Keener, J. P., Schnyder, H., and Bowling, D. R.: Sensitivity analysis and quantification of uncertainty for isotopic mixing relationships in carbon cycle research, Agric. For. Meteorol., 136, 56-75, 10.1016/j.agrformet.2006.01.003, 2006.

**Deleted:** ¶

**Formatted:** Font color: Text 1

**Formatted:** Font: 10 pt, Font color: Text 1

**Formatted:** Font color: Text 1

**Formatted:** Font: 10 pt, Font color: Text 1

**Formatted:** Font color: Text 1

**Formatted:** Font: 10 pt, Font color: Text 1

**Formatted:** Font color: Text 1

**Formatted:** Font: 10 pt, Font color: Text 1

**Formatted:** Font color: Text 1

**Formatted:** Font: 10 pt, Font color: Text 1

**Formatted:** Font color: Text 1

**Formatted:** Font: 10 pt, Font color: Text 1

**Formatted:** Font color: Text 1

**Formatted:** Font: 10 pt, Font color: Text 1

**Formatted:** Font color: Text 1

**Deleted:** 30¶

# Figures and Tables

**Table 1**: The four main CO sources and the OH sink listed with their isotopic signatures and uncertainties.

**Isotopic Sources and Sinks**

| Source/Sink | $\delta^{13}$C (VPDB) | Uncertainty | $\delta^{18}$O (VSMOW) | Uncertainty |
|---|---|---|---|---|
| **Global Sources** | | | | |
| Fossil Fuel Combustion [a,b] | -27.5‰ | ≤1‰ | 23.5‰ | ≤1‰ |
| Biomass Burning [c,d,e,f,*] | -12-25‰ | 1-3‰ | 10-18‰ | 1-3‰ |
| $CH_4$ Oxidation [f,g] | -52.6‰ | 1-3‰ | 0‰ | >3‰ |
| VOC Oxidation (prior estimates) [c,g] | -32‰ | 1-3‰ | 0‰ | >3‰ |
| **VOC Oxidation (this study)** | **-32.8‰** | **0.5‰** | **3.6‰** | **1.2‰** |
| CO Oxidation by OH Fractionation Factors [**] | ~ 5‰ | -3‰ – +6‰ | ~-10‰ | -11‰ – -9‰ |

[a] Stevens et al. (1972)

[b] Brenninkmeijer (1993)

[c] Stevens and Wagner (1989)

[d] Bergamaschi et al. (1998)

[e] Saurer et al. (2009)

[f] Manning et al. (1997)

[g] Brenninkmeijer and Röckmann (1997)

* Isotopic signatures vary based on type of vegetation burned (C3/C4) and temperature of fire

** These factors are the "best estimate" provided Brenninkmeijer et al. (1999). These are based on data from Röckmann et al. (1998), and Stevens et al. (1980). These studies report pressure dependent fractionation factors for $\varepsilon^{13}$C and very little pressure dependence for ε18O (pressure range ~200 mbar to 1100 mbar). The variability in the fractionation factors is reported here as the uncertainty.

**Deleted:** ¶
*<object>*

**Deleted:** ¶
¶
¶

**Formatted:** Font: 10 pt, Font color: Text 1

**Formatted:** Font color: Text 1

**Deleted:** , with values as in (Brenninkmeijer et al., 1999)...*<object>*
*<object>*

**Formatted:** Font color: Text 1

**Formatted:** Font: (Default) Cambria, 10 pt, Font color: Text 1

**Deleted:** *<object>*

**Formatted:** Centered

**Deleted:** 31¶

**Table 2:** VOC signature calculation table using data from Indianapolis, IN, USA. $\Delta^{14}CO_2$ and $X_{CO2-FF}$ values reported from Turnbull et al. (2015,2018). $X_{CO-ENH}$ 1σ uncertainty is ± 0.7 nmol:mol, $\Delta^{14}CO_2$ 1σ uncertainty is ~±1.8‰ (Turnbull et al., 2015,2018), and $X_{CO2-FF}$ 1σ uncertainty is ±1 µmol:mol (Turnbull et al., 2015,2018).

| Date | $X_{CO-ENH}$ (nmol:mol) | $\Delta^{14}CO_2$ (‰) | $X_{CO2-FF}$ (µmol:mol) | $X_{CO-FF}$ (nmol:mol) | $X_{CO-VOC}$ (nmol:mol) | $\delta^{13}C_{VOC}$ (‰) | $\delta^{18}O_{VOC}$ (‰) |
|---|---|---|---|---|---|---|---|
| 5/5/15 | 11.1 | 10.6 | 0.7 | 5.1 | 6.0 | -31.2 | 8.0 |
| 5/12/14 | 9.5 | 17.4 | 0.6 | 4.0 | 5.5 | -31.0 | 8.6 |
| 5/28/14 | 12.5 | 14.6 | 0.8 | 5.9 | 6.6 | -31.2 | 7.8 |
| 6/8/15 | 38.7 | 9.4 | 3.2 | 22.2 | 16.6 | -32.1 | 5.5 |
| 6/30/15 | 12.7 | 12.5 | 1.3 | 8.9 | 3.8 | -34.0 | 0.1 |
| 6/3/14 | 13.2 | 18.0 | 1.4 | 9.6 | 3.7 | -34.5 | -1.1 |
| 7/27/13 | 19.9 | 22.7 | 1.9 | 13.1 | 6.8 | -33.2 | 2.4 |
| 8/1/13 | 12.3 | 26.1 | 1.3 | 9.4 | 2.9 | -35.6 | -4.4 |
| 8/20/14 | 9.8 | 16.1 | 0.8 | 5.3 | 4.5 | -31.8 | 6.3 |
| 8/12/14 | 25.0 | 17.7 | 2.6 | 18.1 | 6.9 | -34.5 | -1.3 |
| 8/21/14 | 27.1 | 9.6 | 2.6 | 17.9 | 9.2 | -33.2 | 2.4 |
| 9/2/14 | 25.6 | 12.6 | 1.4 | 9.9 | 15.7 | -30.8 | 9.2 |

**Deleted:** ¶
*<object>*

**Deleted:** *<object>*¶
¶

**Formatted:** Font color: Text 1

**Formatted:** No page break before

**Formatted:** Font: 10 pt, Font color: Text 1

**Formatted:** Font color: Text 1

**Deleted:**

| Date | $X_{CO-ENH}$ (nmol:mol) | $\Delta^{14}CO_2$ (‰) |
|---|---|---|
| 5/5/15 | 11.1 | 10.6 |
| 5/12/14 | 9.5 | 17.4 |
| 5/28/14 | 12.5 | 14.6 |
| 5/16/14 | 20.3 | 6.7 |
| 6/8/15 | 38.7 | 9.4 |
| 6/30/15 | 12.7 | 12.5 |
| 6/3/14 | 13.2 | 18.0 |
| 7/29/13 | 27.5 | 23.9 |
| 7/27/13 | 19.9 | 22.7 |
| 8/1/13 | 12.3 | 26.1 |
| 8/22/14 | 46.2 | 5.2 |
| 8/20/14 | 9.8 | 16.1 |
| 8/12/14 | 25.0 | 17.7 |
| 8/21/14 | 27.1 | 9.6 |
| 9/1/14 | 9.2 | 19.4 |
| 9/2/14 | 25.6 | 12.6 |

**Deleted:** 32¶

**Figure 1:** Satellite Image of INFLUX tower locations. Arrow indicates predominant wind direction during sampling. Samples from this study were taken from towers 1 and 2 (shown). Also note the vegetation cover between the two towers.

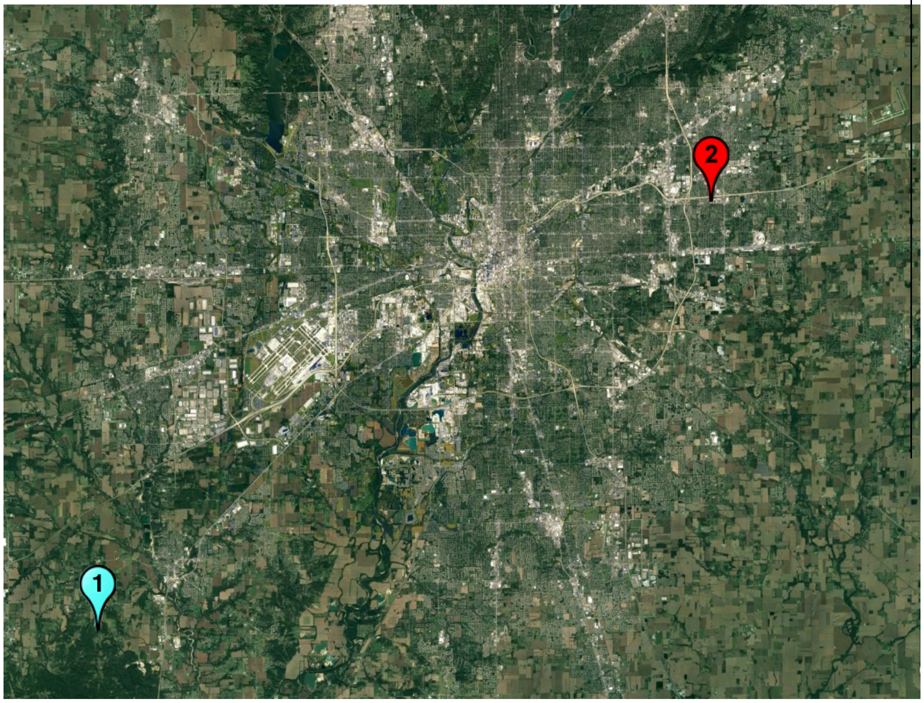

**Deleted:** ¶
*<object>*

**Deleted:**

| Date | $X_{CO\text{-}ENH}$ (nmol:mol) | $\Delta^{14}CO_2$ (‰) |
|---|---|---|
| 5/5/15 | 11.1 | 10.6 |
| 5/12/14 | 9.5 | 17.4 |
| 5/28/14 | 12.5 | 14.6 |
| 5/16/14 | 20.3 | 6.7 |
| 6/8/15 | 38.7 | 9.4 |
| 6/30/15 | 12.7 | 12.5 |
| 6/3/14 | 13.2 | 18.0 |
| 7/29/13 | 27.5 | 23.9 |
| 7/27/13 | 19.9 | 22.7 |
| 8/1/13 | 12.3 | 26.1 |
| 8/22/14 | 46.2 | 5.2 |
| 8/20/14 | 9.8 | 16.1 |
| 8/12/14 | 25.0 | 17.7 |
| 8/21/14 | 27.1 | 9.6 |
| 9/1/14 | 9.2 | 19.4 |
| 9/2/14 | 25.6 | 12.6 |

**Formatted:** Font color: Text 1

**Formatted:** Font: 10 pt, Font color: Text 1

**Formatted:** Font color: Text 1

**Deleted:** 33¶

**Figure 2:** Indianapolis Miller Tans plots for late spring through summer (May, June, July, August, September). The error bars represent the propagated error for the calculation of the enhancements (see text for details).

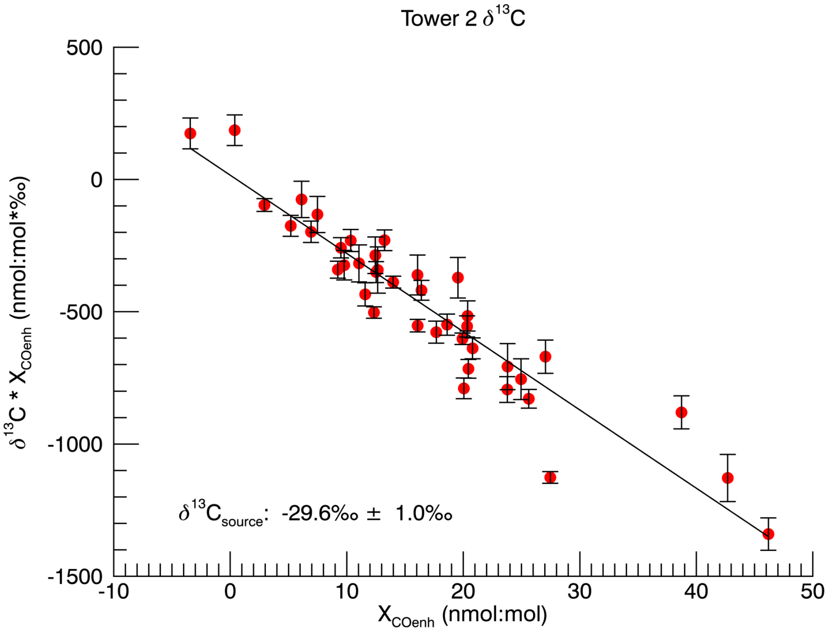

**Deleted:** ¶
***<object>***

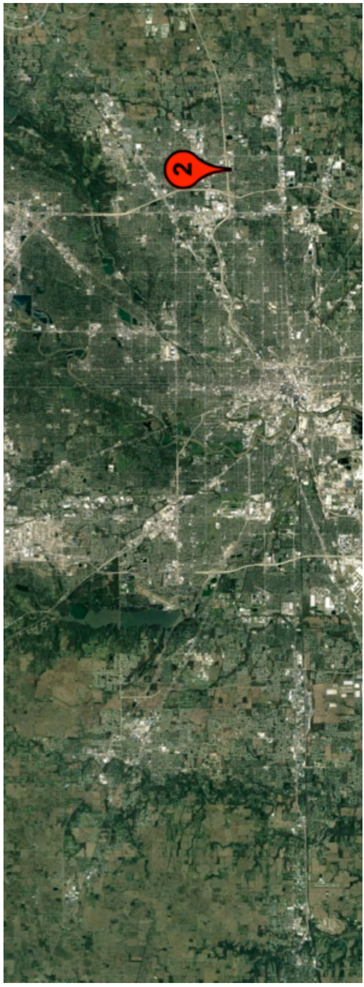

**Deleted:**
¶
¶
¶
... [172]

**Formatted:** Font color: Text 1

**Formatted:** No page break before

**Formatted:** Font: (Default) Cambria, 10 pt, Font color: Text 1

**Deleted:** 34¶

**Deleted:** ¶
***<object>***

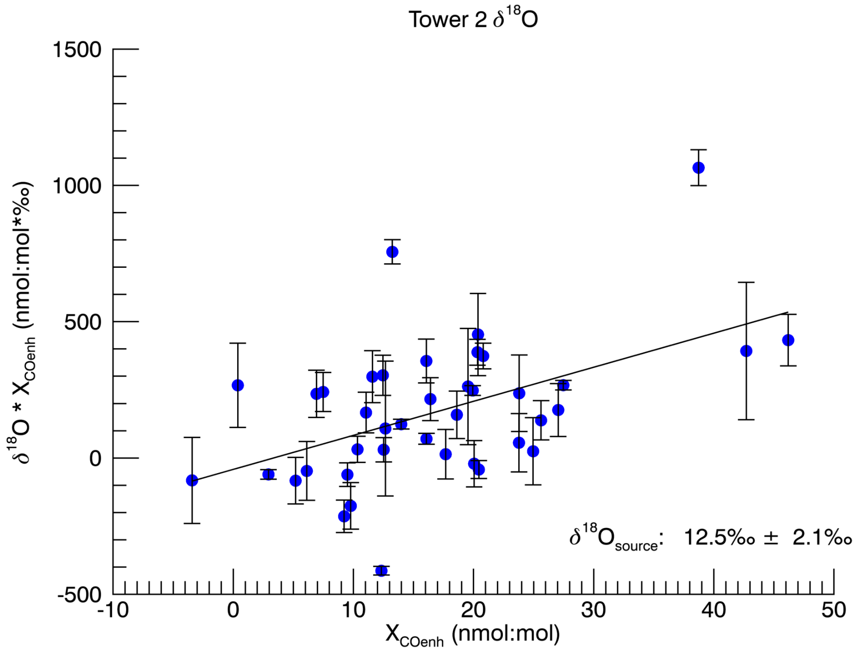

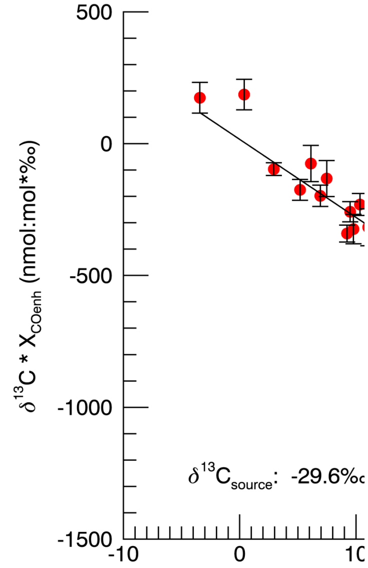

**Deleted:** ... [173]

**Formatted:** Font color: Text 1

**Deleted:** 35¶

**Deleted:** ¶
***<object>***

**Figure 3:** Time series of towers 1 and 2 at Indianapolis. These data were previously shown in Vimont et al. (2017), but are reproduced here for the convenience of the reader. The curves shown are for sighting purposes only. They are a simple single harmonic polynomial smoothing and are meant to aid the reader in viewing the seasonal variability. The error bars represent 1σ uncertainty. CO mole fraction 1σ uncertainty is ± 0.5 nmol:mol. The red arrows indicate the time periods used in this study, and these data, along with $\delta^{13}$C and $\delta^{18}$O 1σ uncertainty is listed in the supplementary material (Table S2).

**Deleted:** table

**Formatted:** Font color: Text 1

**Formatted:** Font: 10 pt, Font color: Text 1

**Formatted:** Font color: Text 1

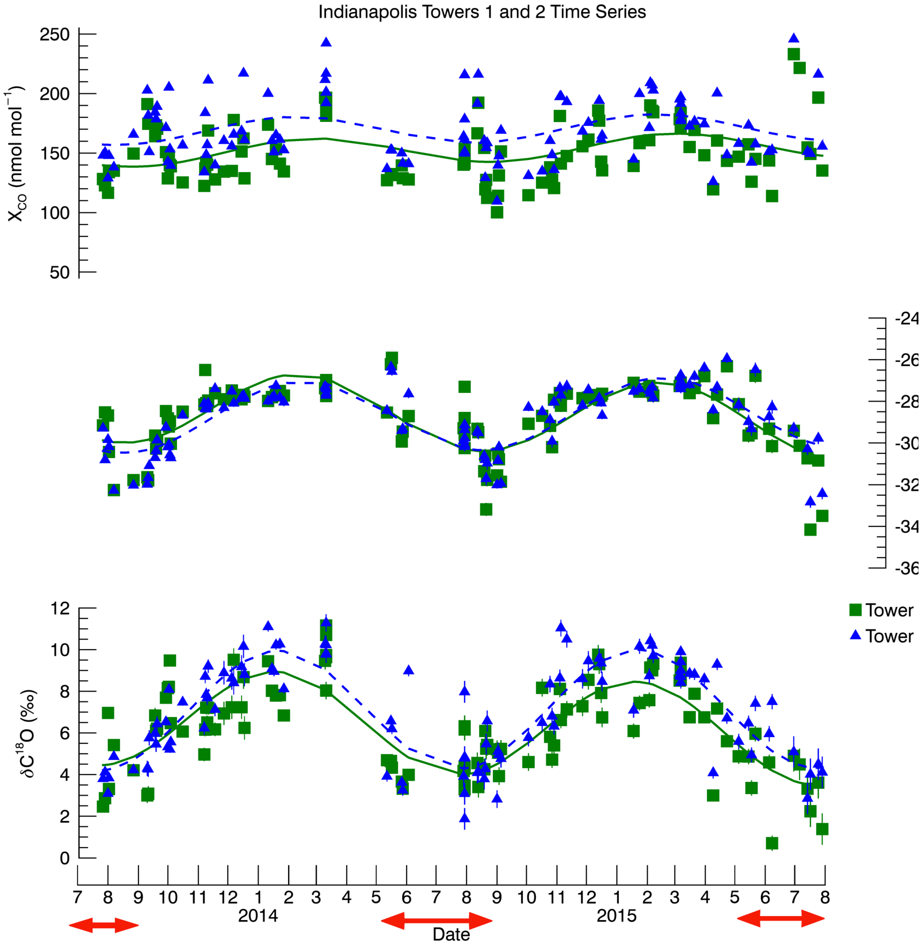

**Deleted:** 36¶

**Figure 4:** Time series for Beech Island, South Carolina. No curves were fit to the data due to the short time frame for the measurements. The error bars represent 1σ analytical uncertainty. CO mole fraction 1σ uncertainty is ±0.5 nmol:mol. Uncertainty for $\delta^{13}C$ and $\delta^{18}O$ is listed in the supplementary material (Table S3). The CO mole fraction data are taken from the NOAA GGGRN dataset (Andrews et al., 2009). The green and blue arrows indicate the summer and winter periods used in this study, respectively.

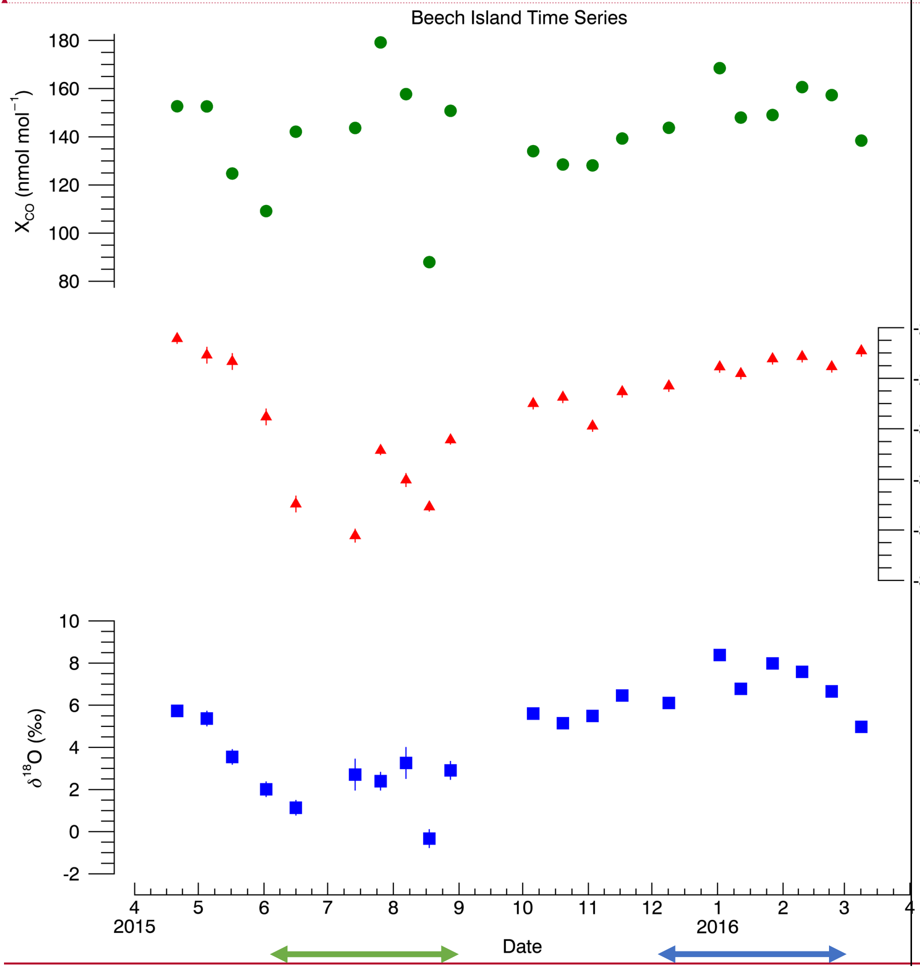

**Deleted:** ¶
***<object>***

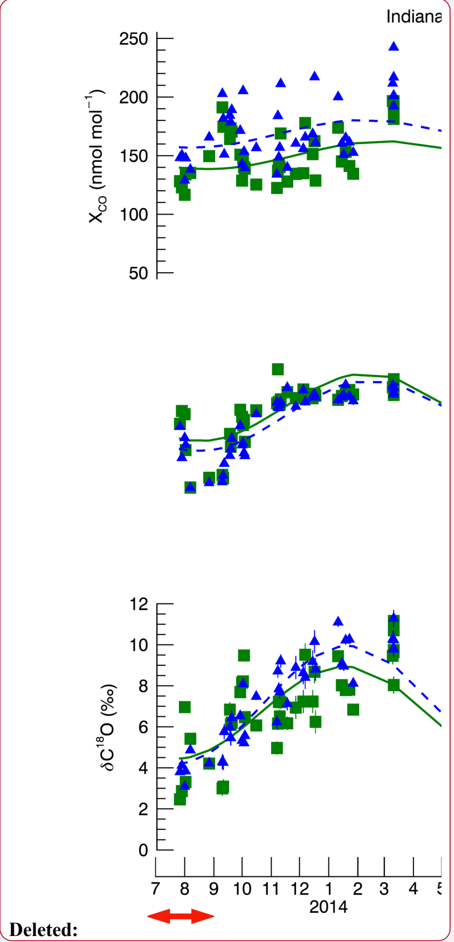

**Deleted:**

**Formatted:** Font color: Text 1

**Formatted:** Font color: Text 1

**Deleted:** table

**Deleted:** is

**Formatted:** Font color: Text 1

**Formatted:** Font color: Text 1

**Formatted:** Font: 10 pt, Font color: Text 1

**Formatted:** Font color: Text 1

**Deleted:** 37¶

**Figure 5:** Beech Island Keeling plots. The reported intercepts and uncertainties are the standard Monte Carlo simulation results. We also performed a bootstrap Monte Carlo. Those results are reported in the text.

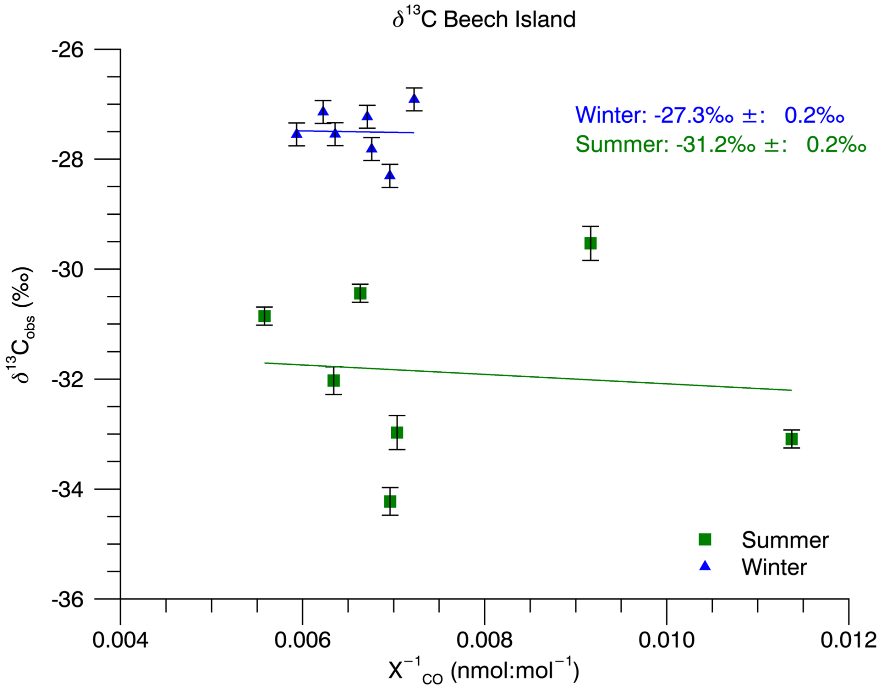

**Deleted:** ¶
***<object>***

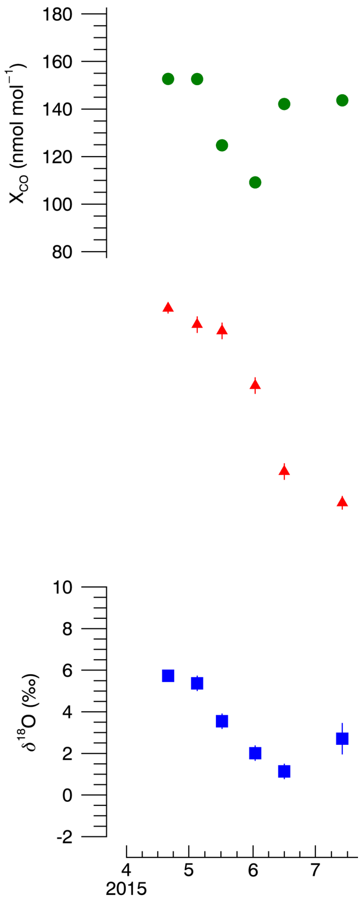

**Deleted:**

**Formatted:** Font color: Text 1

**Formatted:** Font: (Default) Cambria, 10 pt, Font color: Text 1

**Deleted:** 38¶

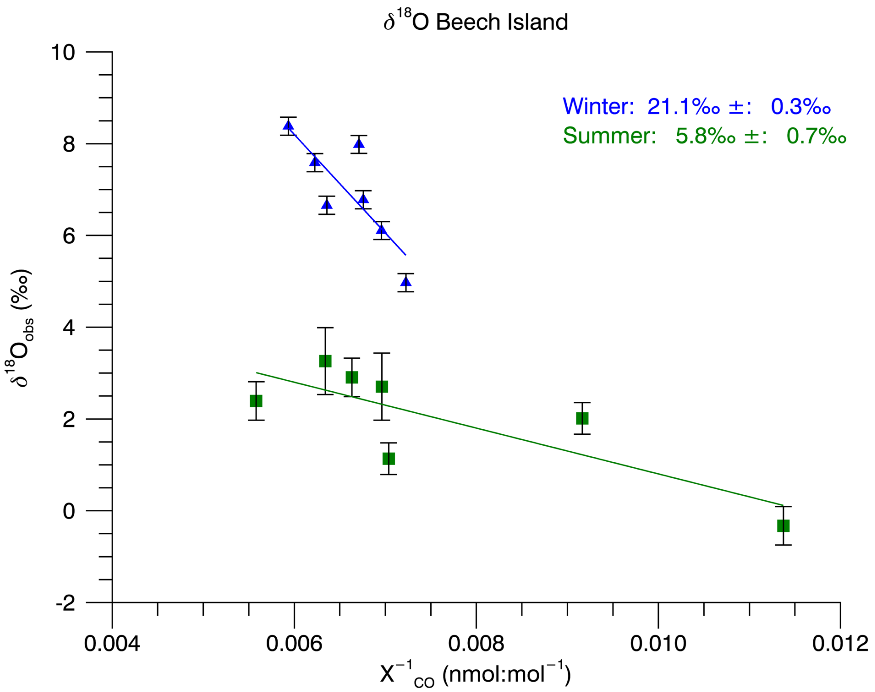

Deleted: ¶
*<object>*

Deleted: 39¶

**Figure 6:** Miller Tans Analysis of Beech Island seasonal source signatures using monthly means from Izaña, Tenerife (Bräunlich, 2000). Green squares indicate summer data, blue triangles indicate winter data. The $\delta^{13}C$ and $\delta^{18}O$ values reported are the mean of 10,000 regression slopes from our Monte Carlo simulation (section 2.5). The uncertainty is the standard deviation of the 10,000 slopes.

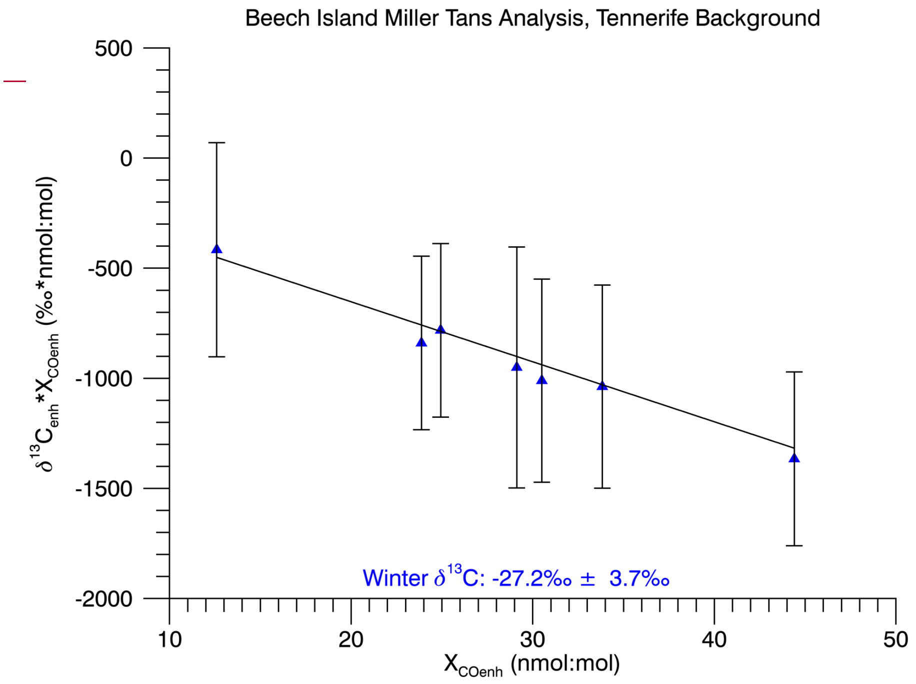

**Deleted:** ¶
*<object>*

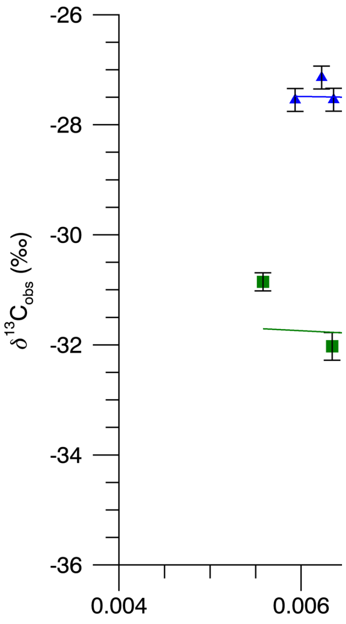

**Deleted:**
¶
... [174]

**Formatted:** Font color: Text 1

**Formatted:** No page break before

**Formatted:** Font: 10 pt, Font color: Text 1

**Formatted:** Font color: Text 1

**Deleted:** 40¶

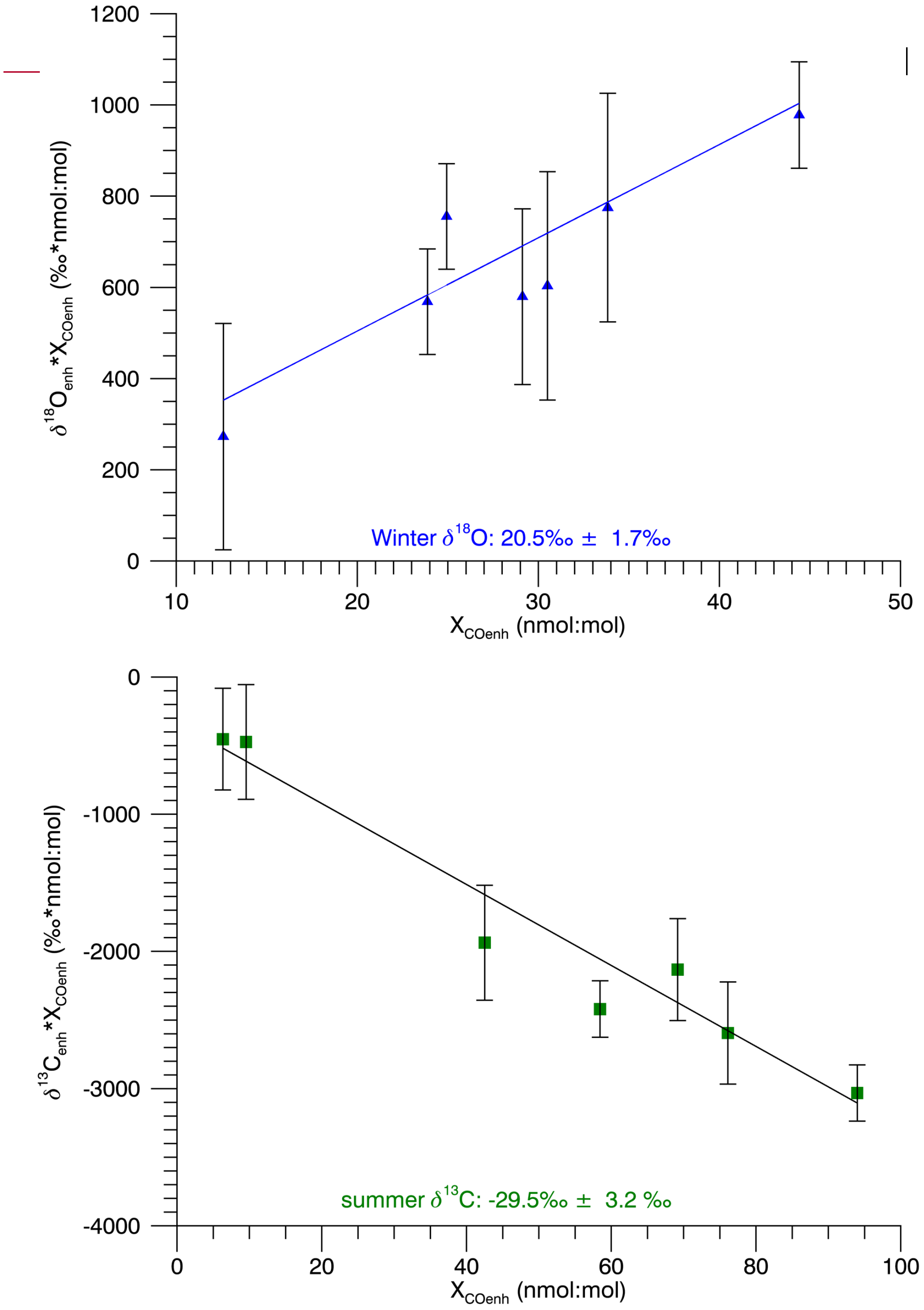

**Deleted:** ¶
***<object>***

**Deleted:** 41¶

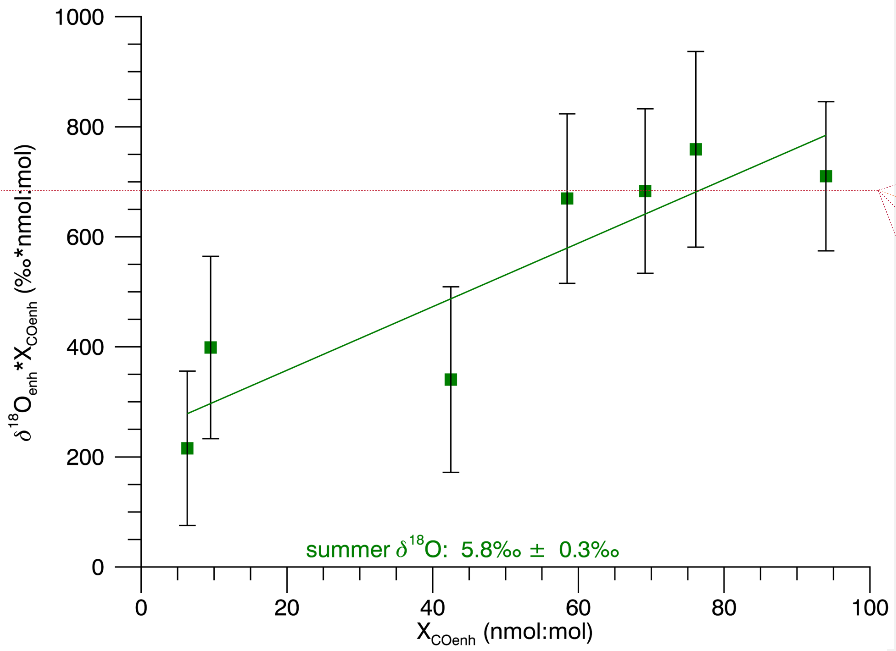

**Deleted:** ¶
*<object>*

**Deleted:** *<object><object>*

**Deleted:** ¶

**Deleted:** *<object><object><object><object><object><object><object><object><object><object><object><object><object><object><object><object>*

**Formatted:** Font: Cambria, Font color: Text 1

**Deleted:** 42¶

**Page 1: [1] Deleted** **Isaac J Vimont** **5/2/19 3:58:00 PM**

**Page 1: [2] Formatted** **Isaac J Vimont** **5/2/19 3:58:00 PM**

Position: Horizontal: Center, Relative to: Margin, Vertical: 0", Relative to: Paragraph, Wrap Around

**Page 1: [3] Formatted** **Isaac J Vimont** **5/2/19 3:58:00 PM**

Page Number

**Page 1: [4] Formatted** **Isaac J Vimont** **5/2/19 3:58:00 PM**

Page Number

**Page 1: [5] Style Definition** **Isaac J Vimont** **5/2/19 3:58:00 PM**

Comment Text: Font: (Default) Times New Roman, 10 pt

**Page 1: [6] Style Definition** **Isaac J Vimont** **5/2/19 3:58:00 PM**

Footer: Font: (Default) Times New Roman, 10 pt, Don't suppress line numbers

**Page 1: [7] Style Definition** **Isaac J Vimont** **5/2/19 3:58:00 PM**

EndNote Bibliography: Font:

**Page 1: [8] Style Definition** **Isaac J Vimont** **5/2/19 3:58:00 PM**

Balloon Text: Font: (Default) Times New Roman, 10 pt

**Page 1: [9] Style Definition** **Isaac J Vimont** **5/2/19 3:58:00 PM**

EndNote Bibliography Char: Font: 12 pt

**Page 1: [10] Style Definition** **Isaac J Vimont** **5/2/19 3:58:00 PM**

Normal: Font: (Default) +Body (Calibri), 12 pt, Hyphenate

**Page 1: [11] Formatted** **Isaac J Vimont** **5/2/19 3:58:00 PM**

Font color: Text 1

**Page 1: [12] Formatted** **Isaac J Vimont** **5/2/19 3:58:00 PM**

Level 1

**Page 1: [13] Formatted** **Isaac J Vimont** **5/2/19 3:58:00 PM**

Formatted

**Page 1: [14] Formatted** **Isaac J Vimont** **5/2/19 3:58:00 PM**

Font: 10 pt, Bold, Font color: Text 1

**Page 1: [15] Formatted** **Isaac J Vimont** **5/2/19 3:58:00 PM**

Font color: Text 1

**Page 1: [16] Formatted** **Isaac J Vimont** **5/2/19 3:58:00 PM**

Level 1

**Page 1: [17] Formatted** **Isaac J Vimont** **5/2/19 3:58:00 PM**

Font: 10 pt, Font color: Text 1

**Page 1: [18] Formatted** **Isaac J Vimont** **5/2/19 3:58:00 PM**

Font color: Text 1

**Page 1: [19] Formatted** **Isaac J Vimont** **5/2/19 3:58:00 PM**

Font: 10 pt, Font color: Text 1

**Page 1: [20] Formatted** **Isaac J Vimont** **5/2/19 3:58:00 PM**

Font color: Text 1

**Page 1: [21] Formatted** **Isaac J Vimont** **5/2/19 3:58:00 PM**

Font: 10 pt, Font color: Text 1

**Page 1: [22] Formatted** **Isaac J Vimont** **5/2/19 3:58:00 PM**

Font: 10 pt, Font color: Text 1, Not Superscript/ Subscript

**Page 1: [23] Formatted** **Isaac J Vimont** **5/2/19 3:58:00 PM**

Font: 10 pt, Font color: Text 1

**Page 1: [24] Formatted** **Isaac J Vimont** **5/2/19 3:58:00 PM**

Font: 10 pt, Font color: Text 1, Not Superscript/ Subscript

**Page 1: [25] Formatted** **Isaac J Vimont** **5/2/19 3:58:00 PM**

Font: 10 pt, Font color: Text 1

**Page 1: [26] Formatted** **Isaac J Vimont** **5/2/19 3:58:00 PM**

Font color: Text 1

**Page 1: [27] Formatted** **Isaac J Vimont** **5/2/19 3:58:00 PM**

Font: 10 pt, Font color: Text 1

**Page 1: [28] Formatted** **Isaac J Vimont** **5/2/19 3:58:00 PM**

Font color: Text 1

**Page 1: [29] Formatted** **Isaac J Vimont** **5/2/19 3:58:00 PM**

Font: 10 pt, Font color: Text 1, Not Superscript/ Subscript

**Page 1: [30] Formatted** **Isaac J Vimont** **5/2/19 3:58:00 PM**

Font: 10 pt, Font color: Text 1

**Page 1: [31] Formatted** **Isaac J Vimont** **5/2/19 3:58:00 PM**

Font: 10 pt, Font color: Text 1, Not Superscript/ Subscript

**Page 1: [32] Formatted** **Isaac J Vimont** **5/2/19 3:58:00 PM**

Font: 10 pt, Font color: Text 1

**Page 1: [33] Formatted** **Isaac J Vimont** **5/2/19 3:58:00 PM**

Font color: Text 1

**Page 1: [34] Formatted** **Isaac J Vimont** **5/2/19 3:58:00 PM**

Font: 10 pt, Font color: Text 1, Not Superscript/ Subscript

**Page 1: [35] Formatted** **Isaac J Vimont** **5/2/19 3:58:00 PM**

Font: 10 pt, Font color: Text 1

**Page 1: [36] Formatted** **Isaac J Vimont** **5/2/19 3:58:00 PM**

Font color: Text 1

**Page 1: [37] Formatted** **Isaac J Vimont** **5/2/19 3:58:00 PM**

Font: 10 pt, Font color: Text 1

**Page 1: [38] Formatted** **Isaac J Vimont** **5/2/19 3:58:00 PM**

Font color: Text 1

**Page 1: [39] Formatted** **Isaac J Vimont** **5/2/19 3:58:00 PM**

Level 1

**Page 1: [40] Formatted** **Isaac J Vimont** **5/2/19 3:58:00 PM**

Font: 10 pt, Font color: Text 1

**Page 1: [41] Formatted** **Isaac J Vimont** **5/2/19 3:58:00 PM**

Font color: Text 1

**Page 1: [42] Formatted** **Isaac J Vimont** **5/2/19 3:58:00 PM**

Position: Horizontal: Center, Relative to: Margin, Vertical: 0", Relative to: Paragraph, Wrap Around

**Page 1: [43] Formatted** **Isaac J Vimont** **5/2/19 3:58:00 PM**

Page Number

**Page 1: [43] Formatted** **Isaac J Vimont** **5/2/19 3:58:00 PM**

Page Number

**Page 9: [44] Formatted** **Isaac J Vimont** **5/2/19 3:58:00 PM**

Font color: Text 1

**Page 9: [44] Formatted** **Isaac J Vimont** **5/2/19 3:58:00 PM**

Font color: Text 1

**Page 9: [45] Deleted** **Vas Petrenko** **5/1/19 9:30:00 AM**

**Page 9: [46] Deleted** **Isaac J Vimont** **4/25/19 10:09:00 AM**

**Page 9: [46] Deleted** **Isaac J Vimont** **4/25/19 10:09:00 AM**

**Page 9: [46] Deleted** **Isaac J Vimont** **4/25/19 10:09:00 AM**

**Page 9: [47] Deleted** **Isaac J Vimont** **4/25/19 10:13:00 AM**

**Page 9: [47] Deleted** **Isaac J Vimont** **4/25/19 10:13:00 AM**

**Page 9: [48] Commented [Vas Petre1]** **Vas Petrenko** **5/1/19 9:31:00 AM**

Although this statement is not true if a lot of your VOC-derived CO in Indianapolis is produced via ozonolysis. So I think you need to try to assess the possible contribution to 17O excess here (and more importantly the impact on d13C) – presumably showing that it should have a negligible impact on d13C

**Page 9: [49] Formatted** **Isaac J Vimont** **5/2/19 3:58:00 PM**

Font color: Text 1

**Page 9: [49] Formatted** **Isaac J Vimont** **5/2/19 3:58:00 PM**

Font color: Text 1

**Page 9: [50] Formatted** **Isaac J Vimont** **5/2/19 3:58:00 PM**

Font color: Text 1

**Page 9: [50] Formatted** **Isaac J Vimont** **5/2/19 3:58:00 PM**

Font color: Text 1

**Page 10: [51] Formatted** **Isaac J Vimont** **5/2/19 3:58:00 PM**

Font color: Text 1

**Page 10: [51] Formatted** **Isaac J Vimont** **5/2/19 3:58:00 PM**

Font color: Text 1

**Page 10: [52] Formatted** **Isaac J Vimont** **5/2/19 11:58:00 AM**

Font: Not Italic

**Page 10: [52] Formatted** **Isaac J Vimont** **5/2/19 11:58:00 AM**

Font: Not Italic

**Page 10: [52] Formatted** **Isaac J Vimont** **5/2/19 11:58:00 AM**

Font: Not Italic

**Page 10: [52] Formatted** **Isaac J Vimont** **5/2/19 11:58:00 AM**

Font: Not Italic

**Page 10: [52] Formatted** **Isaac J Vimont** **5/2/19 11:58:00 AM**

Font: Not Italic

**Page 10: [52] Formatted** **Isaac J Vimont** **5/2/19 11:58:00 AM**

Font: Not Italic

**Page 10: [52] Formatted** **Isaac J Vimont** **5/2/19 11:58:00 AM**

Font: Not Italic

**Page 10: [52] Formatted** **Isaac J Vimont** **5/2/19 11:58:00 AM**

Font: Not Italic

**Page 10: [52] Formatted** **Isaac J Vimont** **5/2/19 11:58:00 AM**

Font: Not Italic

**Page 10: [52] Formatted** **Isaac J Vimont** **5/2/19 11:58:00 AM**

Font: Not Italic

**Page 10: [52] Formatted** **Isaac J Vimont** **5/2/19 11:58:00 AM**

Font: Not Italic

**Page 10: [52] Formatted** **Isaac J Vimont** **5/2/19 11:58:00 AM**

Font: Not Italic

**Page 10: [52] Formatted** **Isaac J Vimont** **5/2/19 11:58:00 AM**

Font: Not Italic

**Page 10: [52] Formatted** **Isaac J Vimont** **5/2/19 11:58:00 AM**

Font: Not Italic

**Page 10: [52] Formatted** **Isaac J Vimont** **5/2/19 11:58:00 AM**

Font: Not Italic

**Page 10: [52] Formatted** **Isaac J Vimont** **5/2/19 11:58:00 AM**

Font: Not Italic

**Page 10: [52] Formatted** **Isaac J Vimont** **5/2/19 11:58:00 AM**

Font: Not Italic

**Page 10: [52] Formatted** **Isaac J Vimont** **5/2/19 11:58:00 AM**

Font: Not Italic

**Page 10: [52] Formatted** **Isaac J Vimont** **5/2/19 11:58:00 AM**

Font: Not Italic

**Page 10: [52] Formatted** **Isaac J Vimont** **5/2/19 11:58:00 AM**

Font: Not Italic

**Page 10: [52] Formatted** **Isaac J Vimont** **5/2/19 11:58:00 AM**

Font: Not Italic

**Page 10: [52] Formatted** **Isaac J Vimont** **5/2/19 11:58:00 AM**

Font: Not Italic

**Page 10: [52] Formatted** **Isaac J Vimont** **5/2/19 11:58:00 AM**

Font: Not Italic

**Page 10: [52] Formatted** **Isaac J Vimont** **5/2/19 11:58:00 AM**

Font: Not Italic

**Page 10: [52] Formatted** **Isaac J Vimont** **5/2/19 11:58:00 AM**

Font: Not Italic

**Page 10: [52] Formatted** **Isaac J Vimont** **5/2/19 11:58:00 AM**

Font: Not Italic

**Page 10: [52] Formatted** **Isaac J Vimont** **5/2/19 11:58:00 AM**

Font: Not Italic

**Page 10: [52] Formatted** **Isaac J Vimont** **5/2/19 11:58:00 AM**

Font: Not Italic

**Page 10: [53] Formatted** **Isaac J Vimont** **5/2/19 11:57:00 AM**

Not Superscript/ Subscript

**Page 10: [53] Formatted** **Isaac J Vimont** **5/2/19 11:57:00 AM**

Not Superscript/ Subscript

**Page 10: [53] Formatted** **Isaac J Vimont** **5/2/19 11:57:00 AM**

Not Superscript/ Subscript

**Page 10: [53] Formatted** **Isaac J Vimont** **5/2/19 11:57:00 AM**

Not Superscript/ Subscript

**Page 10: [53] Formatted** **Isaac J Vimont** **5/2/19 11:57:00 AM**

Not Superscript/ Subscript

**Page 10: [53] Formatted** **Isaac J Vimont** **5/2/19 11:57:00 AM**

Not Superscript/ Subscript

**Page 10: [53] Formatted** **Isaac J Vimont** **5/2/19 11:57:00 AM**

Not Superscript/ Subscript

**Page 10: [53] Formatted** **Isaac J Vimont** **5/2/19 11:57:00 AM**

Not Superscript/ Subscript

**Page 10: [53] Formatted** **Isaac J Vimont** **5/2/19 11:57:00 AM**

Not Superscript/ Subscript

**Page 10: [53] Formatted** **Isaac J Vimont** **5/2/19 11:57:00 AM**

Not Superscript/ Subscript

**Page 10: [53] Formatted** **Isaac J Vimont** **5/2/19 11:57:00 AM**

Not Superscript/ Subscript

**Page 10: [53] Formatted** **Isaac J Vimont** **5/2/19 11:57:00 AM**

Not Superscript/ Subscript

**Page 10: [53] Formatted** **Isaac J Vimont** **5/2/19 11:57:00 AM**

Not Superscript/ Subscript

**Page 10: [53] Formatted** **Isaac J Vimont** **5/2/19 11:57:00 AM**

Not Superscript/ Subscript

**Page 10: [53] Formatted** **Isaac J Vimont** **5/2/19 11:57:00 AM**

Not Superscript/ Subscript

**Page 10: [53] Formatted** **Isaac J Vimont** **5/2/19 11:57:00 AM**

Not Superscript/ Subscript

**Page 10: [53] Formatted** **Isaac J Vimont** **5/2/19 11:57:00 AM**

Not Superscript/ Subscript

**Page 10: [53] Formatted** **Isaac J Vimont** **5/2/19 11:57:00 AM**

Not Superscript/ Subscript

**Page 10: [53] Formatted** **Isaac J Vimont** **5/2/19 11:57:00 AM**

Not Superscript/ Subscript

**Page 10: [53] Formatted** **Isaac J Vimont** **5/2/19 11:57:00 AM**

Not Superscript/ Subscript

**Page 1: [54] Deleted** **Isaac J Vimont** **5/2/19 3:58:00 PM**

**Page 1: [55] Formatted** **Isaac J Vimont** **5/2/19 3:58:00 PM**

Position: Horizontal: Center, Relative to: Margin, Vertical: 0", Relative to: Paragraph, Wrap Around

**Page 1: [56] Formatted** **Isaac J Vimont** **5/2/19 3:58:00 PM**

Page Number

**Page 1: [56] Formatted** **Isaac J Vimont** **5/2/19 3:58:00 PM**

Page Number

**Page 11: [57] Formatted** **Isaac J Vimont** **5/2/19 3:58:00 PM**

Font color: Text 1

**Page 11: [58] Formatted** **Isaac J Vimont** **5/2/19 4:03:00 PM**

Font: Not Italic

**Page 11: [59] Formatted** **Isaac J Vimont** **5/2/19 3:58:00 PM**

Font color: Text 1

**Page 11: [60] Formatted** **Isaac J Vimont** **5/2/19 3:58:00 PM**

Font color: Text 1

**Page 11: [61] Formatted** **Isaac J Vimont** **5/2/19 3:58:00 PM**

Font color: Text 1

**Page 11: [62] Formatted** **Isaac J Vimont** **5/2/19 3:58:00 PM**

Font color: Text 1

**Page 11: [63] Formatted** **Isaac J Vimont** **5/2/19 3:58:00 PM**

Font color: Text 1

**Page 11: [64] Formatted** **Isaac J Vimont** **5/2/19 3:58:00 PM**

Font color: Text 1

**Page 11: [65] Formatted** **Isaac J Vimont** **5/2/19 3:58:00 PM**

Font color: Text 1

**Page 11: [66] Formatted** **Isaac J Vimont** **5/2/19 3:58:00 PM**

Font color: Text 1

**Page 11: [67] Formatted** **Isaac J Vimont** **5/2/19 3:58:00 PM**

Font color: Text 1

**Page 11: [67] Formatted** **Isaac J Vimont** **5/2/19 3:58:00 PM**

Font color: Text 1

**Page 11: [67] Formatted** **Isaac J Vimont** **5/2/19 3:58:00 PM**

Font color: Text 1

**Page 11: [68] Deleted** **Isaac J Vimont** **4/24/19 12:44:00 PM**

**Page 11: [69] Formatted** **Isaac J Vimont** **5/2/19 3:58:00 PM**

Font: 10 pt, Font color: Text 1

**Page 11: [70] Formatted** **Isaac J Vimont** **5/2/19 3:58:00 PM**

Font color: Text 1

**Page 11: [71] Formatted** **Isaac J Vimont** **5/2/19 3:58:00 PM**

Font: 10 pt, Font color: Text 1

**Page 11: [72] Formatted** **Isaac J Vimont** **5/2/19 3:58:00 PM**

Font color: Text 1

**Page 11: [73] Deleted** **Isaac J Vimont** **4/25/19 9:49:00 AM**

**Page 11: [73] Deleted** **Isaac J Vimont** **4/25/19 9:49:00 AM**

**Page 11: [74] Formatted** **Isaac J Vimont** **5/2/19 3:58:00 PM**

Font color: Text 1

**Page 11: [74] Formatted** **Isaac J Vimont** **5/2/19 3:58:00 PM**

Font color: Text 1

**Page 11: [75] Formatted** **Isaac J Vimont** **5/2/19 3:58:00 PM**

Font color: Text 1

**Page 11: [75] Formatted** **Isaac J Vimont** **5/2/19 3:58:00 PM**

Font color: Text 1

**Page 11: [75] Formatted** **Isaac J Vimont** **5/2/19 3:58:00 PM**

Font color: Text 1

**Page 11: [76] Formatted** **Isaac J Vimont** **5/2/19 3:58:00 PM**

Font color: Text 1

**Page 11: [77] Formatted Isaac J Vimont 5/2/19 3:58:00 PM**

Font color: Text 1

**Page 11: [77] Formatted Isaac J Vimont 5/2/19 3:58:00 PM**

Font color: Text 1

**Page 11: [78] Formatted Isaac J Vimont 5/2/19 3:58:00 PM**

Font color: Text 1

**Page 11: [79] Formatted Isaac J Vimont 4/24/19 12:47:00 PM**

Font: Not Italic

**Page 11: [79] Formatted Isaac J Vimont 4/24/19 12:47:00 PM**

Font: Not Italic

**Page 11: [80] Formatted Isaac J Vimont 4/24/19 12:47:00 PM**

Font: Not Italic

**Page 11: [80] Formatted Isaac J Vimont 4/24/19 12:47:00 PM**

Font: Not Italic

**Page 11: [81] Formatted Isaac J Vimont 4/24/19 12:47:00 PM**

Font: Not Italic

**Page 11: [81] Formatted Isaac J Vimont 4/24/19 12:47:00 PM**

Font: Not Italic

**Page 11: [82] Formatted Isaac J Vimont 5/2/19 3:58:00 PM**

Font color: Text 1

**Page 11: [83] Formatted Isaac J Vimont 5/2/19 3:58:00 PM**

Font color: Text 1

**Page 11: [84] Formatted Isaac J Vimont 5/2/19 3:58:00 PM**

Font color: Text 1

**Page 16: [85] Deleted Isaac J Vimont 4/24/19 12:56:00 PM**

**Page 16: [85] Deleted Isaac J Vimont 4/24/19 12:56:00 PM**

**Page 16: [86] Formatted Isaac J Vimont 5/2/19 3:58:00 PM**

Font color: Text 1

**Page 16: [86] Formatted Isaac J Vimont 5/2/19 3:58:00 PM**

Font color: Text 1

**Page 16: [87] Deleted Isaac J Vimont 4/29/19 1:54:00 PM**

**Page 16: [87] Deleted** **Isaac J Vimont** **4/29/19 1:54:00 PM**

**Page 16: [88] Formatted** **Isaac J Vimont** **5/2/19 3:58:00 PM**

Font color: Text 1

**Page 16: [88] Formatted** **Isaac J Vimont** **5/2/19 3:58:00 PM**

Font color: Text 1

**Page 16: [89] Formatted** **Isaac J Vimont** **5/2/19 3:58:00 PM**

Font: 10 pt, Font color: Text 1

**Page 16: [89] Formatted** **Isaac J Vimont** **5/2/19 3:58:00 PM**

Font: 10 pt, Font color: Text 1

**Page 16: [89] Formatted** **Isaac J Vimont** **5/2/19 3:58:00 PM**

Font: 10 pt, Font color: Text 1

**Page 16: [90] Deleted** **Vas Petrenko** **5/1/19 10:15:00 AM**

**Page 16: [90] Deleted** **Vas Petrenko** **5/1/19 10:15:00 AM**

**Page 16: [91] Deleted** **Isaac J Vimont** **5/2/19 1:19:00 PM**

**Page 16: [91] Deleted** **Isaac J Vimont** **5/2/19 1:19:00 PM**

**Page 16: [92] Deleted** **Isaac J Vimont** **5/2/19 4:16:00 PM**

**Page 16: [92] Deleted** **Isaac J Vimont** **5/2/19 4:16:00 PM**

**Page 16: [92] Deleted** **Isaac J Vimont** **5/2/19 4:16:00 PM**

**Page 16: [92] Deleted** **Isaac J Vimont** **5/2/19 4:16:00 PM**

**Page 16: [92] Deleted** **Isaac J Vimont** **5/2/19 4:16:00 PM**

**Page 1: [93] Deleted** **Isaac J Vimont** **5/2/19 3:58:00 PM**

**Page 18: [94] Formatted** **Isaac J Vimont** **5/2/19 3:58:00 PM**

Font: 10 pt, Font color: Text 1

**Page 18: [95] Formatted** **Isaac J Vimont** **5/2/19 3:58:00 PM**

Font color: Text 1

**Page 18: [96] Formatted** **Isaac J Vimont** **5/2/19 3:58:00 PM**

Font: 10 pt, Font color: Text 1

**Page 18: [97] Formatted** **Isaac J Vimont** **5/2/19 3:58:00 PM**

Font color: Text 1

**Page 18: [98] Formatted** **Isaac J Vimont** **5/2/19 3:58:00 PM**

Font color: Text 1

**Page 18: [99] Formatted** **Isaac J Vimont** **5/2/19 3:58:00 PM**

Font color: Text 1

**Page 18: [100] Formatted** **Isaac J Vimont** **5/2/19 3:58:00 PM**

Font color: Text 1

**Page 18: [101] Formatted** **Isaac J Vimont** **5/2/19 3:58:00 PM**

Font color: Text 1

**Page 18: [102] Formatted** **Isaac J Vimont** **5/2/19 3:58:00 PM**

Font color: Text 1

**Page 18: [103] Formatted** **Isaac J Vimont** **5/2/19 3:58:00 PM**

Font color: Text 1

**Page 18: [104] Formatted** **Isaac J Vimont** **5/2/19 3:58:00 PM**

Font color: Text 1

**Page 18: [105] Formatted** **Isaac J Vimont** **5/2/19 3:58:00 PM**

Font: 10 pt, Font color: Text 1

**Page 18: [106] Formatted** **Isaac J Vimont** **5/2/19 3:58:00 PM**

Font color: Text 1

**Page 18: [107] Formatted** **Isaac J Vimont** **5/2/19 3:58:00 PM**

Font color: Text 1

**Page 18: [108] Formatted** **Isaac J Vimont** **5/2/19 3:58:00 PM**

Font color: Text 1

**Page 18: [109] Formatted** **Isaac J Vimont** **5/2/19 4:28:00 PM**

English (US)

**Page 18: [110] Formatted** **Isaac J Vimont** **5/2/19 3:58:00 PM**

Font color: Text 1

**Page 18: [111] Formatted** **Isaac J Vimont** **5/2/19 3:58:00 PM**

Font color: Text 1

**Page 18: [112] Formatted** **Isaac J Vimont** **5/2/19 3:58:00 PM**

Font color: Text 1

**Page 18: [113] Formatted** **Isaac J Vimont** **5/2/19 3:58:00 PM**

Font color: Text 1

**Page 18: [114] Formatted** **Isaac J Vimont** **5/2/19 3:58:00 PM**

Font color: Text 1

**Page 18: [115] Formatted** **Isaac J Vimont** **5/2/19 3:58:00 PM**

Font: 10 pt, Font color: Text 1

**Page 1: [116] Formatted** **Isaac J Vimont** **5/2/19 3:58:00 PM**

Page Number

**Page 1: [116] Formatted** **Isaac J Vimont** **5/2/19 3:58:00 PM**

Page Number

**Page 19: [117] Formatted** **Isaac J Vimont** **5/2/19 3:58:00 PM**

Font color: Text 1

**Page 19: [117] Formatted** **Isaac J Vimont** **5/2/19 3:58:00 PM**

Font color: Text 1

**Page 19: [117] Formatted** **Isaac J Vimont** **5/2/19 3:58:00 PM**

Font color: Text 1

**Page 19: [117] Formatted** **Isaac J Vimont** **5/2/19 3:58:00 PM**

Font color: Text 1

**Page 19: [117] Formatted** **Isaac J Vimont** **5/2/19 3:58:00 PM**

Font color: Text 1

**Page 19: [117] Formatted** **Isaac J Vimont** **5/2/19 3:58:00 PM**

Font color: Text 1

**Page 19: [117] Formatted** **Isaac J Vimont** **5/2/19 3:58:00 PM**

Font color: Text 1

**Page 19: [117] Formatted** **Isaac J Vimont** **5/2/19 3:58:00 PM**

Font color: Text 1

**Page 19: [117] Formatted** **Isaac J Vimont** **5/2/19 3:58:00 PM**

Font color: Text 1

**Page 19: [117] Formatted** **Isaac J Vimont** **5/2/19 3:58:00 PM**

Font color: Text 1

**Page 19: [117] Formatted** **Isaac J Vimont** **5/2/19 3:58:00 PM**

Font color: Text 1

| | | |
|---|---|---|
| **Page 19: [117] Formatted** | **Isaac J Vimont** | **5/2/19 3:58:00 PM** |

Font color: Text 1

| | | |
|---|---|---|
| **Page 19: [118] Deleted** | **Vas Petrenko** | **5/1/19 10:55:00 AM** |
| **Page 19: [118] Deleted** | **Vas Petrenko** | **5/1/19 10:55:00 AM** |
| **Page 19: [119] Deleted** | **Isaac J Vimont** | **5/2/19 3:58:00 PM** |
| **Page 19: [119] Deleted** | **Isaac J Vimont** | **5/2/19 3:58:00 PM** |
| **Page 19: [119] Deleted** | **Isaac J Vimont** | **5/2/19 3:58:00 PM** |
| **Page 19: [120] Formatted** | **Isaac J Vimont** | **5/2/19 3:58:00 PM** |

Font color: Text 1

| | | |
|---|---|---|
| **Page 19: [120] Formatted** | **Isaac J Vimont** | **5/2/19 3:58:00 PM** |

Font color: Text 1

| | | |
|---|---|---|
| **Page 19: [120] Formatted** | **Isaac J Vimont** | **5/2/19 3:58:00 PM** |

Font color: Text 1

| | | |
|---|---|---|
| **Page 19: [120] Formatted** | **Isaac J Vimont** | **5/2/19 3:58:00 PM** |

Font color: Text 1

| | | |
|---|---|---|
| **Page 19: [120] Formatted** | **Isaac J Vimont** | **5/2/19 3:58:00 PM** |

Font color: Text 1

| | | |
|---|---|---|
| **Page 19: [120] Formatted** | **Isaac J Vimont** | **5/2/19 3:58:00 PM** |

Font color: Text 1

| | | |
|---|---|---|
| **Page 19: [120] Formatted** | **Isaac J Vimont** | **5/2/19 3:58:00 PM** |

Font color: Text 1

| | | |
|---|---|---|
| **Page 19: [120] Formatted** | **Isaac J Vimont** | **5/2/19 3:58:00 PM** |

Font color: Text 1

| | | |
|---|---|---|
| **Page 19: [120] Formatted** | **Isaac J Vimont** | **5/2/19 3:58:00 PM** |

Font color: Text 1

| | | |
|---|---|---|
| **Page 1: [121] Deleted** | **Isaac J Vimont** | **5/2/19 3:58:00 PM** |
| **Page 20: [122] Deleted** | **Isaac J Vimont** | **4/25/19 10:43:00 AM** |
| **Page 20: [122] Deleted** | **Isaac J Vimont** | **4/25/19 10:43:00 AM** |

**Page 20: [122] Deleted Isaac J Vimont 4/25/19 10:43:00 AM**

**Page 20: [122] Deleted Isaac J Vimont 4/25/19 10:43:00 AM**

**Page 20: [122] Deleted Isaac J Vimont 4/25/19 10:43:00 AM**

**Page 20: [123] Formatted Isaac J Vimont 5/2/19 3:58:00 PM**

Font color: Text 1

**Page 20: [124] Deleted Vas Petrenko 5/1/19 11:22:00 AM**

**Page 20: [124] Deleted Vas Petrenko 5/1/19 11:22:00 AM**

**Page 20: [125] Formatted Isaac J Vimont 5/2/19 3:58:00 PM**

Font color: Text 1

**Page 20: [126] Deleted Vas Petrenko 5/1/19 10:43:00 AM**

**Page 20: [126] Deleted Vas Petrenko 5/1/19 10:43:00 AM**

**Page 20: [127] Formatted Isaac J Vimont 5/2/19 3:58:00 PM**

Font color: Text 1

**Page 20: [128] Formatted Isaac J Vimont 5/2/19 3:58:00 PM**

Font color: Text 1

**Page 20: [129] Formatted Isaac J Vimont 5/2/19 3:58:00 PM**

Font color: Text 1

**Page 20: [130] Formatted Isaac J Vimont 5/2/19 3:58:00 PM**

Font color: Text 1

**Page 20: [131] Formatted Isaac J Vimont 5/2/19 3:58:00 PM**

Font color: Text 1

**Page 20: [132] Formatted Isaac J Vimont 5/2/19 3:58:00 PM**

Font color: Text 1

**Page 20: [133] Formatted Isaac J Vimont 5/2/19 3:58:00 PM**

Font: 10 pt, Font color: Text 1

**Page 20: [133] Formatted Isaac J Vimont 5/2/19 3:58:00 PM**

Font: 10 pt, Font color: Text 1

**Page 20: [134] Deleted Vas Petrenko 5/1/19 10:48:00 AM**

**Page 20: [135] Formatted Isaac J Vimont 5/2/19 3:58:00 PM**

Font: 10 pt, Font color: Text 1

**Page 20: [135] Formatted Isaac J Vimont 5/2/19 3:58:00 PM**

Font: 10 pt, Font color: Text 1

**Page 20: [135] Formatted Isaac J Vimont 5/2/19 3:58:00 PM**

Font: 10 pt, Font color: Text 1

**Page 20: [135] Formatted Isaac J Vimont 5/2/19 3:58:00 PM**

Font: 10 pt, Font color: Text 1

**Page 20: [135] Formatted Isaac J Vimont 5/2/19 3:58:00 PM**

Font: 10 pt, Font color: Text 1

**Page 20: [135] Formatted Isaac J Vimont 5/2/19 3:58:00 PM**

Font: 10 pt, Font color: Text 1

**Page 20: [135] Formatted Isaac J Vimont 5/2/19 3:58:00 PM**

Font: 10 pt, Font color: Text 1

**Page 20: [135] Formatted Isaac J Vimont 5/2/19 3:58:00 PM**

Font: 10 pt, Font color: Text 1

**Page 20: [135] Formatted Isaac J Vimont 5/2/19 3:58:00 PM**

Font: 10 pt, Font color: Text 1

**Page 20: [135] Formatted Isaac J Vimont 5/2/19 3:58:00 PM**

Font: 10 pt, Font color: Text 1

**Page 20: [136] Deleted Isaac J Vimont 4/29/19 11:58:00 AM**

**Page 20: [137] Formatted Isaac J Vimont 5/2/19 3:58:00 PM**

Font: 10 pt, Font color: Text 1

**Page 20: [137] Formatted Isaac J Vimont 5/2/19 3:58:00 PM**

Font: 10 pt, Font color: Text 1

**Page 20: [138] Formatted Isaac J Vimont 5/2/19 3:58:00 PM**

Font color: Text 1

**Page 20: [139] Formatted Isaac J Vimont 5/2/19 3:58:00 PM**

Font color: Text 1

**Page 20: [140] Formatted Isaac J Vimont 5/2/19 3:58:00 PM**

Font color: Text 1

**Page 20: [140] Formatted** **Isaac J Vimont** **5/2/19 3:58:00 PM**

Font color: Text 1

**Page 20: [141] Formatted** **Isaac J Vimont** **5/2/19 3:58:00 PM**

Font color: Text 1

**Page 20: [142] Formatted** **Isaac J Vimont** **5/2/19 3:58:00 PM**

Font color: Text 1

**Page 20: [143] Formatted** **Isaac J Vimont** **5/2/19 3:58:00 PM**

Font color: Text 1

**Page 20: [143] Formatted** **Isaac J Vimont** **5/2/19 3:58:00 PM**

Font color: Text 1

**Page 20: [144] Formatted** **Isaac J Vimont** **5/2/19 3:58:00 PM**

Font color: Text 1

**Page 20: [145] Formatted** **Isaac J Vimont** **5/2/19 3:58:00 PM**

Font color: Text 1

**Page 20: [146] Deleted** **Vas Petrenko** **5/1/19 11:29:00 AM**

**Page 20: [146] Deleted** **Vas Petrenko** **5/1/19 11:29:00 AM**

**Page 20: [147] Formatted** **Isaac J Vimont** **5/2/19 3:58:00 PM**

Font color: Text 1

**Page 20: [147] Formatted** **Isaac J Vimont** **5/2/19 3:58:00 PM**

Font color: Text 1

**Page 20: [148] Formatted** **Isaac J Vimont** **5/2/19 3:58:00 PM**

Font color: Text 1

**Page 20: [149] Formatted** **Isaac J Vimont** **5/2/19 3:58:00 PM**

Font color: Text 1

**Page 20: [149] Formatted** **Isaac J Vimont** **5/2/19 3:58:00 PM**

Font color: Text 1

**Page 20: [149] Formatted** **Isaac J Vimont** **5/2/19 3:58:00 PM**

Font color: Text 1

**Page 20: [149] Formatted** **Isaac J Vimont** **5/2/19 3:58:00 PM**

Font color: Text 1

**Page 20: [149] Formatted** **Isaac J Vimont** **5/2/19 3:58:00 PM**

Font color: Text 1

**Page 20: [149] Formatted Isaac J Vimont 5/2/19 3:58:00 PM**

Font color: Text 1

**Page 20: [149] Formatted Isaac J Vimont 5/2/19 3:58:00 PM**

Font color: Text 1

**Page 1: [150] Formatted Isaac J Vimont 5/2/19 3:58:00 PM**

Page Number

**Page 1: [150] Formatted Isaac J Vimont 5/2/19 3:58:00 PM**

Page Number

**Page 21: [151] Formatted Isaac J Vimont 5/2/19 3:58:00 PM**

Font color: Text 1

**Page 21: [151] Formatted Isaac J Vimont 5/2/19 3:58:00 PM**

Font color: Text 1

**Page 21: [151] Formatted Isaac J Vimont 5/2/19 3:58:00 PM**

Font color: Text 1

**Page 21: [151] Formatted Isaac J Vimont 5/2/19 3:58:00 PM**

Font color: Text 1

**Page 21: [151] Formatted Isaac J Vimont 5/2/19 3:58:00 PM**

Font color: Text 1

**Page 21: [152] Formatted Isaac J Vimont 5/2/19 3:58:00 PM**

Font color: Text 1

**Page 21: [152] Formatted Isaac J Vimont 5/2/19 3:58:00 PM**

Font color: Text 1

**Page 21: [152] Formatted Isaac J Vimont 5/2/19 3:58:00 PM**

Font color: Text 1

**Page 21: [152] Formatted Isaac J Vimont 5/2/19 3:58:00 PM**

Font color: Text 1

**Page 21: [153] Formatted Isaac J Vimont 5/2/19 3:58:00 PM**

Font color: Text 1

**Page 21: [153] Formatted Isaac J Vimont 5/2/19 3:58:00 PM**

Font color: Text 1

**Page 21: [153] Formatted Isaac J Vimont 5/2/19 3:58:00 PM**

Font color: Text 1

**Page 21: [153] Formatted Isaac J Vimont 5/2/19 3:58:00 PM**

Font color: Text 1

**Page 21: [153] Formatted Isaac J Vimont 5/2/19 3:58:00 PM**

Font color: Text 1

**Page 21: [153] Formatted Isaac J Vimont 5/2/19 3:58:00 PM**

Font color: Text 1

**Page 21: [153] Formatted Isaac J Vimont 5/2/19 3:58:00 PM**

Font color: Text 1

**Page 21: [153] Formatted Isaac J Vimont 5/2/19 3:58:00 PM**

Font color: Text 1

**Page 21: [153] Formatted Isaac J Vimont 5/2/19 3:58:00 PM**

Font color: Text 1

**Page 21: [153] Formatted Isaac J Vimont 5/2/19 3:58:00 PM**

Font color: Text 1

**Page 21: [153] Formatted Isaac J Vimont 5/2/19 3:58:00 PM**

Font color: Text 1

**Page 21: [153] Formatted Isaac J Vimont 5/2/19 3:58:00 PM**

Font color: Text 1

**Page 21: [153] Formatted Isaac J Vimont 5/2/19 3:58:00 PM**

Font color: Text 1

**Page 21: [154] Formatted Isaac J Vimont 5/2/19 3:58:00 PM**

Font color: Text 1

**Page 21: [154] Formatted Isaac J Vimont 5/2/19 3:58:00 PM**

Font color: Text 1

**Page 21: [154] Formatted Isaac J Vimont 5/2/19 3:58:00 PM**

Font color: Text 1

**Page 21: [154] Formatted Isaac J Vimont 5/2/19 3:58:00 PM**

Font color: Text 1

**Page 21: [154] Formatted Isaac J Vimont 5/2/19 3:58:00 PM**

Font color: Text 1

**Page 21: [155] Formatted Isaac J Vimont 5/2/19 4:44:00 PM**

Superscript

**Page 21: [155] Formatted Isaac J Vimont 5/2/19 4:44:00 PM**

Superscript

**Page 21: [155] Formatted Isaac J Vimont 5/2/19 4:44:00 PM**

Superscript

**Page 21: [156] Formatted Isaac J Vimont 5/2/19 3:58:00 PM**

Font color: Text 1

**Page 21: [156] Formatted Isaac J Vimont 5/2/19 3:58:00 PM**

Font color: Text 1

**Page 22: [157] Formatted Isaac J Vimont 5/2/19 3:58:00 PM**

Font: (Default) Cambria, 10 pt, Font color: Text 1

**Page 22: [158] Formatted Isaac J Vimont 5/2/19 4:48:00 PM**

Font color: Text 1, Not Superscript/ Subscript

**Page 22: [159] Deleted Vas Petrenko 5/1/19 12:05:00 PM**

**Page 22: [160] Formatted Isaac J Vimont 5/2/19 3:58:00 PM**

Font: (Default) Cambria, 10 pt, Font color: Text 1

**Page 1: [161] Formatted Isaac J Vimont 5/2/19 3:58:00 PM**

Position: Horizontal: Center, Relative to: Margin, Vertical: 0", Relative to: Paragraph, Wrap Around

**Page 1: [162] Formatted Isaac J Vimont 5/2/19 3:58:00 PM**

Page Number

**Page 1: [162] Formatted Isaac J Vimont 5/2/19 3:58:00 PM**

Page Number

**Page 23: [163] Deleted Isaac J Vimont 4/30/19 12:36:00 PM**

**Page 23: [163] Deleted Isaac J Vimont 4/30/19 12:36:00 PM**

**Page 23: [164] Deleted Isaac J Vimont 5/2/19 1:19:00 PM**

**Page 23: [164] Deleted Isaac J Vimont 5/2/19 1:19:00 PM**

**Page 23: [165] Formatted Isaac J Vimont 5/2/19 3:58:00 PM**

Font color: Text 1

**Page 23: [165] Formatted Isaac J Vimont 5/2/19 3:58:00 PM**

Font color: Text 1

**Page 23: [166] Deleted Isaac J Vimont 5/3/19 4:23:00 PM**

**Page 23: [167] Formatted Isaac J Vimont 5/2/19 3:58:00 PM**

Font color: Text 1

**Page 23: [167] Formatted Isaac J Vimont 5/2/19 3:58:00 PM**

Font color: Text 1

**Page 23: [167] Formatted Isaac J Vimont 5/2/19 3:58:00 PM**

Font color: Text 1

**Page 23: [168] Deleted Isaac J Vimont 5/2/19 3:58:00 PM**

**Page 23: [169] Formatted Isaac J Vimont 5/2/19 3:58:00 PM**

Font color: Text 1

**Page 23: [169] Formatted Isaac J Vimont 5/2/19 3:58:00 PM**

Font color: Text 1

**Page 23: [170] Formatted Isaac J Vimont 5/2/19 3:58:00 PM**

Font color: Text 1

**Page 23: [170] Formatted Isaac J Vimont 5/2/19 3:58:00 PM**

Font color: Text 1

**Page 23: [171] Formatted Isaac J Vimont 5/2/19 3:58:00 PM**

Font color: Text 1

**Page 23: [171] Formatted Isaac J Vimont 5/2/19 3:58:00 PM**

Font color: Text 1

**Page 34: [172] Deleted Isaac J Vimont 5/2/19 3:58:00 PM**

**Page 35: [173] Deleted Isaac J Vimont 5/2/19 3:58:00 PM**

**Page 40: [174] Deleted Isaac J Vimont 5/2/19 3:58:00 PM**

# Supplementary Material: An improved estimate for the $\delta^{13}C$ and $\delta^{18}O$ signatures of carbon monoxide produced from atmospheric oxidation of volatile organic compounds

**Authors:**

*Isaac J Vimont[1,2,3], Jocelyn C. Turnbull[3,4], Vasilii V. Petrenko[5], Philip F. Place[5], Colm Sweeney[2], Natasha Miles[6], Scott Richardson[6], Bruce H. Vaughn[1], James W.C. White[1]

[1.] Institute of Arctic and Alpine Research, Boulder, CO USA
[2.] National Oceanic and Atmospheric Administration, Global Monitoring Division, Boulder, CO USA
[3.] CIRES, University of Colorado, Boulder, CO, USA
[4.] GNS Science, Lower Hutt, New Zealand
[5.] University of Rochester Earth and Environmental Science Department, Rochester, NY, USA
[6.] Pennsylvania State University, College Station, PA USA

* Corresponding Author: Isaac.vimont@colorado.edu

## *S.1 Broadleaf, Deciduous vegetation cover at Indianapolis and Beech Island*

Using the MEGAN 2.1 model plant functional type (PFT) inputs (Guenther et al., 2012), we created land cover maps for Indianapolis (figure S1) and Beech Island (Figure S2). These plants produce the bulk of biogenic VOC emissions (e.g. Harley et al., 1999) and therefore these plants are most relevant to our study.

**Figure S1:** Broadleaf, deciduous trees and shrubs for the region surrounding Indianapolis, IN. The black circle denotes the location of Indinapolis and its immediate surroundings. The grid is incremented at 0.5° (both latitude and longitude).

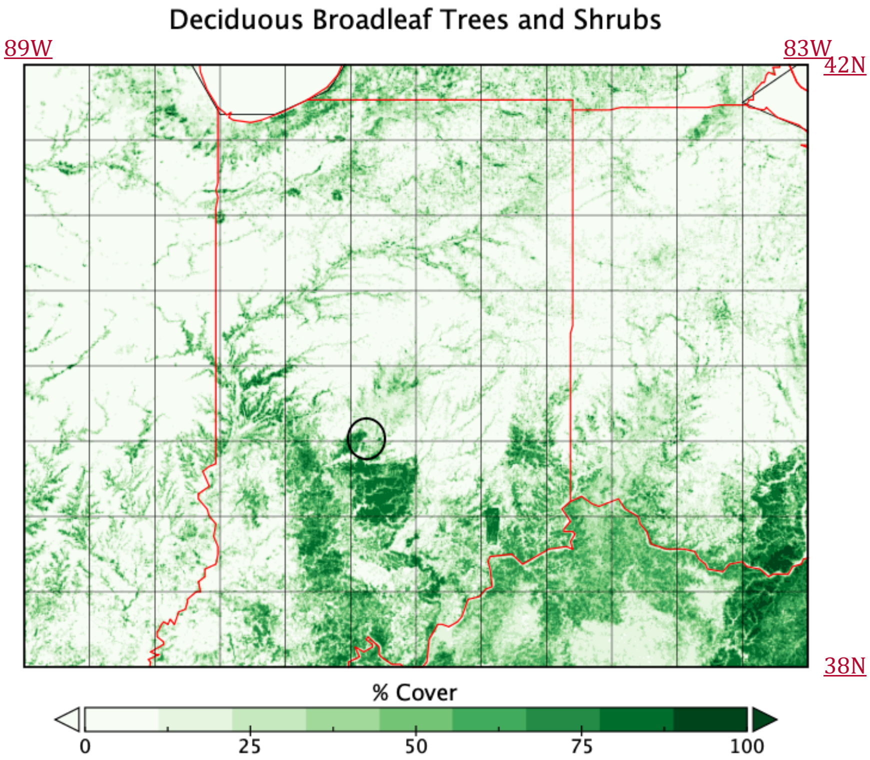
Deciduous Broadleaf Trees and Shrubs

**Figure S2:** Broadleaf, deciduous trees and shrubs for the region surrounding Beech Island, SC. The black circle denotes the location of Beech Island and its immediate surroundings. The grid is incremented at 0.5° (both latitude and longitude).

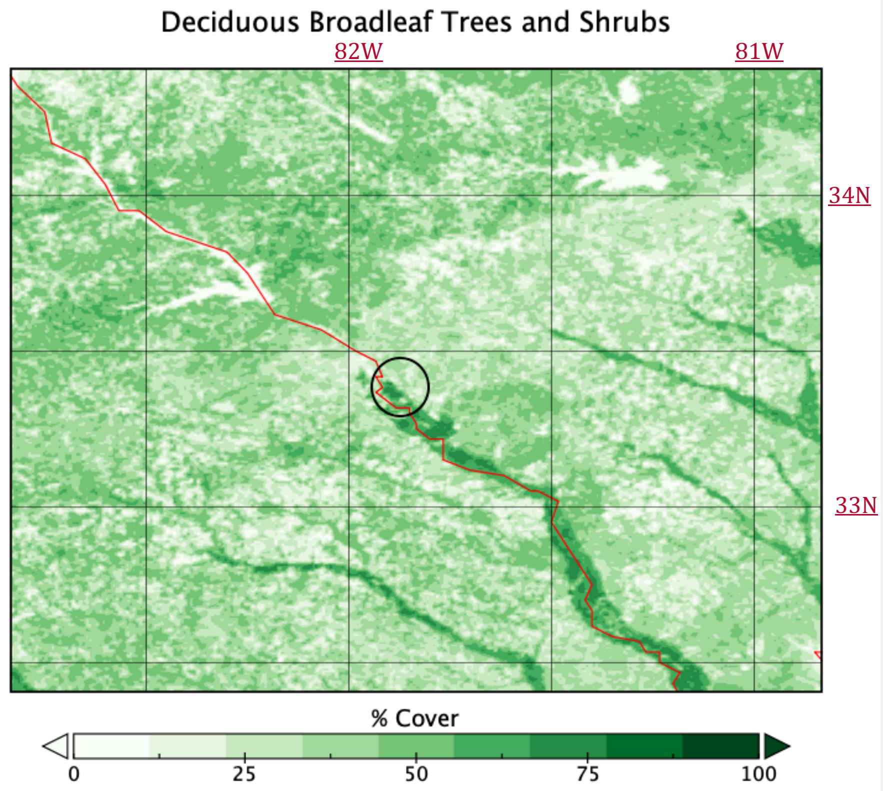

Deciduous Broadleaf Trees and Shrubs

**Formatted:** Font: Not Bold

**Deleted:** *1*

### *S.2 Simplification of the CO Budget*

One of the advantages to the INFLUX experiment is the ability to remove background signals from the urban measurements, and thereby derive the urban enhancement. This approach also allows the CO budget to be simplified. Both the oxidation of $CH_4$ to CO and the oxidation of CO to $CO_2$ via the OH radical are reactions that proceed slowly relative to the experimental scale of a few hours transit time. We can consider only this short time scale because we are only considering reactions that can occur when air masses are transiting between the background and urban sites (table S1). Because of this, we calculate that these two processes have negligible impact on our urban CO enhancements, and can be disregarded given the short reaction time being considered (detailed below, table S1).

The reaction time period can be calculated simply by considering the distance between tower 1 and towers 2 or 3 and the average wind speed. Given the average wind speed during sampling for this study was 4.4 ± 1.3 m $s^{-1}$, a 2.7-hour transit time is required. In this experiment, we correct our results to account for the incoming background CO and examine the urban contribution alone. This short transit time scale allows us to place constraints on the $CH_4$ oxidation source and the OH oxidation sink of CO.

Oxidation of $CH_4$ by OH is a major source of CO globally but $CH_4$ is long lived in the atmosphere relative to CO (Sander et al., 2006; Atkinson et al., 2006; Duncan et al., 2007). The approximate rate for the reaction of CH4 with OH is $6.4 \times 10^{-15}$ $cm^3$ $s^{-1}$ at standard pressure and our mean ambient temperature of 26° C (Atkinson et al., 2006). OH concentration has been determined at urban sites in similar latitude bands and ranges from $1 \times 10^6$ $cm^{-3}$ in cool, winter time conditions to $2 \times 10^7$ $cm^{-3}$ in hot, summertime conditions (Warneke et al., 2007, 2013; Atkinson and Arey, 2003; Park et al., 2011). We do not have OH concentration measurements at Indianapolis, and therefore use the highest reported literature value for OH of $2 \times 10^7$ $cm^{-3}$ (Park et al., 2011) to assess the maximum $CH_4$ oxidation contribution to CO (Park et al., 2011, Table S1). We calculated the change in mole fraction of CO due to oxidation of $CH_4$ by OH by:

$$\Delta X_{CO}=\gamma(X_{CH_{4,i}})\left(1-e^{-k([OH])t}\right) \qquad (S1)$$

where $\Delta X_{CO}$ is the change in CO mole fraction due to $CH_4$ oxidation by OH, γ is the CO yield for the $CH_4$+OH reaction (0.96 mole CO produced per mole $CH_4$), $X_{CH4,i}$ is the initial $CH_4$ mole fraction (the average $CH_4$ mole fraction during the sampling period, 1930 nmol:mol), k is the reaction rate for $CH_4$+OH ($6.4 \times 10^{-15}$ $cm^3$ $s^{-1}$), [OH] is the high end member OH concentration from Park et al. (2011) ($2 \times 10^7$ $cm^{-3}$, and t is the transit time of 2.7 hours. Using (S1), we calculated 1.4 nmol:mol CO produced from oxidation of $CH_4$ between the two towers.

| Species | $k_{OH}$ ($cm^3 molec^{-1} sec^{-1}$) | $k_{O3}$ ($cm^3 molec^{-1} sec^{-1}$) | $k_{NO3}$ ($cm^3 molec^{-1} sec^{-1}$) | Estimated Mole Fraction (nmol:mol) | $\gamma_{OH}$ (%C) | Molec CO per molec VOC | Yield OH (nmol:mol) | Yield $O_3$ (nmol:mol) | Yield $NO_3$ (nmol:mol) | Total CO (nmol:mol) | $\Delta\delta^{13}C$ (‰) | $\Delta\delta^{18}O$ (‰) |
|---|---|---|---|---|---|---|---|---|---|---|---|---|
| Methane | 6.40E-15 | | 1.00E-18 | 1930 | 0.96 | 0.96 | 1.4 | 0 | 0.005 | 1.4 | -0.21 | -0.04 |
| CO | 1.44E-13 | | N/A | 166 | N/A | N/A | 2.4 | N/A | N/A | 2.4 | -0.08 | 0.17 |

**Table S1:** $CH_4$ and CO deviations caused by oxidation of $CH_4$ to CO, and oxidation of CO to $CO_2$ by OH. Assumed [OH] = $2\times10^7$ molec $cm^{-3}$ (Park et al., 2011). CO yield from oxidation of $CH_4$ taken from Grant et al. (2010).

We further assessed the impact on CO isotopes (Table S1) by using the reported isotopic values for $CH_4$ oxidation (Table 1, main text). We calculated the change in $\delta^{13}C$ and $\delta^{18}O$ by

$$\Delta\delta=\delta_{CO,i}-\frac{\left(\delta_{CO,i}(X_{CO_i})\right)+\left(\delta_{CH_4}(X_{CO_{CH_4}})\right)}{\left(X_{CO_i}+X_{CO_{CH_4}}\right)} \qquad (S2)$$

where $\Delta\delta$ is the change in either $\delta^{13}C$ or $\delta^{18}O$, $\delta_{COi}$ is the initial delta value at the polluted towers (average of the two towers (non-enhancement) of -29.6‰ for $\delta^{13}C$ and 5.1‰ for $\delta^{18}O$), $X_{COi}$ is the CO mole fraction at the two polluted towers (average value of 166 nmol:mol), $\delta_{CH4}$ is the $\delta^{13}C$ or $\delta^{18}O$ value of CO produced by $CH_4$ oxidation (-52.6‰ and 0‰ for $\delta^{13}C$ and $\delta^{18}O$ respectively, Brenninkmeijer et al., 1999), and $X_{COCH4}$ is the mole fraction of CO produced from oxidation of $CH_4$ by OH, calculated above.

Using these parameters and the average transit time between the towers of 2.7 hours, we calculate that during the transit across the city, $CH_4$ oxidation could contribute up to 1.4 nmol:mol CO, changing $\delta^{13}C$ by up to -0.21‰, and $\delta^{18}O$ by up to -0.04‰. These values are below our 1σ measurement uncertainties (0.23‰ $\delta^{13}C$ and 0.46‰ $\delta^{18}O$), and thus we do not consider $CH_4$ oxidation to be a significant source of CO in our analyses.

OH oxidation is the main sink of CO, and will directly impact the isotopic signatures of CO measured within the city (Röckmann and Brenninkmeijer, 1997; Duncan et al., 2007). Using the same method and OH concentration as for $CH_4$ oxidation above, and a reaction rate for CO+OH of $1.44 \times 10^{-13}$ $cm^3$ $s^{-1}$ (Atkinson et al., 2006), we calculated the loss of CO during the transit of an air mass across the city:

$$\Delta X_{CO}=(X_{CO_i})\left(1-e^{-k([OH])t}\right) \qquad (S3)$$

We obtained a loss of 2.4 nmol:mol CO. However, to calculate changes to the isotopic budget, we use the fractionation factors for OH oxidation found in Table 1, main text and a Rayleigh distillation approach to compute the impact of the OH sink on $\delta^{13}C$ and $\delta^{18}O$ of CO:

$$\frac{\delta_f}{10^3‰}+1=\left(\frac{\delta_i}{10^3‰}\right)f_f^{\alpha-1}+f_f^{\alpha-1} \qquad (S4)$$

f refers to the final change in either $\delta^{13}C$ or $\delta^{18}O$, and i refers to the mean value of $\delta^{13}C$ or $\delta^{18}O$ measured at the two downwind towers (-29.9‰ for $\delta^{13}C$ and 4.1‰ for $\delta^{18}O$). $f_f$ is the final fraction of CO left after the amount of CO lost is removed, determined by:

$$f_f=\frac{X_{CO_T}-X_{CO_{lost}}}{X_{CO_T}} \qquad (S5)$$

where $X_{COT}$ is the total CO mole fraction measured at tower 1 (mean value of 146 nmol:mol), and $X_{COlost}$ is the amount of CO removed by oxidation with OH. α is the fractionation factor for either $\delta^{13}C$ or $\delta^{18}O$ from the literature (Table 1, main text). The estimated total effect of OH oxidation on the CO mole fraction is 2.4 nmol:mol CO lost, -0.08‰ change in $\delta^{13}C$, and 0.17‰ change in $\delta^{18}O$. These changes in the isotopic values can also be neglected in our quantification of the CO isotopic budget given our estimated measurement uncertainty.

Biomass burning can be a source of CO in urban regions, though it is primarily used as a heat source (Saurer et al., 2009). Within Indianapolis, 2/3 of residential and commercial heating is done by natural gas combustion, and the remaining 1/3 is electrical (Gurney et al., 2012). Vimont et al. (2017) estimated that biomass burning for heat was only about 1% of the CO budget during the winter, and did not impact the isotopic budget significantly. As there should be much less (if any) biomass burning for heat during the summer, we assume that biomass burning is not a significant source of CO. Any biomass burning outside the city (burning off of crop fields or forest fires) is accounted for by removing the background.

The remaining sources of CO that must be considered are oxidation of VOC's (both biogenic and anthropogenic), and fossil fuel combustion. Fossil fuel combustion has long been considered the primary source of CO within urban regions (Stevens et al., 1972; EPA, 2014), whereas only recently has biogenic VOC oxidation been shown to be a significant urban source (Cheng et al., 2017).

### *S.3 Bootstrap Monte Carlo Results*

**Deleted:** *2*

The bootstrap Monte Carlo method was used to determine the isotopic signatures at Beech Island, South Carolina. A Keeling plot analysis was used to determine these signatures by performing a linear regression on the measured isotopic values plotted against the inverse of the measured mole fraction values. In the bootstrap Monte Carlo, these data were randomly sampled with replacement 1000 times, producing 1000 intercepts from which we took the mean and standard error of the mean as the reported values. To give the reader an idea of the spread in each value, we have included the histograms of the 1000 intercept data sets generated for each isotope in both summer and winter (Figure S1)

**Figure S3**

Deleted: 1

(a) Winter $\delta^{13}C$ at Beech Island, South Carolina

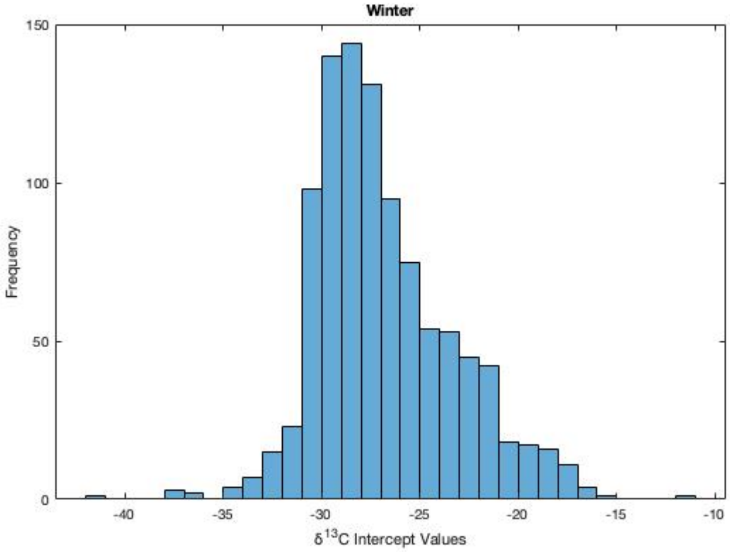

(b) Winter $\delta^{18}O$ at Beech Island, South Carolina

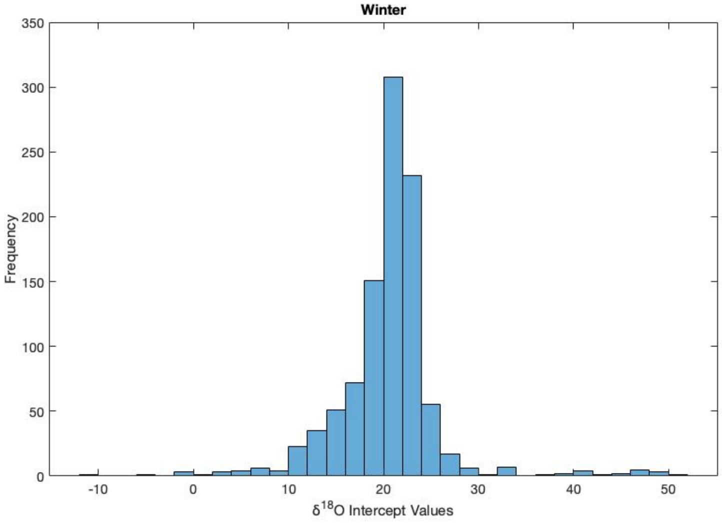

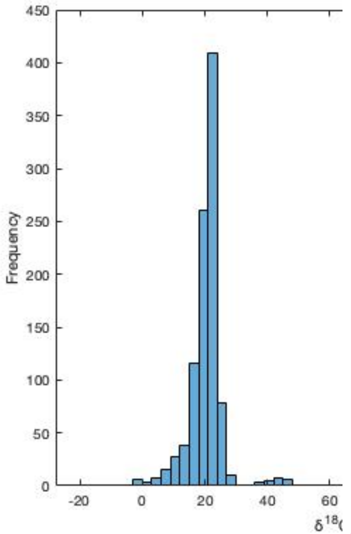

Deleted:

(c) Summer $\delta^{13}C$ at Beech Island, South Carolina

**Deleted:** C

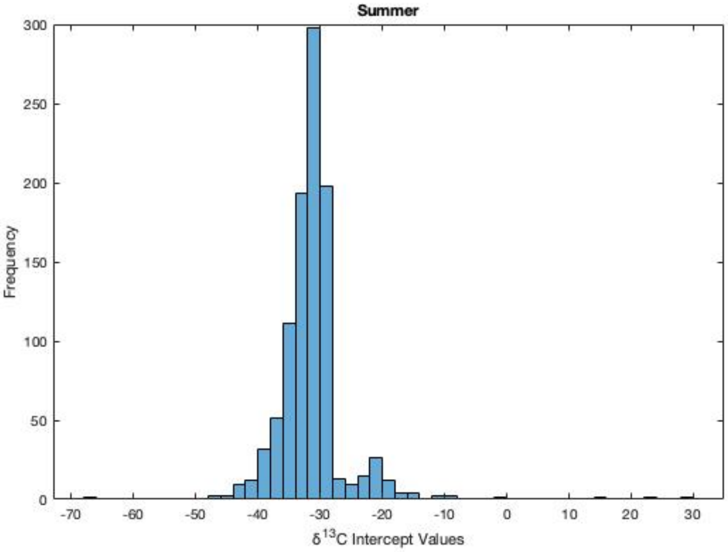

(d) Summer $\delta^{18}O$ at Beech Island, South Carolina

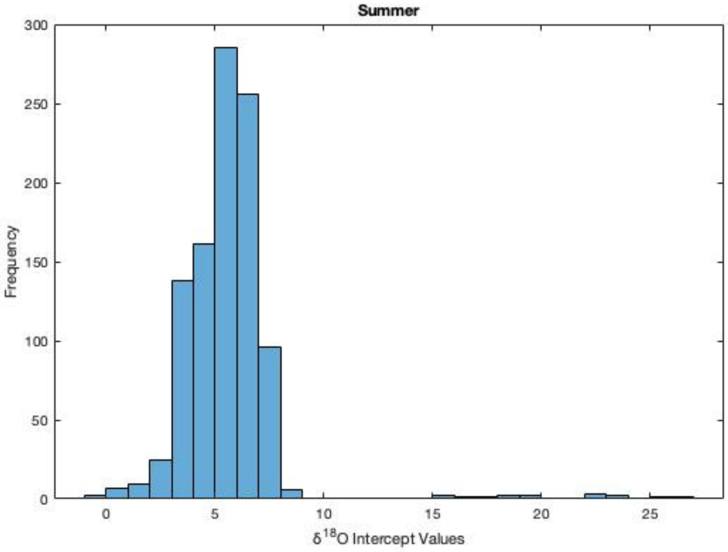

### *S.4 Mole Fraction and Isotopic Data From Indianapolis, IN, and Beech Island, SC.*

**Deleted:** *3*

**Table S2:** Indianapolis Tower 1 and Tower 2 mole fraction and isotopic data used in this study. Mole fraction uncertainty is reported as ± 0.5 nmol:mol (1σ).

| Date | $X_{CO}$ T1 (nmol:mol) | $\delta^{13}$C T1 (‰) | 1σ $\delta^{13}$C T1 (‰) | $\delta^{18}$O T1 (‰) | 1σ $\delta^{18}$O T1 (‰) | $X_{CO}$ T2 (nmol:mol) | $\delta^{13}$C T2 (‰) | 1σ $\delta^{13}$C T2 (‰) | $\delta^{18}$O T2 (‰) |
|---|---|---|---|---|---|---|---|---|---|
| 7/27/13 | 128.2 | -29.2 | 0.04 | 2.5 | 0.09 | 148.1 | -29.3 | 0.04 | 3.8 |
| 7/29/13 | 122.9 | -28.5 | 0.04 | 2.9 | 0.09 | 150.4 | -30.8 | 0.04 | 4.1 |
| 8/1/13 | 116.6 | -28.7 | 0.04 | 7.0 | 0.09 | 129.0 | -29.8 | 0.04 | 3.1 |
| 8/2/13 | 133.9 | -30.4 | 0.04 | 3.3 | 0.09 | 147.9 | -30.2 | 0.04 | 3.8 |
| 8/7/13 | 135.2 | -32.3 | 0.04 | 5.4 | 0.09 | 138.1 | -32.3 | 0.04 | 4.9 |
| 8/27/13 | 149.6 | -31.8 | 0.04 | 4.2 | 0.09 | 165.7 | -32.0 | 0.04 | 4.2 |
| 9/10/13 | 191.1 | -31.6 | 0.13 | 3.0 | 0.34 | 202.7 | -32.0 | 0.13 | 4.3 |
| 9/11/13 | 174.6 | -31.8 | 0.13 | 3.1 | 0.34 | 181.6 | -31.7 | 0.13 | 4.3 |
| 9/18/13 | 164.2 | -29.6 | 0.13 | 6.8 | 0.34 | 184.2 | -30.7 | 0.13 | 6.0 |
| 9/19/13 | 173.3 | -30.3 | 0.13 | 6.1 | 0.34 | 178.5 | -30.4 | 0.13 | 5.5 |
| 9/20/13 | 170.5 | -29.9 | 0.13 | 6.2 | 0.34 | 189.1 | -29.9 | 0.13 | 6.4 |
| 9/29/13 | 150.8 | -28.5 | 0.13 | 7.7 | 0.14 | 171.3 | -29.2 | 0.13 | 6.5 |
| 5/12/14 | 127.2 | -28.5 | 0.18 | 4.7 | 0.23 | 136.7 | -28.4 | 0.18 | 3.9 |
| 5/16/14 | 132.4 | -26.2 | 0.18 | 4.7 | 0.23 | 152.7 | -26.4 | 0.18 | 6.6 |
| 5/17/14 | 131.5 | -25.9 | 0.18 | 4.3 | 0.23 | 152.3 | -26.6 | 0.18 | 6.2 |
| 5/27/14 | 139.6 | -29.9 | 0.18 | 3.7 | 0.23 | 150.0 | -29.4 | 0.18 | 3.6 |
| 5/28/14 | 128.9 | -29.5 | 0.18 | 3.3 | 0.23 | 141.4 | -29.3 | 0.18 | 3.2 |
| 6/3/14 | 127.8 | -28.7 | 0.18 | 4.0 | 0.23 | 141.0 | -27.6 | 0.18 | 9.0 |
| 7/29/14 | 140.2 | -29.3 | 0.20 | 4.2 | 0.50 | 164.0 | -29.9 | 0.20 | 3.9 |
| 8/12/14 | 166.6 | -29.3 | 0.29 | 4.6 | 0.48 | 191.5 | -29.4 | 0.29 | 4.1 |
| 8/13/14 | 192.3 | -29.5 | 0.29 | 3.4 | 0.48 | 216.1 | -29.5 | 0.29 | 4.1 |
| 8/19/14 | 154.4 | -31.4 | 0.29 | 4.3 | 0.48 | 160.5 | -30.6 | 0.29 | 3.8 |
| 8/20/14 | 119.5 | -30.6 | 0.29 | 6.1 | 0.48 | 129.2 | -30.8 | 0.29 | 4.3 |
| 8/21/14 | 127.4 | -33.2 | 0.29 | 5.2 | 0.48 | 154.5 | -31.7 | 0.29 | 5.5 |
| 8/22/14 | 112.4 | -31.8 | 0.29 | 5.4 | 0.48 | 158.6 | -31.0 | 0.29 | 6.6 |
| 9/1/14 | 100.3 | -31.6 | 0.15 | 5.2 | 0.40 | 109.5 | -32.0 | 0.15 | 2.8 |
| 9/2/14 | 114.1 | -30.5 | 0.15 | 5.1 | 0.40 | 139.7 | -30.8 | 0.15 | 5.1 |
| 9/3/14 | 131.1 | -30.8 | 0.15 | 3.9 | 0.40 | 147.6 | -30.2 | 0.15 | 5.0 |
| 9/5/14 | 151.3 | -31.9 | 0.15 | 5.2 | 0.40 | 169.0 | -31.9 | 0.15 | 4.8 |
| 5/5/15 | 146.9 | -28.1 | 0.31 | 4.9 | 0.34 | 158.0 | -28.2 | 0.31 | 5.6 |
| 5/15/15 | 157.3 | -29.6 | 0.31 | 4.9 | 0.34 | 173.4 | -29.0 | 0.31 | 6.5 |
| 5/22/15 | 145.1 | -26.8 | 0.31 | 6.0 | 0.34 | 157.5 | -26.5 | 0.31 | 7.4 |
| 6/5/15 | 143.8 | -29.3 | 0.31 | 4.6 | 0.34 | 151.3 | -28.7 | 0.31 | 6.0 |
| 6/8/15 | 113.9 | -30.1 | 0.31 | 0.7 | 0.34 | 152.7 | -28.3 | 0.31 | 7.5 |
| 6/30/15 | 233.1 | -29.4 | 0.25 | 4.9 | 0.73 | 245.8 | -29.3 | 0.25 | 5.1 |
| 7/6/15 | 221.6 | -30.1 | 0.25 | 4.5 | 0.73 | 264.3 | -29.5 | 0.25 | 5.3 |
| 7/14/15 | 154.7 | -30.7 | 0.25 | 3.3 | 0.73 | 151.3 | -30.3 | 0.25 | 2.9 |
| 7/17/15 | 149.2 | -34.2 | 0.25 | 2.2 | 0.73 | 149.6 | -32.8 | 0.25 | 4.0 |
| 7/25/15 | 196.6 | -30.8 | 0.25 | 3.6 | 0.73 | 216.1 | -29.8 | 0.25 | 4.5 |
| 7/29/15 | 135.3 | -33.5 | 0.25 | 1.4 | 0.73 | 155.7 | -32.4 | 0.25 | 4.1 |

**Table S3:** Beech Island mole fraction and isotopic data. Mole fraction uncertainty is ± 0.5 nmol:mol (1σ).

| Date | $X_{CO}$ (nmol:mol) | $\delta^{13}C$ (‰) | $\delta^{13}C$ 1σ (‰) | $\delta^{18}O$ (‰) | $\delta^{18}O$ 1σ (‰) |
|---|---|---|---|---|---|
| 4/21/15 | 152.7 | -26.4 | 0.2 | 5.7 | 0.3 |
| 5/5/15 | 152.6 | -27.1 | 0.3 | 5.4 | 0.3 |
| 5/17/15 | 124.7 | -27.3 | 0.3 | 3.5 | 0.3 |
| 6/2/15 | 109.1 | -29.5 | 0.3 | 2.0 | 0.3 |
| 6/16/15 | 142.1 | -33.0 | 0.3 | 1.1 | 0.3 |
| 7/14/15 | 143.7 | -34.2 | 0.3 | 2.7 | 0.7 |
| 7/26/15 | 179.2 | -30.9 | 0.2 | 2.4 | 0.4 |
| 8/7/15 | 157.7 | -32.0 | 0.3 | 3.3 | 0.7 |
| 8/18/15 | 87.9 | -33.1 | 0.2 | -0.3 | 0.4 |
| 8/28/15 | 150.8 | -30.4 | 0.2 | 2.9 | 0.4 |
| 10/6/15 | 134.0 | -29.0 | 0.2 | 5.6 | 0.2 |
| 10/20/15 | 128.5 | -28.8 | 0.2 | 5.1 | 0.2 |
| 11/3/15 | 128.1 | -29.9 | 0.2 | 5.5 | 0.2 |
| 11/17/15 | 139.3 | -28.5 | 0.2 | 6.5 | 0.2 |
| 12/9/15 | 143.7 | -28.3 | 0.2 | 6.1 | 0.2 |
| 1/2/16 | 168.5 | -27.5 | 0.2 | 8.4 | 0.2 |
| 1/12/16 | 148.0 | -27.8 | 0.2 | 6.8 | 0.2 |
| 1/27/16 | 149.0 | -27.2 | 0.2 | 8.0 | 0.2 |
| 2/10/16 | 160.6 | -27.1 | 0.2 | 7.6 | 0.2 |
| 2/24/16 | 157.3 | -27.5 | 0.2 | 6.7 | 0.2 |
| 3/9/16 | 138.4 | -26.9 | 0.2 | 5.0 | 0.2 |

**Table S4:** Monthly mean CO mole fraction and isotope data extracted from Bräunlich (2000). We were unable to locate a table for these data in the literature, so we used freely available graphical digitizing software (WebPlotDigitizer-4.2, https://automeris.io/WebPlotDigitizer) to extract the data. This software works by selecting points along the axes of a plot, and implements a grid based on the number of pixels between each point. The operator then selects the data from the image, and a table of values is generated by the software. From this data, we took the mean and standard deviation for each month for the sampling period (1996-1999) reported by Bräunlich (2000). We then used the monthly mean values from this data set as a background for the Beech Island Miller Tans analysis.

| MONTH | CO | σCO | $\delta^{13}$C | σ$\delta^{13}$C | $\delta^{18}$O | σ$\delta^{18}$O |
|---|---|---|---|---|---|---|
| 1 | 124.1 | 14.6 | -26.4 | 0.6 | 3.5 | 0.8 |
| 2 | 126.8 | 17.3 | -26.2 | 0.6 | 3.5 | 1.9 |
| 3 | 125.8 | 18.3 | -26.3 | 0.5 | 3.3 | 1.9 |
| 4 | 122.5 | 20.7 | -26.1 | 0.4 | 1.8 | 1.7 |
| 5 | 120.7 | 15.3 | -26.1 | 0.8 | 1.5 | 1.5 |
| 6 | 99.6 | 14.8 | -27.6 | 0.8 | -1.8 | 1.6 |
| 7 | 85.2 | 6.6 | -29.3 | 0.7 | -3.3 | 1.3 |
| 8 | 81.6 | 12.0 | -30.1 | 1.0 | -3.0 | 1.6 |
| 9 | 78.4 | 11.1 | -30.2 | 1.1 | -3.0 | 1.7 |
| 10 | 91.1 | 16.4 | -28.9 | 0.9 | -1.2 | 1.4 |
| 11 | 105.5 | 8.5 | -27.9 | 0.6 | 1.4 | 1.6 |
| 12 | 114.6 | 19.9 | -27.2 | 0.6 | 2.6 | 1.6 |

**Formatted:** Centered

**Deleted:** ----------Page Break----------

## References

Atkinson, R., and Arey, J.: Gas-phase tropospheric chemistry of biogenic volatile organic compounds: a review, Atmospheric Environment, 37, Supplement 2, 197-219, http://dx.doi.org/10.1016/S1352-2310(03)00391-1, 2003.

Atkinson, R., Baulch, D. L., Cox, R. A., Crowley, J. N., Hampson, R. F., Hynes, R. G., Jenkin, M. E., Rossi, M. J., and Troe, J.: Evaluated kinetic and photochemical data for atmospheric chemistry: Volume II - gas phase reactions of organic species, Atmospheric Chemistry and Physics, 6, 3625-4055, 2006.

Bräunlich, M.: Study of atmospheric carbon monoxide and methane using isotopic analysis, PhD, Institute of Environmental Physics, Rupertus Carola University, Heidelberg, Germany, 2000.

Brenninkmeijer, C. A. M., Rockmann, T., Braunlich, M., Jockel, P., and Bergamaschi, P.: Review of Progress in Isotope Sutdies of Atmospheric Carbon Monoxide, ChemoSphere- Global Change Science, 1, 33-52, 1999.

Cheng, Y., Wang, Y. H., Zhang, Y. Z., Chen, G., Crawford, J. H., Kleb, M. M., Diskin, G. S., and Weinheimer, A. J.: Large biogenic contribution to boundary layer O-3-CO regression slope in summer, Geophysical Research Letters, 44, 7061-7068, 10.1002/2017gl074405, 2017.

Duncan, B. N., Logan, J. A., Bey, I., Megretskaia, I. A., Yantosca, R. M., Novelli, P. C., Jones, N. B., and Rinsland, C. P.: Global budget of CO, 1988–1997: Source estimates and validation with a global model, Journal of Geophysical Research: Atmospheres, 112, D22301, 10.1029/2007jd008459, 2007.

Guenther, A. B., Jiang, X., Heald, C. L., Sakulyanontvittaya, T., Duhl, T., Emmons, L. K., and Wang, X.: The Model of Emissions of Gases and Aerosols from Nature version 2.1 (MEGAN2.1): an extended and updated framework for modeling biogenic emissions, Geosci. Model Dev., 5, 1471-1492, 10.5194/gmd-5-1471-2012, 2012.

Gurney, K. R., Razlivanov, I., Song, Y., Zhou, Y. Y., Benes, B., and Abdul-Massih, M.: Quantification of Fossil Fuel CO2 Emissions on the Building/Street Scale for a Large US City, Environ. Sci. Technol., 46, 12194-12202, 10.1021/es3011282, 2012.

Park, C., Schade, G. W., and Boedeker, I.: Characteristics of the flux of isoprene and its oxidation products in an urban area, J. Geophys. Res.-Atmos., 116, 13, 10.1029/2011jd015856, 2011.

Rockmann, T., and Brenninkmeijer, C. A. M.: CO and CO2 isotopic composition in Spitsbergen during the 1995 ARCTOC campaign, Tellus, 49B, 455-465, 1997.

Röckmann, T., Brenninkmeijer, C. A. M., Saueressig, G., Bergamaschi, P., Crowley, J. N., Fischer, H., and Crutzen, P. J.: Mass-Independent Oxygen Isotope Fractionation in Atmospheric CO as a Result of the Reaction CO+OH, Science, 281, 544-546, 10.1126/science.281.5376.544, 1998.

Sander, S. P., Friedl, R., Golden, D., Kurylo, M., Moortgat, G., Keller-Rudek, H., Wine, P., Ravishankara, A., Kolb, C., and Molina, M.: Chemical kinetics and photochemical data for use in atmospheric studies: evaluation number 15, National Aeronautics and Space Administration, Jet Propulsion Laboratory, California Institute of Technology Pasadena, CA, 2006.

Saurer, M., Prevot, A. S. H., Dommen, J., Sandradewi, J., Baltensperger, U., and Siegwolf, R. T. W.: The influence of traffic and wood combustion on the stable isotopic composition of carbon monoxide, Atmospheric Chemistry and Physics, 9, 3147-3161, 2009.

Stevens, C. M., Kaplan, L., Gorse, R., Durkee, S., Compton, M., Cohen, S., and Bielling, K.: The kinetic isotope effect for carbon and oxygen in the reaction CO + OH, Int. J. Chem. Kinet., 12, 935-948, 10.1002/kin.550121205, 1980.

Stevens, C. M., Krout, L., Walling, D., and Venters, A.: The Isotopic Composition of Atmospheric Carbon Monoxide, Earth and Planetary Science Letters, 16, 147-165, 1972.

Deleted: ¶

Vimont, I. J., Turnbull, J. C., Petrenko, V. V., Place, P. F., Karion, A., Miles, N. L., Richardson, S. J., Gurney, K. R., Patarasuk, R., Sweeney, C., Vaughn, B., and White, J. W. C.: Carbon monoxide isotopic measurements in Indianapolis constrain urban source isotopic signatures and support mobile fossil fuel emissions as the dominant wintertime CO source, Elem Sci Anth, 5, 10.1525/elementa.136, 2017.

Warneke, C., de Gouw, J. A., Edwards, P. M., Holloway, J. S., Gilman, J. B., Kuster, W. C., Graus, M., Atlas, E., Blake, D., Gentner, D. R., Goldstein, A. H., Harley, R. A., Alvarez, S., Rappenglueck, B., Trainer, M., and Parrish, D. D.: Photochemical aging of volatile organic compounds in the Los Angeles basin: Weekday-weekend effect, J. Geophys. Res.-Atmos., 118, 5018-5028, 10.1002/jgrd.50423, 2013.

Warneke, C., McKeen, S. A., de Gouw, J. A., Goldan, P. D., Kuster, W. C., Holloway, J. S., Williams, E. J., Lerner, B. M., Parrish, D. D., Trainer, M., Fehsenfeld, F. C., Kato, S., Atlas, E. L., Baker, A., and Blake, D. R.: Determination of urban volatile organic compound emission ratios and comparison with an emissions database, J. Geophys. Res.-Atmos., 112, 13, 10.1029/2006jd007930, 2007.